DOT/FAA/PM-88/9

Project Report
ATC-158

Selected Wind Shear Events Observed During the 1987 Evaluation of Enhancements to the FAA Low Level Wind Shear Alert System at Stapleton International Airport

M. F. Donovan
M. M. Wolfson

15 February 1989

Lincoln Laboratory
MASSACHUSETTS INSTITUTE OF TECHNOLOGY
LEXINGTON, MASSACHUSETTS

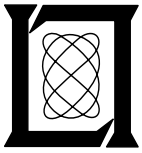

Prepared for the Federal Aviation Administration,
Washington, D.C. 20591

TECHNICAL REPORT STANDARD TITLE PAGE

1. Report No.	2. Government Accession No.	3. Recipient's Catalog No.
DOT/FAA/PS-88-9		

4. Title and Subtitle	5. Report Date
Selected Wind Shear Events Observed During the 1987 Evaluation of Enhancements to the FAA Low Level Wind Shear Alert System at Stapleton International Airport	15 February 1989
	6. Performing Organization Code

7. Author(s)	8. Performing Organization Report No.
Michael F. Donovan and Marilyn M. Wolfson	ATC-158

9. Performing Organization Name and Address	10. Work Unit No. (TRAIS)
Lincoln Laboratory, MIT P.O. Box 73 Lexington, MA 02173-0073	11. Contract or Grant No. DTFA-01-80-Y-10546
	13. Type of Report and Period Covered
12. Sponsoring Agency Name and Address Department of Transportation Federal Aviation Administration Program Engineering Service Washington, DC 20591	Project Report
	14. Sponsoring Agency Code

15. Supplementary Notes

The work reported in this document was performed at Lincoln Laboratory, a center for research operated by Massachusetts Institute of Technology, under Air Force Contract F19628-85-C-0002.

16. Abstract

The Federal Aviation Administration (FAA) Technical Center (FAATC) conducted a test of the enhancements to the FAA Low Level Wind Shear Alert System (LLWAS) at Denver Stapleton International Airport from 3 August through 4 September 1987. Upon completion of the test, the performance of the LLWAS during selected microburst and gust front test cases was investigated in detail. Additional sources of "true" wind shear information were sought to help evaluate the performance of the LLWAS. In support of these efforts, Lincoln Laboratory supplied complete data sets, including single Doppler radar data from the FAA-Lincoln Laboratory FL-2 radar, dual Doppler radar data from the FAA-Lincoln Laboratory FL-2 radar, dual Doppler analyses of the surface wind fields (when possible), mesonet data from the Lincoln network of 30 automatic weather stations in the vicinity of Stapleton, and LLWAS data to the FAATC. This report provides a summary of salient features for a number of FAATC selected wind shear events which occurred during the evaluation of the enhanced LLWAS, and documents the data that Lincoln Laboratory has provided to the FAA as part of its project responsibilities.

17. Key Words		18. Distribution Statement
FAATC	low level wind shear	Document is available to the public through the National Technical Information Service, Springfield, VA 22161.
LLWAS	microburst	
mesonet	gust front	
dual Doppler	FL-2	
TDWR	UND	

19. Security Classif. (of this report)	20. Security Classif. (of this page)	21. No. of Pages	22. Price
Unclassified	Unclassified	146	

FORM DOT F 1700.7 (8-69)

ABSTRACT

The Federal Aviation Administration (FAA) Technical Center (FAATC) conducted a test of the enhancements to the FAA Low Level Wind Shear Alert System (LLWAS) at Denver Stapleton International Airport from 3 August through 4 September, 1987. Upon completion of the test, the performance of the LLWAS during selected microburst and gust front test cases was investigated in detail. Additional sources of "true" wind shear information were sought to help evaluate the performance of the LLWAS. In support of these efforts, Lincoln Laboratory supplied complete data sets, including single Doppler radar data from the FAA–Lincoln Laboratory FL–2 radar, dual Doppler analyses of the surface wind fields (when possible), mesonet data from the Lincoln network of 30 automatic weather stations in the vicinity of Stapleton, and LLWAS data to the FAATC. This report provides a summary of salient features for a number of FAATC selected wind shear events which occurred during the evaluation of the enhanced LLWAS, and documents the data that Lincoln Laboratory has provided to the FAA as part of its project responsibilities.

TABLE OF CONTENTS

LIST OF ILLUSTRATIONS

LIST OF TABLES

LIST OF ACRONYMS AND ABBREVIATIONS

BPI	bits per inch
CEF	Cartesian Exchange Format
CO	Colorado
EOF	end of file
FAA	Federal Aviation Administration
FAATC	Federal Aviation Administration Technical Center
FLOWS	FAA-Lincoln Laboratory Operational Weather Studies
FL-2	FAA-Lincoln Laboratory S-band Doppler weather radar
GF	gust front
LLWAS	Low Level Wind Shear Alert System
MB/div line	microburst/divergent line
NCAR	National Center for Atmospheric Research
SEIC	System Engineering and Integration Contractor
TDWR	Terminal Doppler Weather Radar
UND	University of North Dakota C-band Doppler weather radar
UTC	Universal Coordinated Time

ACKNOWLEDGMENTS

Without the help of many people in Group 43 at Lincoln Laboratory, the reported work could not have been accomplished on time. We especially thank Paul Biron for assisting in all of the data processing and Robert Hallowell for helping with the dual Doppler analyses. Efforts by Richard DeLaura, Benjamin Stevens and Sharon Stanfill in altering portions of the software to accomodate the needs of this project are also gratefully acknowledged. In addition, we thank Diana Klingle-Wilson for her help in analyzing the 26 August 1987 case, and John DiStefano for his help in analyzing of the 2 September 1987 microburst case. The daily weather summaries, written by Mark Isaminger for each day FL-2 collected data during the 1987 season, provided a very useful source of information for the case studies presented in this report.

I. INTRODUCTION

The Federal Aviation Administration (FAA) evaluation of the enhancements to the Low Level Wind Shear Alert System (LLWAS) at the Denver Stapleton International Airport took place from 3 August through 4 September, 1987. The test was designed to determine the effectiveness of the new LLWAS wind shear and microburst detection algorithms developed at the National Center for Atmospheric Research (NCAR; Wilson and Flueck, 1986), of the new 12-station LLWAS configuration at Stapleton, and of the new alphanumeric display message formats and a prototype color graphic wind shear display (O'Brien, 1987; LLWAS Program Staff, 1987).

The FAA Technical Center (FAATC) had the overall responsibility for the enhanced LLWAS evaluation. The other organizations that participated were The Martin Marietta Corp. (as System Engineering and Integration Contractor (SEIC)), NCAR, and Lincoln Laboratory. The project responsibilities taken on by Lincoln Laboratory are described below.

A. Lincoln Laboratory's Role

A color workstation display, showing radar reflectivity and Doppler velocity data in the vicinity of the airport, was provided by Lincoln Laboratory for FAATC and SEIC meteorologists conducting the evaluation. The workstation was located in the TDWR S-band Doppler weather radar testbed (FL-2), located 15 km southeast of Stapleton (Fig. I-1). This radar was being operated by Lincoln for the FAA as part of the Terminal Doppler Weather Radar (TDWR) program (Evans and Johnson, 1984; Evans and Turnbull, 1985). The FL-2 radar data were used for the real-time color workstation display. Overlays of the LLWAS station locations, and of the automated FL-2 radar based detections of microbursts (Merritt, 1987) and gust fronts (Sanford *et al.*, 1988) could also be shown on the color display. Two additional VT-240 (Tektronix graphics-emulating) terminals were provided in the same area for display of the alphanumeric LLWAS messages and alarms generated by the LLWAS computer at Stapleton.

Lincoln Laboratory also continuously operated a network of automatic weather stations (Wolfson, 1987) in support of the TDWR program during the enhanced LLWAS evaluation. Wind speed measurements from this network, situated around Stapleton airport (Fig. I-1), were made available by Lincoln after the operational test period to supplement the LLWAS measurements. These were useful for meteorological evaluation of the wind shear events impacting the LLWAS network.

Lincoln Laboratory's project responsibilities also included the provision of dual Doppler radar derived two dimensional surface wind fields that covered the entire Stapleton terminal area. These wind fields were calculated on a 100 x 100 point grid with 250 m spacing by combining, at each grid point, the single Doppler radar

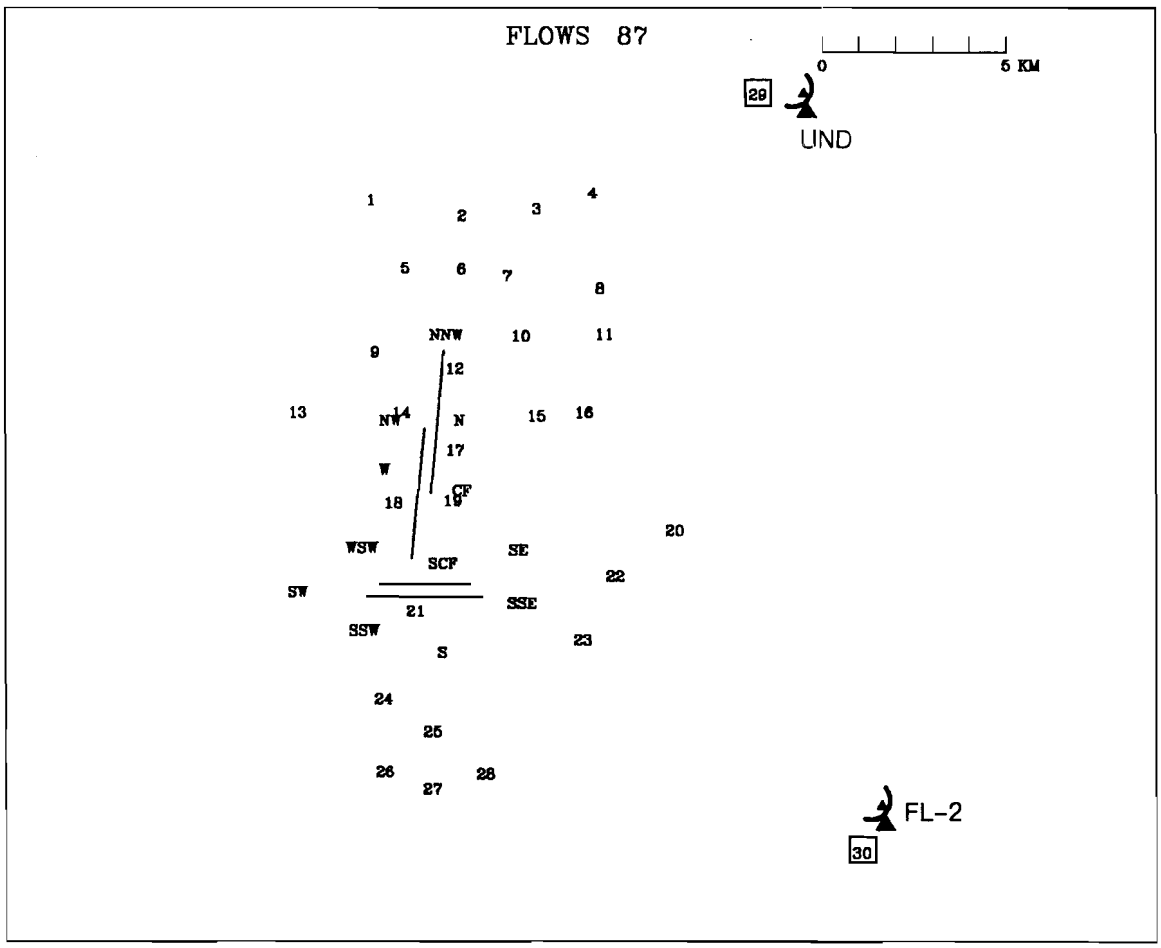

Figure I–1. Map showing 1987 Lincoln mesonet and LLWAS network in relation to Stapleton International Airport. The UND and FL–2 Doppler radars are located at mesonet station Nos. 29 and 30, respectively. The Lincoln mesonet stations are numbered from 1 to 30, and the LLWAS stations are identified by their position relative to the airport, e.g. CF = centerfield, NW = northwest.

measurements from the FL-2 Doppler radar with those from the University of North Dakota (UND) Doppler radar. The UND radar, located 15 km northeast of Stapleton (Fig. I-1), was also being operated in support of the TDWR project. By combining these two, nearly orthogonal views of the wind field, it was possible to derive the true wind speed and direction at most points on the grid (Doviak *et al.*, 1976; Kessinger *et al.*, 1987).

A surface wind field was computed for virtually every minute during the wind shear events for which data from both radars were available. Never before have dual Doppler analyses of wind shear events, with this high spatial and temporal resolution, for these long durations (30 min - 80 min) been produced. These analyses were particularly useful for visualizing the surface wind fields and for determining what type of wind shear events were approaching, or impacting the Stapleton area. They were also used as an independent source of "true" wind information by FAATC in subsequently evaluating the detection performance of the enhanced LLWAS.

B. Provision of Wind Shear Case Studies from Stapleton

The FAATC selected seven wind shear cases from the enhanced LLWAS evaluation period for provision by Lincoln Laboratory. These cases are listed below in Table I-1. The predominant type of shear present, the requested time period, and the actual time period for which data were sent are given. Throughout the report, times are given in Universal coordinates (UTC); subtract 6 hours to get local time for the Denver area (Mountain Daylight Time).

Table I-1. Wind shear events requested by the FAA Technical Center.

Event date (1987)	Shear type	Time requested (UTC)	Time sent (UTC)
August 5	Thermal	1800-2030	1927-2031
August 11	Thermal	1950-2105	1949-2105
August 20	Microburst	2100-2200	2133-2203
*August 21	Gust Front	2200-2300	2138-2245
*August 26	Microburst	0000-0100	0000-0055
*August 28	Gust Front	2200-2300	2205-2235
*September 2	Microburst	2200-2315	2200-2330

*Cases for which it was possible to compute dual Doppler wind fields.

These wind shear events were chosen by FAATC based on visual observations by meteorologists located in the Denver Air Traffic Control Tower; thus they were not always events for which Doppler radar data were available. It was possible to

derive dual Doppler wind fields for four of the seven cases selected. The other cases either had no data recorded from one of the radars, or the time difference between the FL-2 and UND radar scans was too large for the data to be combined (nearly simultaneous scans are required). However, all of the other available data were provided for these cases.

Lincoln Laboratory provided the following data for each requested wind shear case:

1) plots of the combined Lincoln mesonet and LLWAS wind fields,

2) plots of dual Doppler wind vectors and streamlines (where available; see Appendix A for details of the dual Doppler analysis process),

3) color plots of layered FL-2 radar data (at lowest elevation angle available),

4) inventories of FL-2 and UND radar scans,

5) magnetic tape of dual Doppler data in Lincoln Laboratory's Cartesian Exchange Format (see Appendix B),

6) magnetic tape of Lincoln mesonet and LLWAS wind data* (ASCII listing),

7) magnetic tape of "raw" LLWAS wind data* (ASCII listing),

8) magnetic tapes of all corresponding FL-2 and UND radar scans in "Universal" format (Common Doppler Radar Data Exchange format; see Barnes, 1980), and

9) a table of all FL-2 and UND radar scans used to compute the dual Doppler wind fields during the requested time periods (where applicable).

The datasets were prepared and sent to FAATC over a roughly two month period (24 September - 16 November, 1987) following the LLWAS test in Denver. The FAA has permitted Lincoln Laboratory to make all of these data available for research studies. The data request procedure is outlined in Appendix C.

The following chapters of this report each document a wind shear event that occurred during the FAA evaluation of the new enhanced LLWAS at the Stapleton

* The LLWAS data provided with the Lincoln mesonet data were processed to create a one-minute average wind speed and direction, and a one-minute peak wind speed for each minute. This allowed direct comparison with the mesonet data. The unprocessed "raw" LLWAS data were separately provided.

International Airport. For each case requested by FAATC personnel, a summary of the available data is given. For cases for which it was possible to perform dual Doppler wind analyses, a summary of the synoptic weather situation is also included. At least two examples are presented for each case that depict the wind shear events in the vicinity of the LLWAS network. This report can thus be used as a comprehensive wind shear data summary for a number of salient events that occurred during the 1987 enhanced LLWAS evaluation. It also serves to document the datasets that Lincoln Laboratory has provided to the FAA as part of its project responsibilities.

II. 5 August 1987

This was a day on which thermals (observed by FAATC personnel) over the airport triggered LLWAS alarms. No significant wind shear (defined as at least a 10 m/s radial velocity differential over 4 km) was found in the Doppler radar data taken on this day.

A. Available Data

The time period of interest was 1800–2030 UTC; the time period for which the FL–2 single Doppler data and mesonet data were provided was 1927–2031. The UND radar was not operating on this day, so no dual Doppler data were provided. The FL–2 system failed to record the LLWAS data for this day. (FAATC LLWAS recorders were operating.)

B. Wind Shear Events

At 1927 UTC weak and variable wind conditions existed over the eastern half of the network while moderate wind speeds from the west were present over the western portion of the network. According to FL–2 single Doppler data (not shown), a core of stronger approaching velocities (5–9 m/s) had been moving eastward from the west. By 1936, this region of moderate west–northwest winds had passed through the center of the mesonet/LLWAS network (Fig. II–1). Associated with a wind shift and a stronger flow, the boundary of this core initiated a weak divergent flow (7 m/s velocity differential) at LLWAS stations SE and SSE. FL–2 single Doppler radar data did not detect this signature perhaps because it was so weak, or perhaps because it was short–lived; the closest corresponding surface scan to the mesonet/LLWAS wind plot in Fig. II–1 was at 1937 UTC (one minute later).

By 2000 UTC, all mesonet and LLWAS stations were influenced by the westerly flow of approximately 10 m/s (not shown). Twenty minutes later, wind conditions were again very weak and variable. Another small, weak divergent flow occurred at LLWAS stations NW and N at 2030 UTC, as can be seen in Fig. II–2 (the wind direction at LLWAS station NW is from the east–southeast). Again, FL–2 surface radar scans around 2030 UTC (not shown) did not reveal the divergent flow; wind conditions were highly variable, and the divergence probably dissipated by the time the radar was scanning at the surface (2031 UTC).

Cloud conditions of the central U.S. (taken at 2031 UTC) are shown in Fig. II–3. With the state of Colorado highlighted, it is obvious that the sky was clear in and around the Denver region. In fact, throughout the entire time period of interest (1800–2030 UTC), eastern Colorado was free from clouds. This image helps to illustrate that the LLWAS alarms which were triggered during the requested time period were more likely the result of thermals (gusty winds with variable wind directions) rather than microbursts or any other large–scale weather systems occurring within the mesonet/LLWAS network.

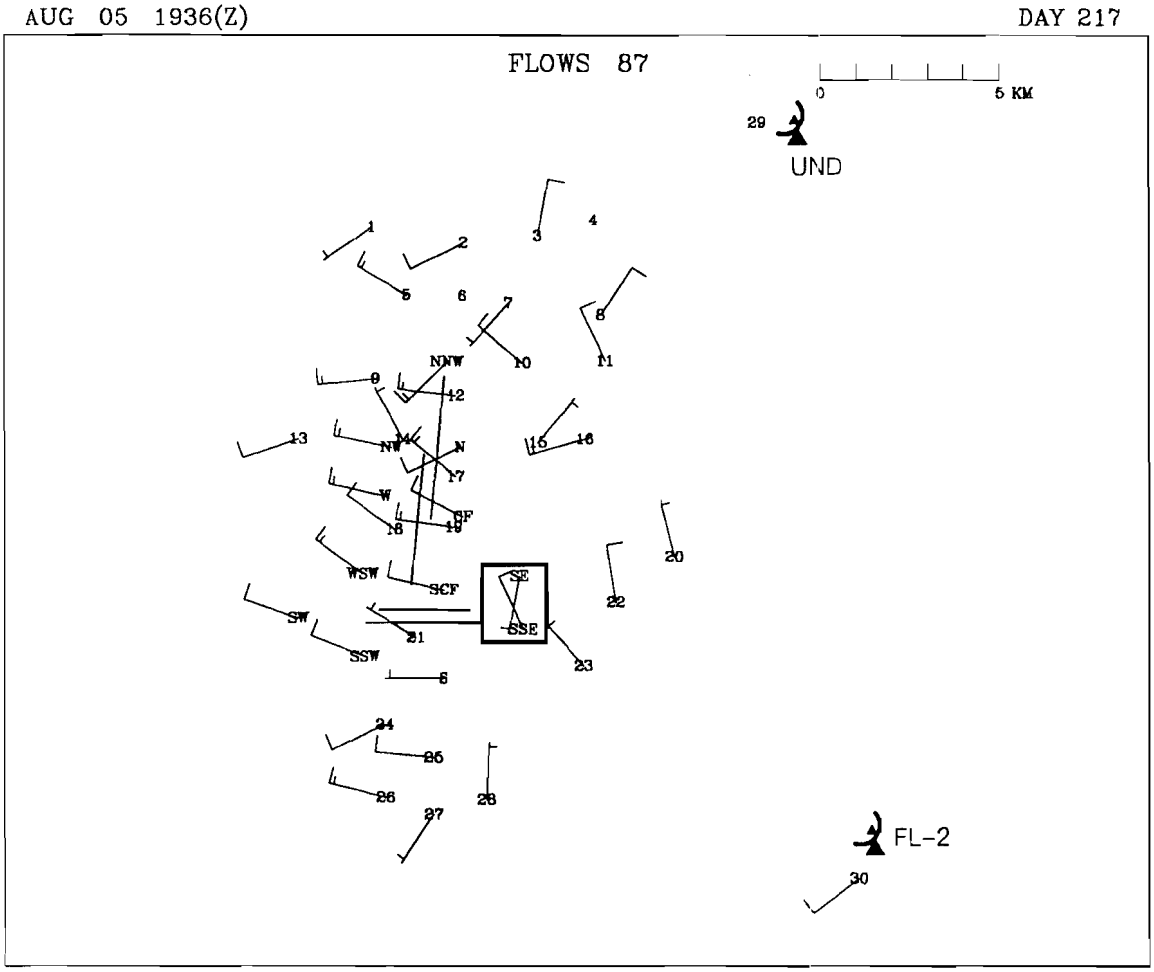

Figure II-1. Mesonet/LLWAS winds at 1936 UTC on 5 August 1987. A core of stronger winds has moved through the center of the network and has initiated a small divergent wind pattern near LLWAS stations SE and SSE(enclosed by the box). A full barb on the wind direction arrow represents 5 m/s and a half barb represents 2.5 m/s.

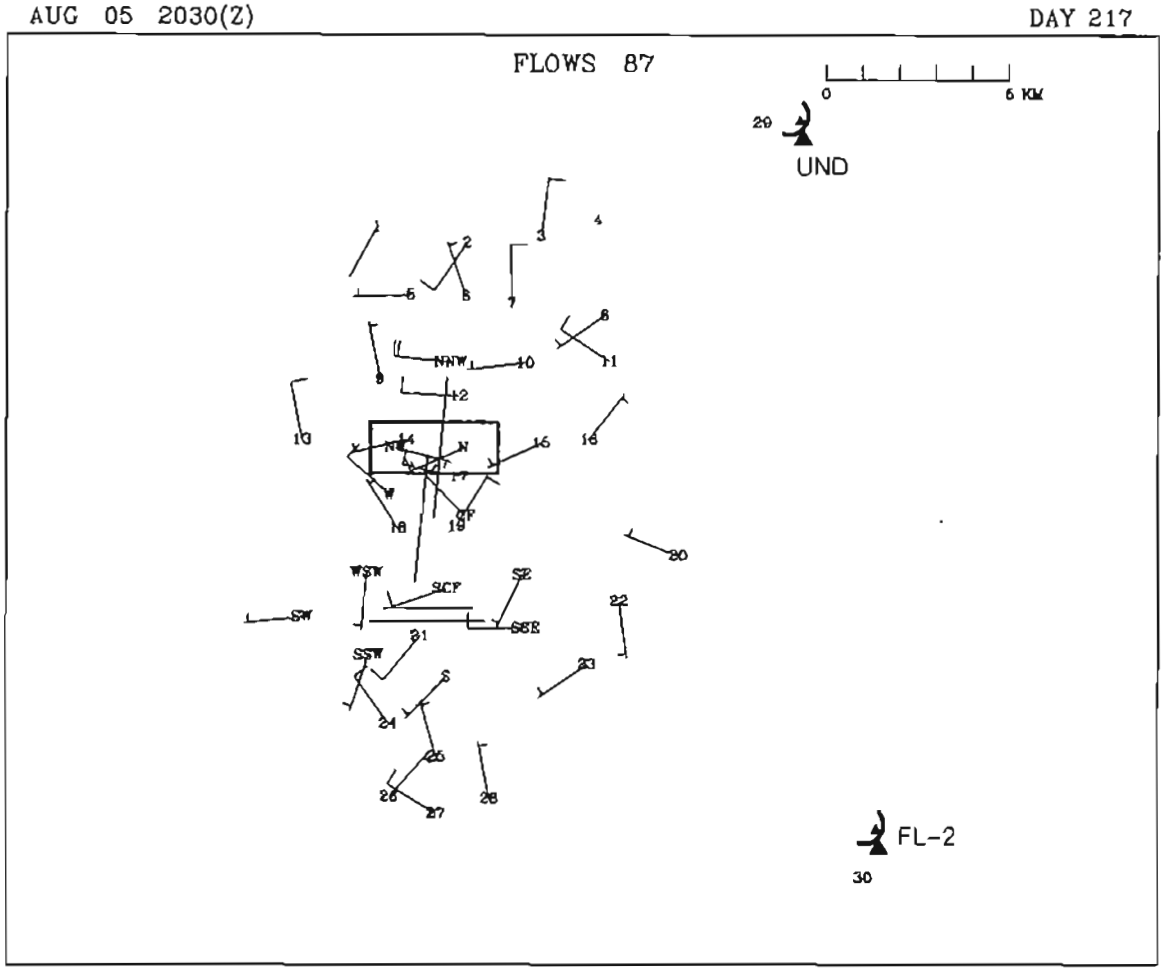

Figure II-2. Mesonet/LLWAS winds at 2030 UTC on 5 August 1987. Wind conditions are light and variable. A weak divergent flow exists between LLWAS stations NW and N (enclosed by the rectangle).

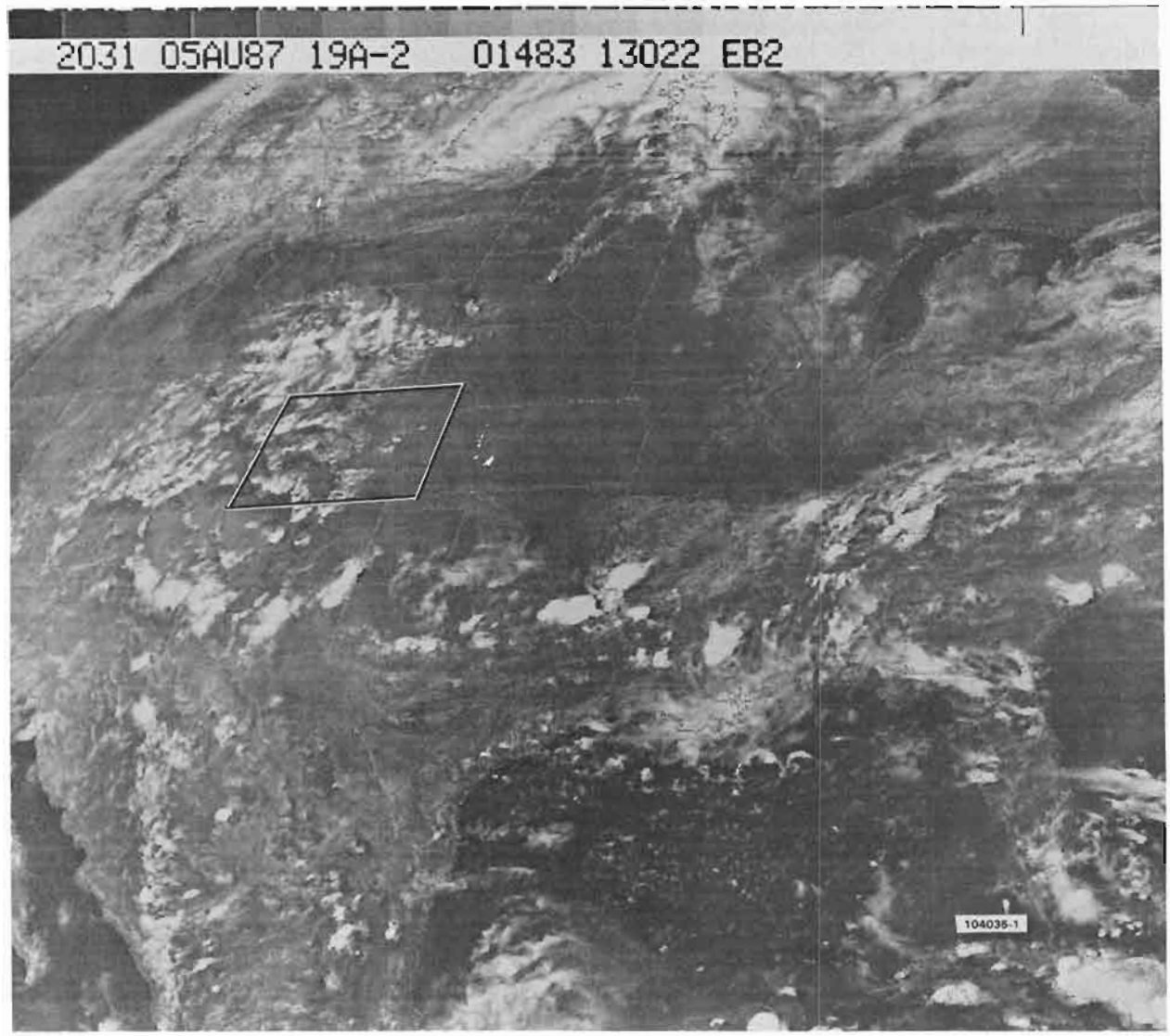

Figure II-3. Visible satellite image of the central U.S. taken at 2031 UTC on 5 August 1987. The clear skies over central and eastern Colorado in this image are representative of cloud conditions throughout the time period of interest (1800-2030 UTC).

III. 11 August 1987

This was a day on which thermals (observed by FAATC personnel) over the airport triggered LLWAS alarms. No significant wind shear (defined as at least a 10 m/s radial velocity differential over 4 km) was found in the Doppler radar data taken on this day.

A. Available Data

The time period of interest was 1950–2105 UTC; the time period for which the FL–2 single Doppler data and mesonet/LLWAS data were provided was 1949–2105 UTC. Coordinated dual Doppler scanning between the FL–2 and UND radar did not begin until 2118, after the requested time period.

B. Wind Shear Events

During the first 15 minutes of the time period of interest, a predominantly easterly wind flow was present over much of the network. The following minutes featured highly variable wind conditions with occasional divergent flows impacting the stations closest to the Stapleton runways. Figure III–1 shows an easterly flow over most of the network at 1957 UTC, with divergent wind shear (10 m/s differential velocity) between LLWAS stations NW, N, and W. The FL–2 single Doppler radar data (not shown) agreed with Fig. III–1 by revealing a somewhat weaker divergent flow (7 m/s outflow) over these LLWAS stations. According to mesonet/LLWAS wind plots, this shear dissipated by 2002.

Another divergent shear pattern had developed over LLWAS stations W, WSW, and CF by 2047 UTC (Fig. III–2). This significant divergent flow (13 m/s outflow) appears to have been more organized, and impacted many more stations, than any other shear found within the time period of interest. However, this divergent flow quickly dissipated within a few minutes. The FL–2 layered reflectivity plot from 500 meters to 6 km above ground level (Fig. III–3) shows that only insignificant echoes (0–5 dBZ) were present throughout the mesonet/LLWAS network at the time (2045–2047). In addition, fair weather was reported over the entire network during the time period of interest. The layered reflectivity plot (Fig. III–3) is an indication that the gusty winds and variable wind directions detected at LLWAS stations W, WSW, and CF (associated with 0 dBZ) could be attributed to thermals rather than a particular weather system moving into the area.

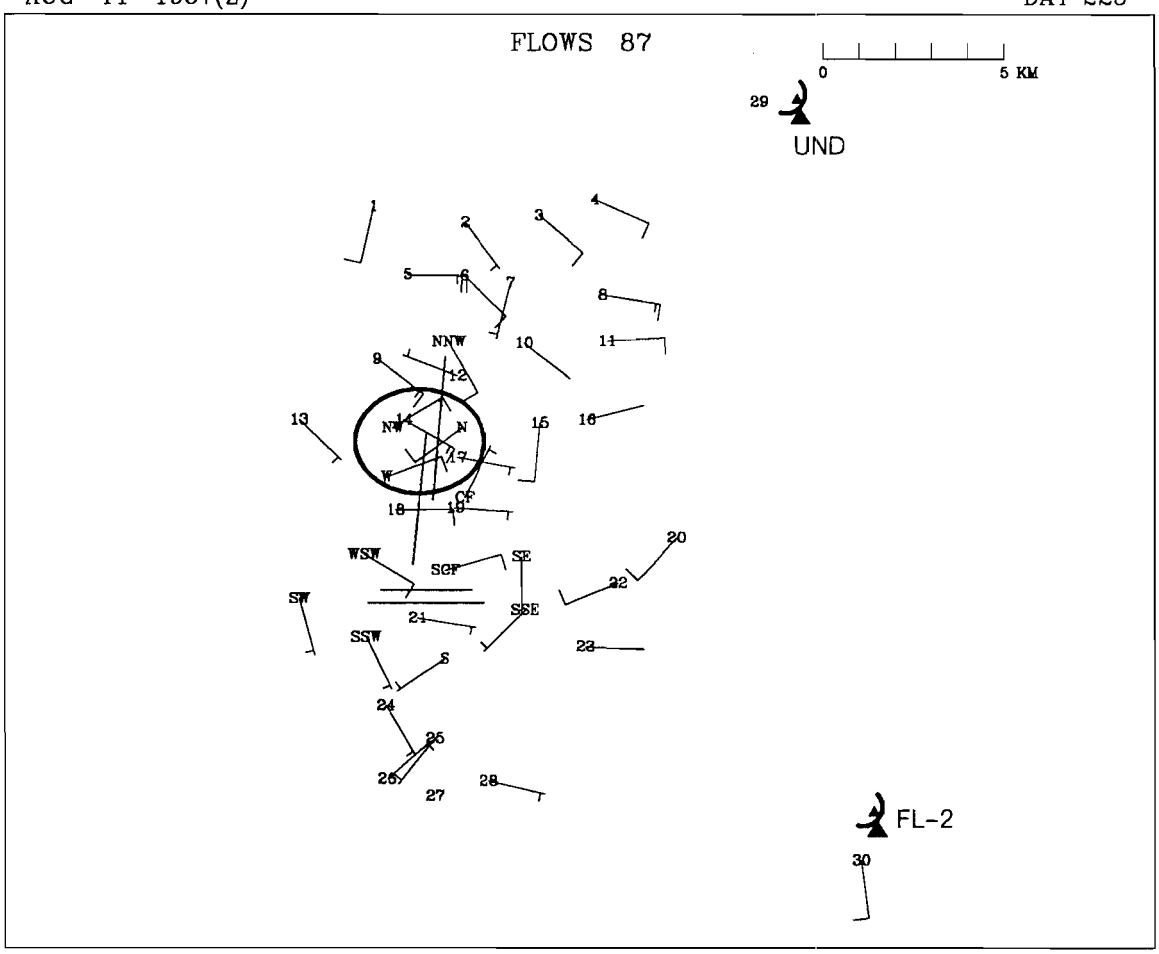

Figure III-1. Mesonet/LLWAS winds at 1957 UTC on 11 August 1987. Divergent wind shear is present between LLWAS stations NW, W, and N (enclosed by the oval). A full barb on the wind direction arrow represents 5 m/s and a half barb represents 2.5 m/s.

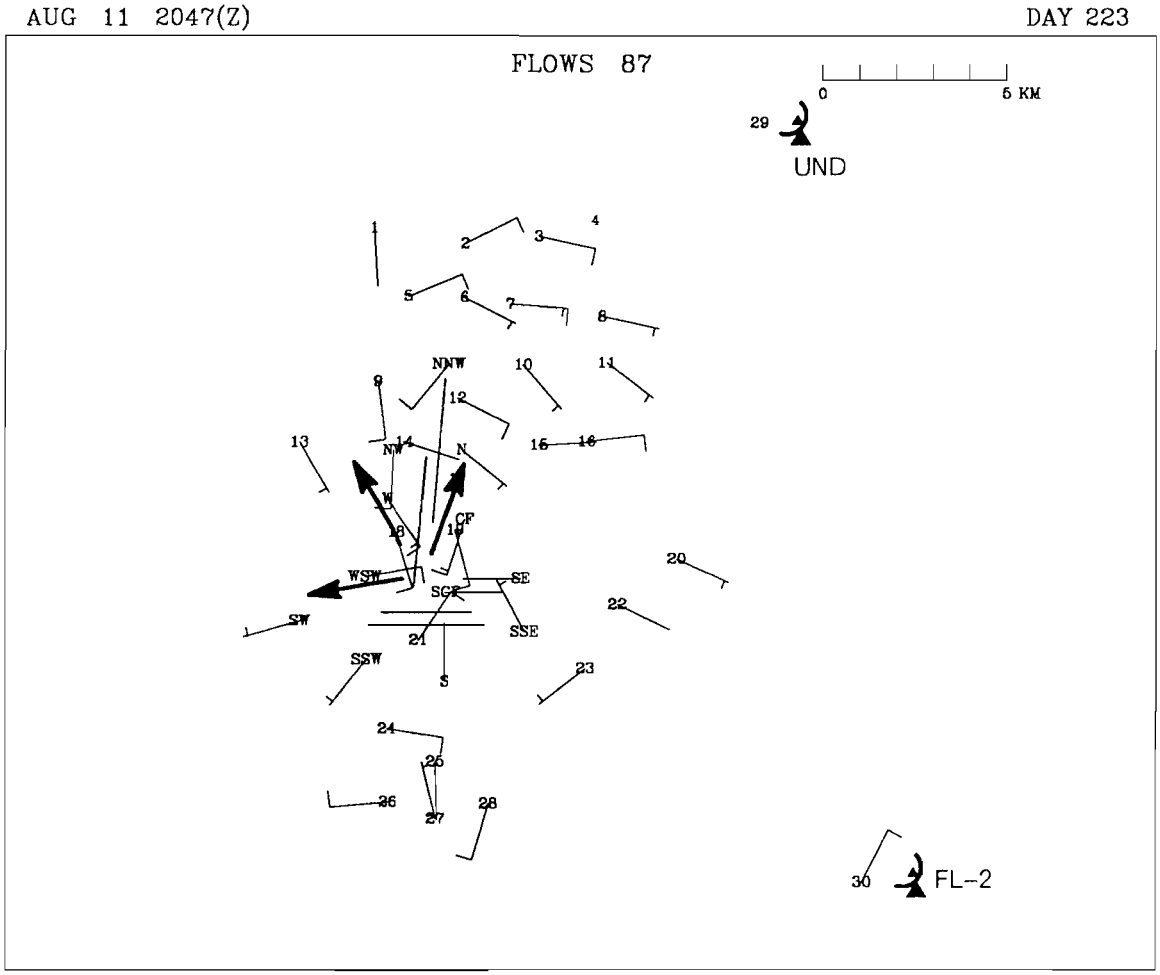

Figure III-2. Mesonet/LLWAS winds at 2047 UTC on 11 August 1987. Wind flow is weak over much of the network except at LLWAS stations W, WSW, and CF, where a divergent wind pattern is present.

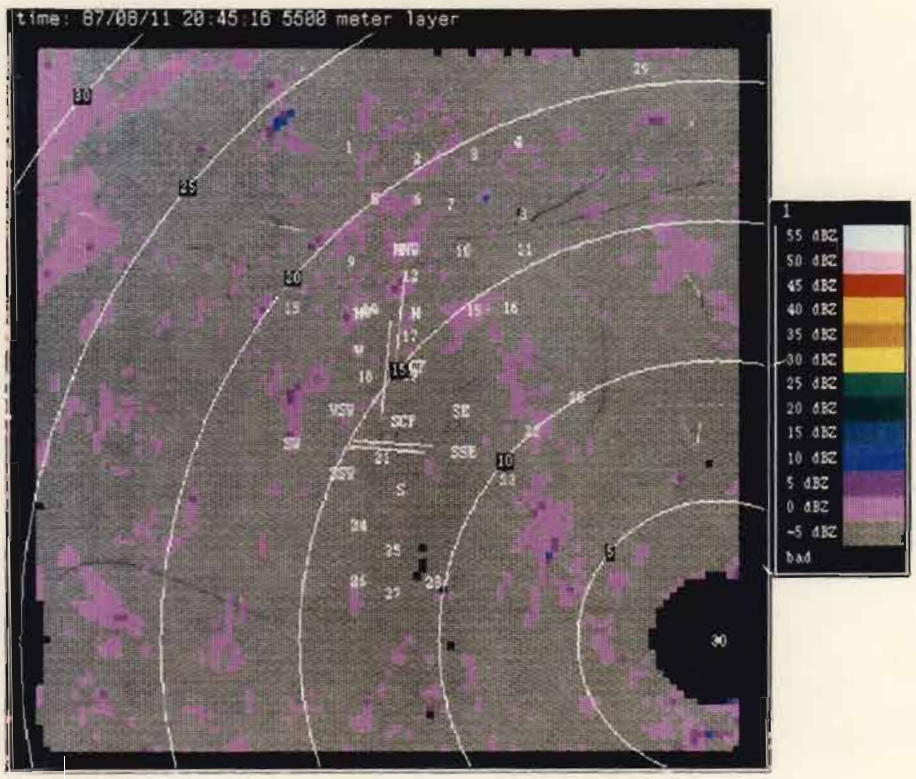

Figure III–3. Layered single Doppler FL–2 reflectivity plot representing the 500 m to 6 km layer at 2045:16 UTC on 11 August 1987. It is clearly evident from the very weak echoes (0–5 dBZ) detected over the mesonet/LLWAS network that the weather occurring at this time was insignificant.

IV. 20 August 1987

This was a day on which the LLWAS indicated microbursts were present over the airport; however, radar data collection began after the microbursts occurred. No significant shear (defined as at least a 10 m/s radial velocity differential over 4 km) was found in the available Doppler radar data taken on this day

A. Available Data

The time period of interest was 2100–2200 UTC. Mesonet, LLWAS, and FL–2 single Doppler data were provided for the period 2133–2203 UTC. Apparently the significant microburst wind shear occurred in the first half of the requested time period.

B. Wind Shear Events

Significant microbursts occurred in the first 30 minutes of the requested time period. In the last 30 minutes of the time period, only one weak shear event was detected. At 2105 UTC, two small weak outflows occurred in the center and eastern regions of the network (not shown). These two outflows quickly dissipated.

Another more significant microburst wind shear event occurred at the southwest edge of the network at 2116 UTC. This outflow progressed northeastward and strengthened with time. Figure IV–1 shows this microburst (22 m/s outflow) impacting the eastern edge of the airport at 2125 (stations CF, SE, 19, and SSE). From 2125 to 2132, the microburst remained relatively stationary and weakened considerably. This divergent outflow was classified as a microburst rather than a thermal because a slight temperature decrease (1–2 °C) was recorded at all of the above stations during the surface outflow passage.

For the next several minutes, the wind flow over much of the network was light from the southwest. At 2151 UTC, one other wind shear event was detected, albeit weak. Figure IV–2 illustrates how weak the surface winds were at this time. However, a very small and weak divergent flow (10 m/s outflow) is evident at stations 12 and N.

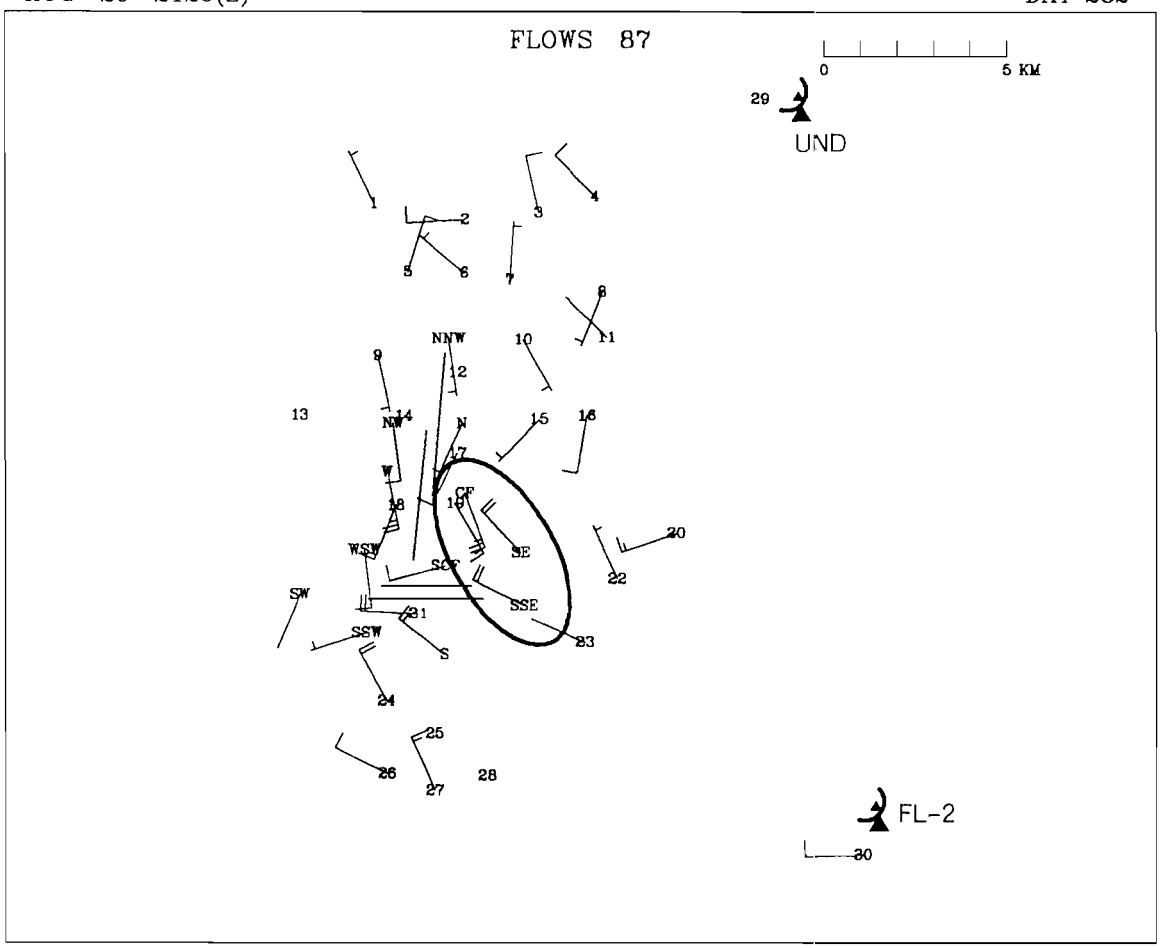

Figure IV–1. Mesonet/LLWAS winds at 2125 UTC on 20 August 1987. Strong peak wind speeds indicate the presence of a microburst outflow at stations 19, CF, SE, and SSE (enclosed by the oval). A full barb on the wind direction arrow represents 5 m/s and a half barb represents 2.5 m/s.

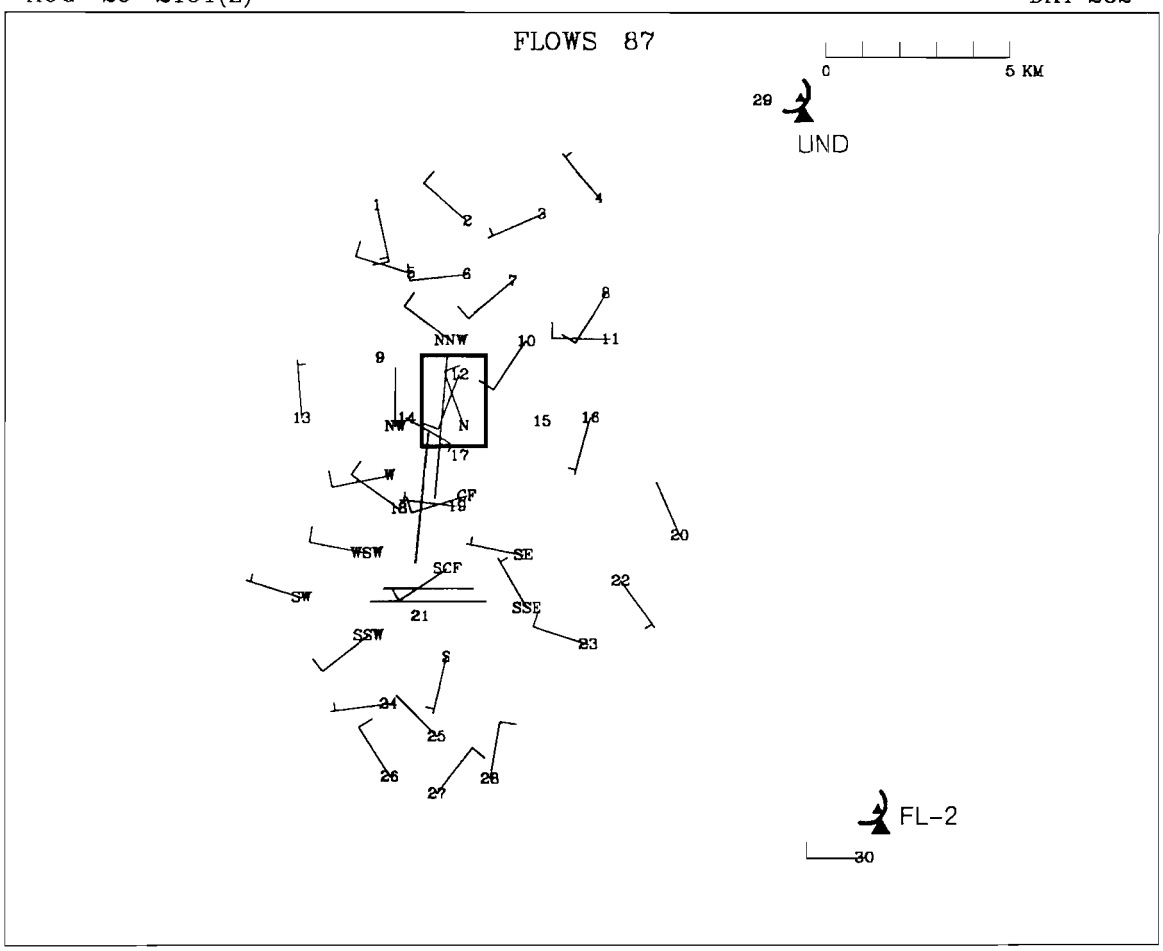

Figure IV–2. Mesonet/LLWAS winds at 2151 UTC on 20 August 1987. A small and weak divergent flow is present over stations 12 and N (enclosed by the box); otherwise tranquil conditions prevail.

V. 21 August 1987

A strong gust front, which moved across Stapleton airport from the northwest, was the predominant wind shear event for the day. A weaker gust front, which crossed Stapleton from the southeast about 15 minutes earlier, also created wind shear over the LLWAS network.

A. Available Data

The time period of interest was 2200-2300 UTC. This was later revised to include the preceding half hour. Mesonet, LLWAS, and FL-2 single Doppler data were provided for the period 2138 to 2245 UTC. It was possible to perform dual Doppler analyses for this same time period, at roughly one minute intervals. The FL-2 and UND radar scan times, and the difference between these scan times, for each dual Doppler analysis are given below in Table V-1.

Table V-1. FL-2 and UND scan times used for 21 August 1987 dual Doppler analyses.

Dual Doppler Pair	FL-2 time (UTC)	UND time (UTC)	Time diff. (sec)
1	2138:19	2137:15	64
2	2142:22	2141:33	49
3	2143:21	2143:28	7
4	2144:28	2144:31	3
5	2145:30	2145:32	2
6	2146:29	2146:33	4
7	2147:26	2147:30	4
8	2148:25	2148:31	6
9	2149:32	2149:34	2
10	2150:34	2150:35	1
11	2151:33	2151:35	2
12	2152:31	2152:33	2
13	2153:30	2153:35	5
14	2154:37	2154:38	1
15	2155:40	2155:38	2
16	2156:38	2156:39	1
17	2157:35	2157:36	1
18	2158:34	2158:38	4
19	2159:41	2159:41	0
20	2200:43	2200:42	1
21	2201:42	2201:43	1
22	2202:41	2202:40	1
23	2203:40	2203:42	2

24	2204:47	2204:46	1
25	2205:49	2205:47	2
26	2206:48	2206:48	0
27	2207:44	2207:45	1
28	2208:43	2208:47	4
29	2209:50	2209:51	1
30	2210:52	2210:52	0
31	2211:51	2211:52	1
32	2212:49	2212:49	0
33	2213:48	2213:51	3
34	2214:55	2214:54	1
35	2215:57	2215:54	3
36	2216:55	2216:55	0
37	2217:51	2217:52	1
38	2218:50	2218:55	5
39	2219:56	2219:58	2
40	2220:58	2220:58	0
41	2221:56	2221:59	3
42	2222:55	2222:55	0
43	2223:53	2223:57	4
44	2224:59	2225:00	1
45	2226:01	2226:00	1
46	2227:00	2227:01	1
47	2227:56	2227:58	2
48	2228:54	2229:01	7
49	2230:01	2230:04	3
50	2231:03	2231:05	2
51	2232:01	2232:06	5
52	2232:59	2233:03	4
53	2233:58	2234:04	6
54	2235:04	2235:08	4
55	2236:06	2236:09	3
56	2237:04	2237:09	5
57	2238:00	2238:06	6
58	2238:59	2239:08	9
59	2240:05	2240:11	6
60	2241:07	2241:12	5
61	2242:05	2242:13	8
62	2243:03	2243:10	7
63	2244:02	2244:12	10
64	2245:08	2245:15	7

B. *Synoptic Situation*

By late in the morning a line of echoes had developed along the Rocky Mountain foothills to the west. Most of this activity dissipated after tracking off the mountains. By early afternoon (1849 UTC), a few weak storms were detected 40 km northwest of FL–2. Nearly one hour later, a line of cells formed southeast of FL–2. This line developed into a gust front and tracked northwestward toward Stapleton. At about the same time the stronger outflow and gust front from the storms to the northwest and west reached the Stapleton area. In the wake of the gust front passage, a stratiform rainfall persisted into the evening hours.

At 2100 UTC, one half hour before dual Doppler scanning began, surface temperatures were in the 80's and 90's (°F). However, overall dewpoints were only in the 40's (°F), signifying the presence of a dry air mass. Showers were present in the region northwest of the airport. At the start of dual Doppler coverage, the long range reflectivity map from FL–2 at 2200 UTC exhibited a broad area of 20–30 dBZ echoes over north–central and central Colorado (Fig. V–1). This region had remained about the same size for the last 30 minutes. Thundershowers with reflectivity up to 35 dBZ can be seen south and northeast of Denver (east of the high reflectivity returns from the mountains, but west of the FL–2 radar). The cloud tops of these storms were measured by the National Weather Service radar to be 35,000 ft. The main precipitation area was moving east at 2.5 m/s while individual cells were pushing northeastward at 7.5 m/s.

Figure V–2 shows the strong upper level winds observed over the state of Colorado. This figure represents the upper level wind flow 14 hours after the time period of interest, but conditions at 500 mb were not changing rapidly. This figure shows southwesterly winds at speeds of 20 m/s ($\sim$ 40 knots) over Colorado between a high pressure cell to the east and a developing low pressure cell to the west. The northeastward storm cell motion was apparently influenced by these 500 mb winds.

The visible satellite image (Fig. V–3) taken at the same time as the long range reflectivity map (2200 UTC) confirms the presence of denser clouds located over central Colorado. In addition, the middle and upper level clouds over the southwest U.S. appear to be spreading out towards the northeast. This feature is consistent with the strong upper level flow over Colorado shown in Fig. V–2. The sequence of satellite images from 2130 to 2230 shows tall individual cells south and northeast of Denver that were growing vertically and moving slightly eastward during this time period.

C. *Wind Shear Events*

i. Wind Shear Summary

The gust front that moved across the airport (from the northwest) was the predominant wind shear detected between 2138 and 2245 UTC. At the beginning of

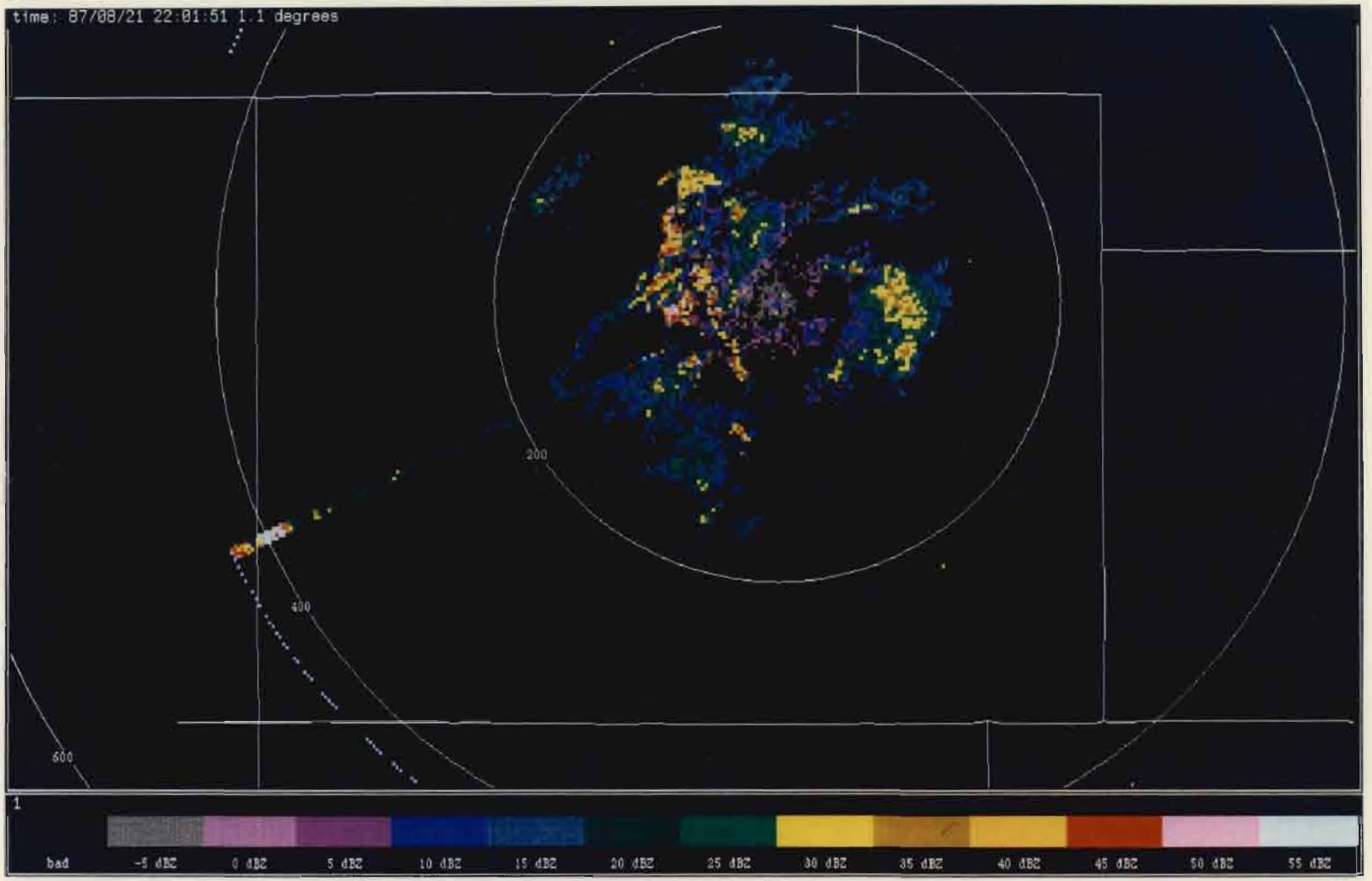

Figure V–1. Long range reflectivity map from FL–2 at 2201 UTC on 21 August 1987. The stronger signals (light blue, pink, and red) detected 40 to 70 km west of FL–2 in a line running from NW to SE are not from weather; they are returns from the Rocky Mountains. The state borders are shown in white. The radial data extending out beyond the 400 km range ring (in southwestern Colorado) is erroneous.

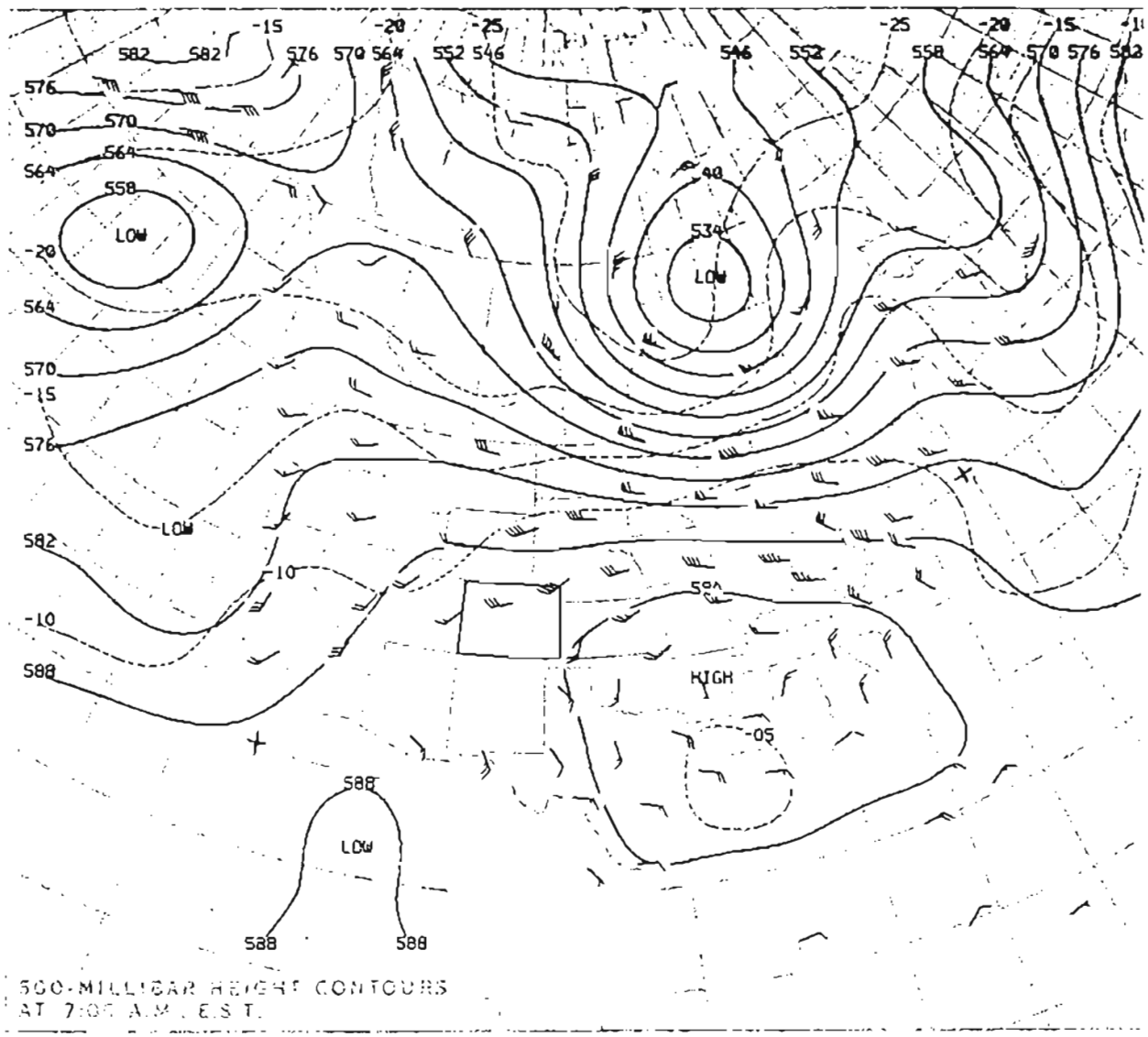

Figure V-2. 500 mb heights/winds representing 1200 UTC observations on 22 August 1987. Map represents upper level winds 14 hours after the gust front had moved through Stapleton. A full barb is 10 knots, a half barb is 5 knots, and a blackened triangle denotes 50 knots. Solid contours are geopotential heights of the 500 mb pressure level in decameters; dotted contours are isotherms in degrees Centigrade.

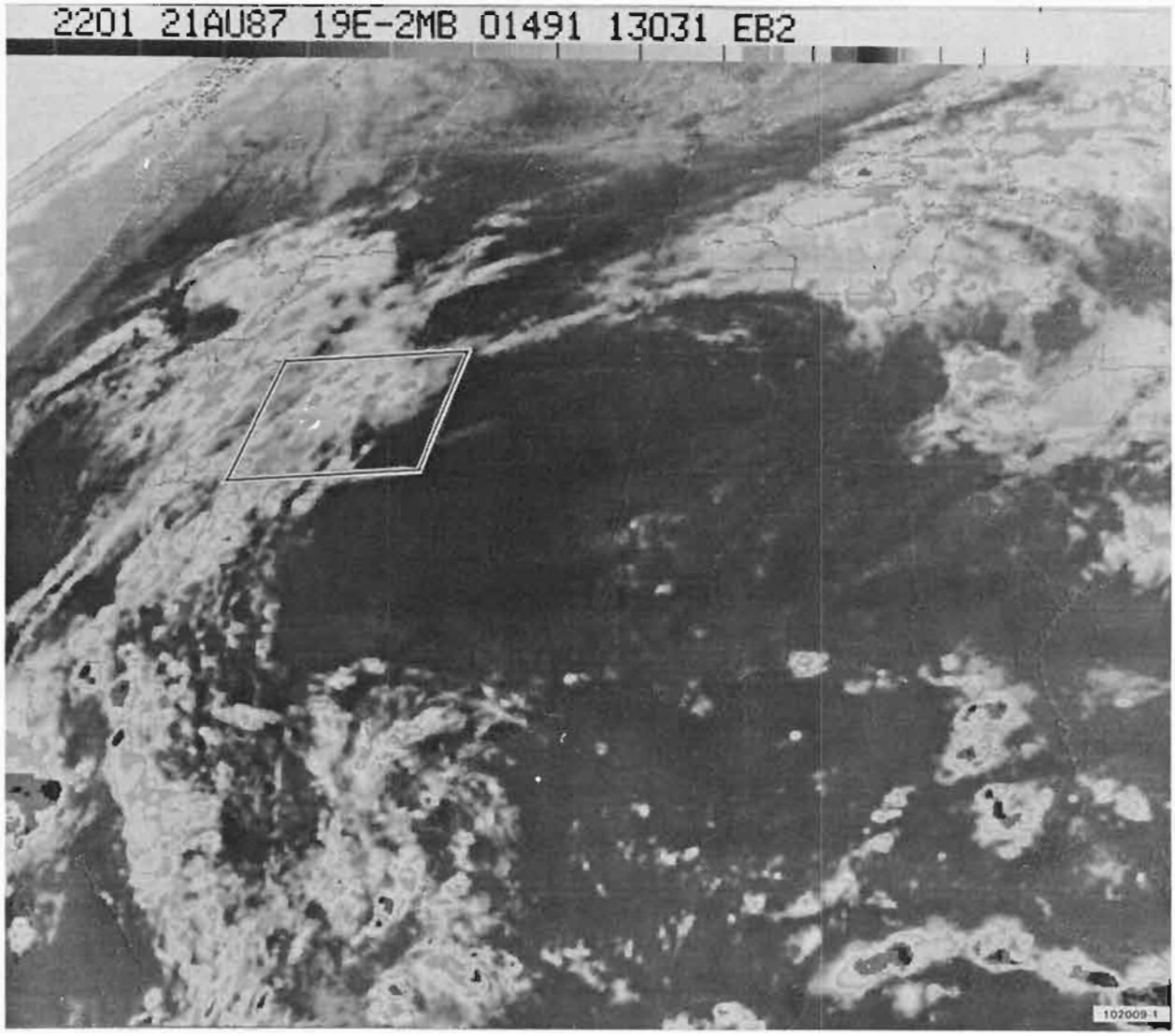

Figure V-3. Infrared satellite image of the central U.S. taken at 2201 UTC on 21 August 1987. The brighter areas denote the colder areas, or equivalently, the higher cloud tops. The cloud temperature scale which wraps around, is shown at the top of the image but below the time and date. Each tick mark denotes a 10 degree interval. The tick mark in the black region (right-hand side) represents -60 degrees Centigrade; to the left of this point are warmer temperatures (lower clouds) and to the right are colder temperatures (higher clouds).

the period, nearly all mesonet and LLWAS sensors were reporting an ESE wind with an average wind speed of 10 m/s; only a couple of stations north of the runways were reporting winds from the NNE at 5 m/s. As the first gust front (moving from SE to NW) crossed the airport at 2147 UTC, LLWAS alarms were triggered. Simultaneously, a second gust front moving southeastward was located a small distance northwest from Stapleton. Both gust fronts collided just west of the airport and the resultant flow movement continued toward the southeast. The change in velocity, 5 km northwest of the runways, was estimated to be 17 m/s at 2158 UTC. At this same time, surface reflectivity was beginning to increase 10–15 km southwest of Stapleton. Weak convection was initiated with at least one divergent outflow observed in the FL-2 data at range 27 km, azimuth 268°. The FL-2 and UND radars were operating in a dual Doppler mode throughout this gust front event (2138–2245 UTC). Figure V-4 shows the progression of these gust fronts based on dual Doppler data.

ii. Wind Shear Examples

By 2204 UTC, the gust front previously to the west of the mesonet area had entered the network area, and was influencing the winds at station Nos. 1, 2, 5, and 13 (Fig. V-5). The depicted mesonet winds represent the peak wind speed and the average wind direction in the minute from 2204:05 to 2205:05 UTC. The dual Doppler wind vectors and streamlines for the 2204:47 analysis time are shown in Fig. V-6 for comparison. The position of the gust front based on the mesonet data agrees fairly well with that indicated by the dual Doppler analysis (the streamline analysis in Fig. V-6b is useful in locating the gust front). There are small differences however; the dual Doppler analysis shows the gust front impacting station No. 9 while the mesonet map shows the gust front still to the west of this station. Curvature in the lowest 100 m of the leading edge or "nose" of a gust front could account for the difference between the radar and mesonet data (Fig. V-7). A small divergent outflow or weak microburst can also be seen at this time northwest of station No. 13 in Fig. V-6a. This event did not impact the mesonet.

The second gust front had overtaken the first by 2211 UTC. At this time, the leading edge of this now dominant gust front had moved over the center of the north/south runways. A difference between the mesonet and LLWAS wind field (Fig. V-8) and the dual Doppler wind field (Fig. V-9a) at this time is apparent at station No. 2. In Fig. V-8 this station reporting a peak wind speed of 5 m/s with an average wind direction from the SW. In Figure V-9a, a moderate uniform wind flow from the NW is present at station No. 2 and at all surrounding stations. Several minutes later, the mesonet plots continue to show a SW wind flow impacting station No. 2. This discrepancy may be real; the small lobe of reflectivity over station 5 (Fig. V-9) might indicate that virga or light rain was falling in the area. If so, this could have produced a weak outflow at the surface which was too shallow for the radar to

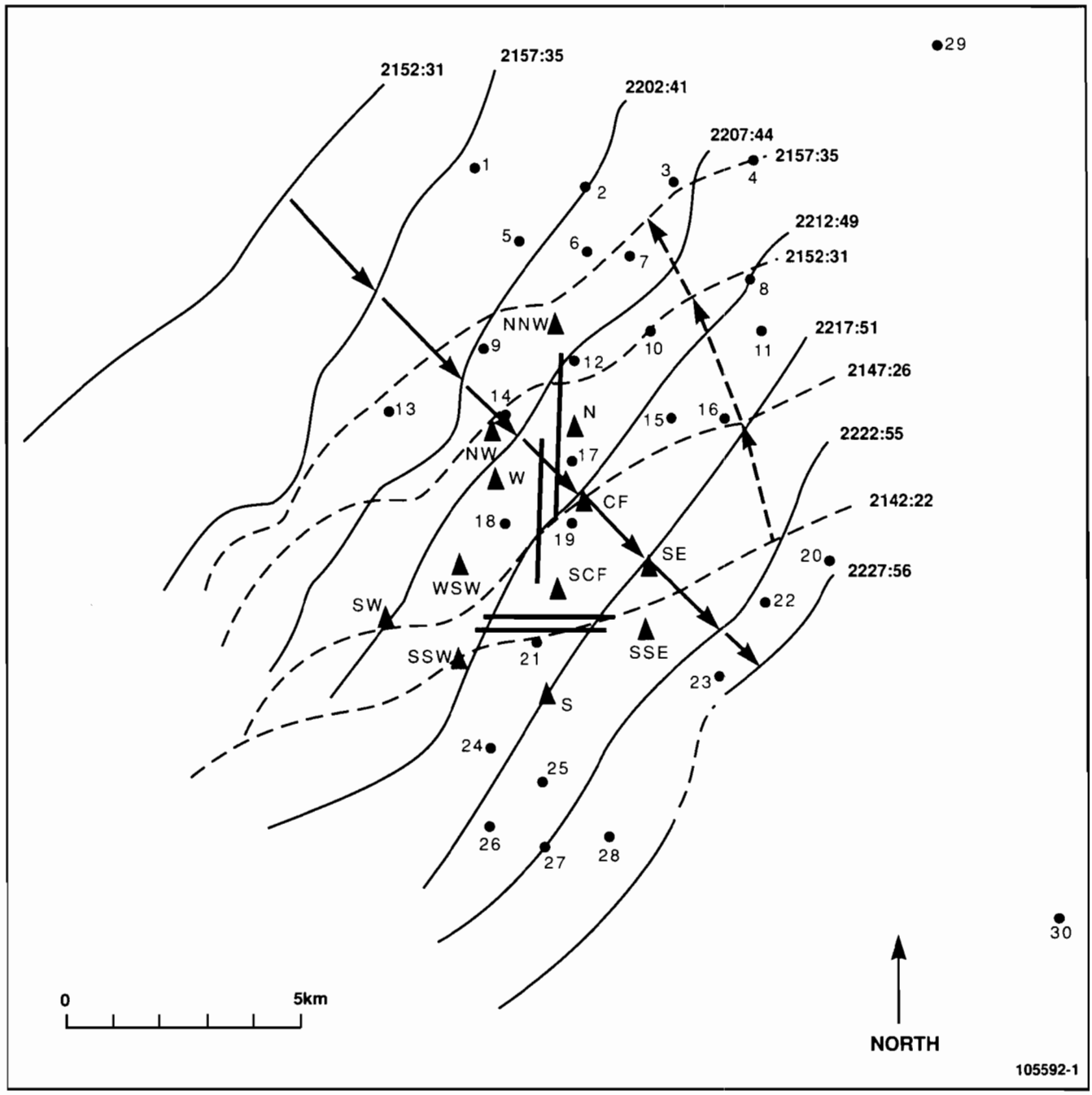

Figure V–4. Map illustrating the progression of two gust fronts during the 2138 to 2245 UTC time period for 21 August 1987. Map is based on dual Doppler data. Solid lines show the progression of the gust front moving from the northwest toward the southeast, and dashed lines show the progression of the weaker gust front moving from the southeast toward the northwest. Lines are drawn at roughly 5 min. intervals.

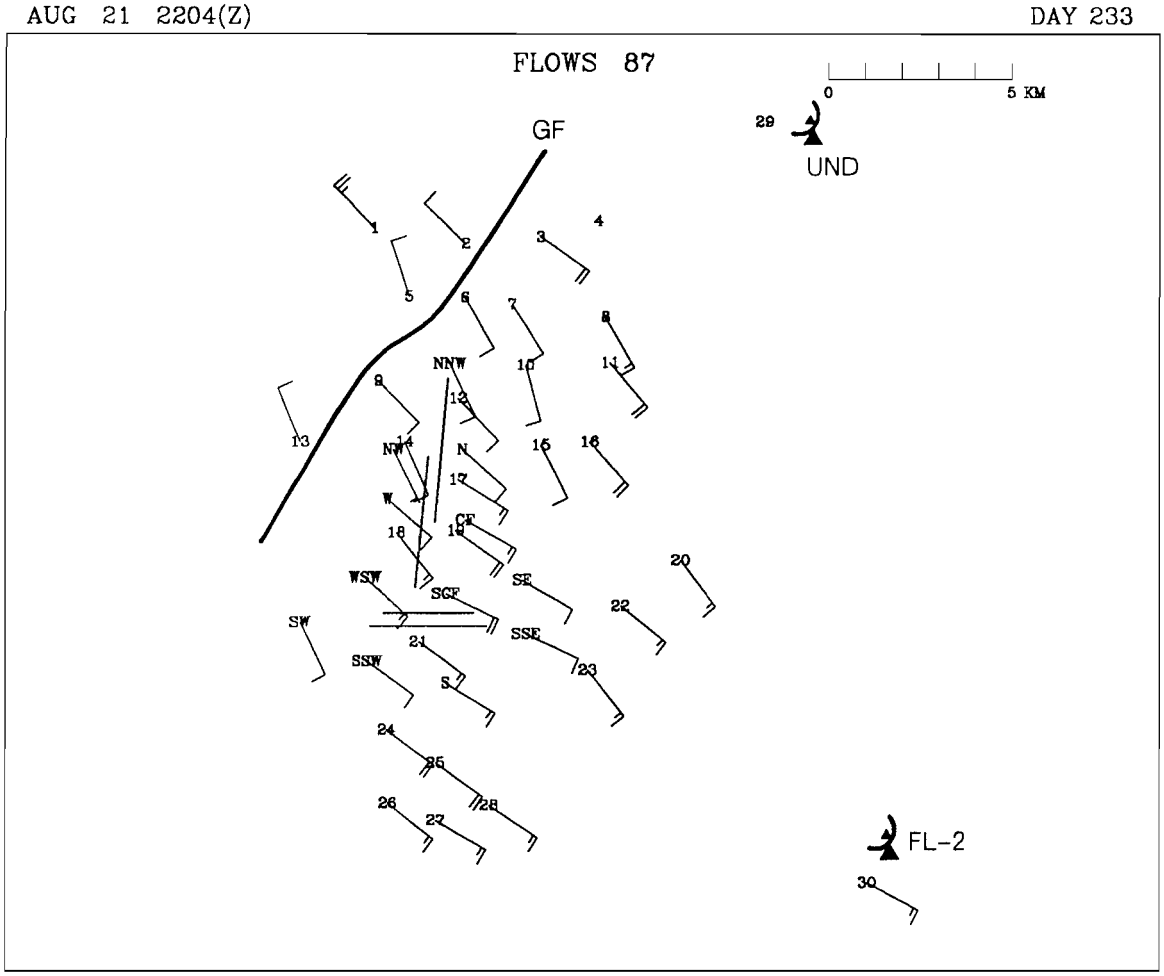

Figure V-5. Mesonet/LLWAS winds at 2204 UTC on 21 August 1987. Gust front (GF) is located in the northwest quadrant of the network. A full barb on the wind direction arrow represents 5 m/s and a half barb represents 2.5 m/s.

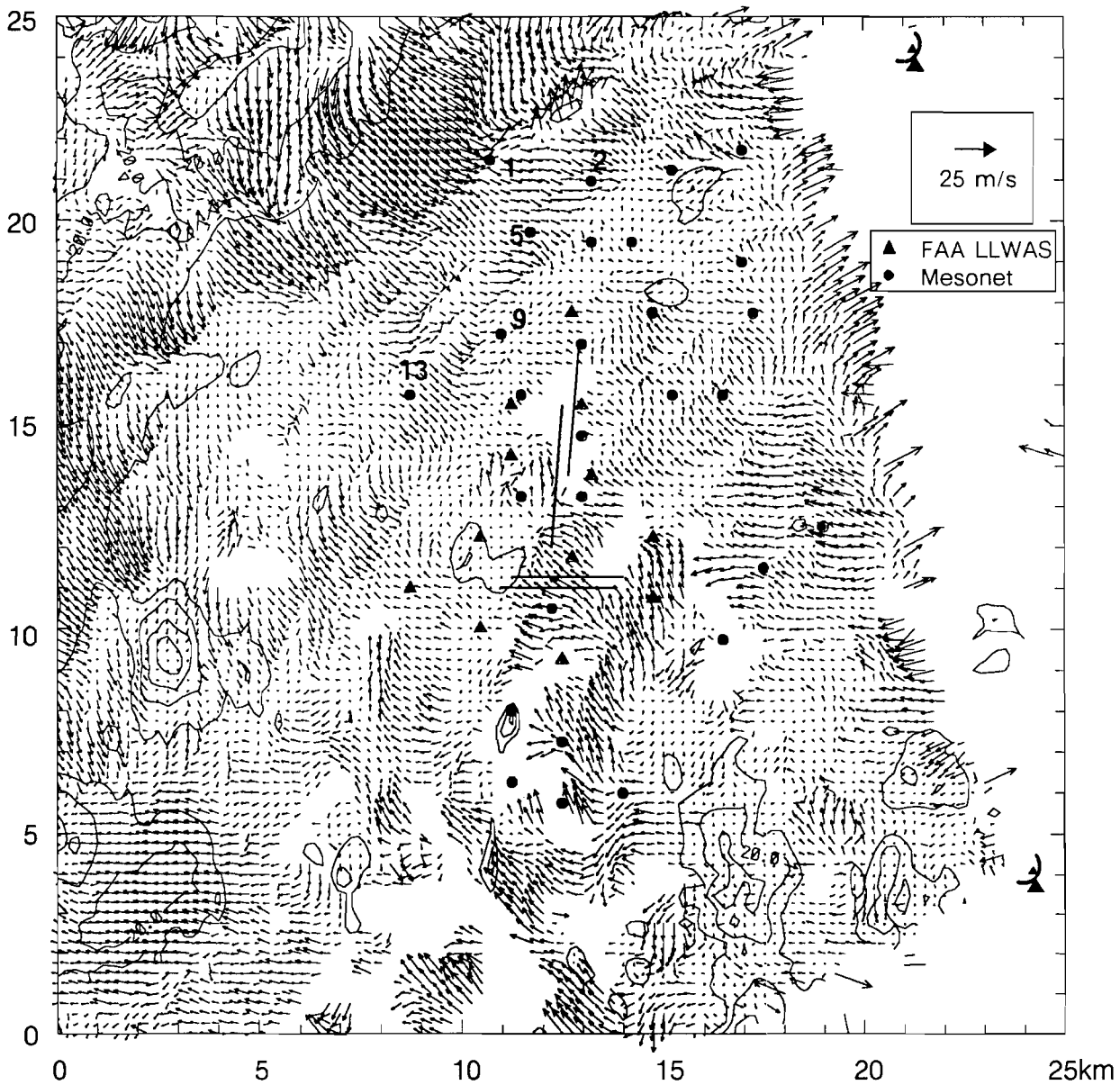

Figure V-6a. Dual Doppler plot of the wind and reflectivity field at 2204:47 UTC on 21 August 1987. Radar coverage encompasses entire mesonet/LLWAS network. The large wind vectors at the edge of the radar coverage are erroneous, and should be ignored. Dots denote the FLOWS mesonet stations and triangles denote the LLWAS stations. The overlaid runways are an approximation to the actual length and placement within the network. Each contour level represents 10 dBZ. The 40 dBZ region, located 10 km west-southwest of the runways, is not from weather; they are the returns from the Denver metropolitan area.

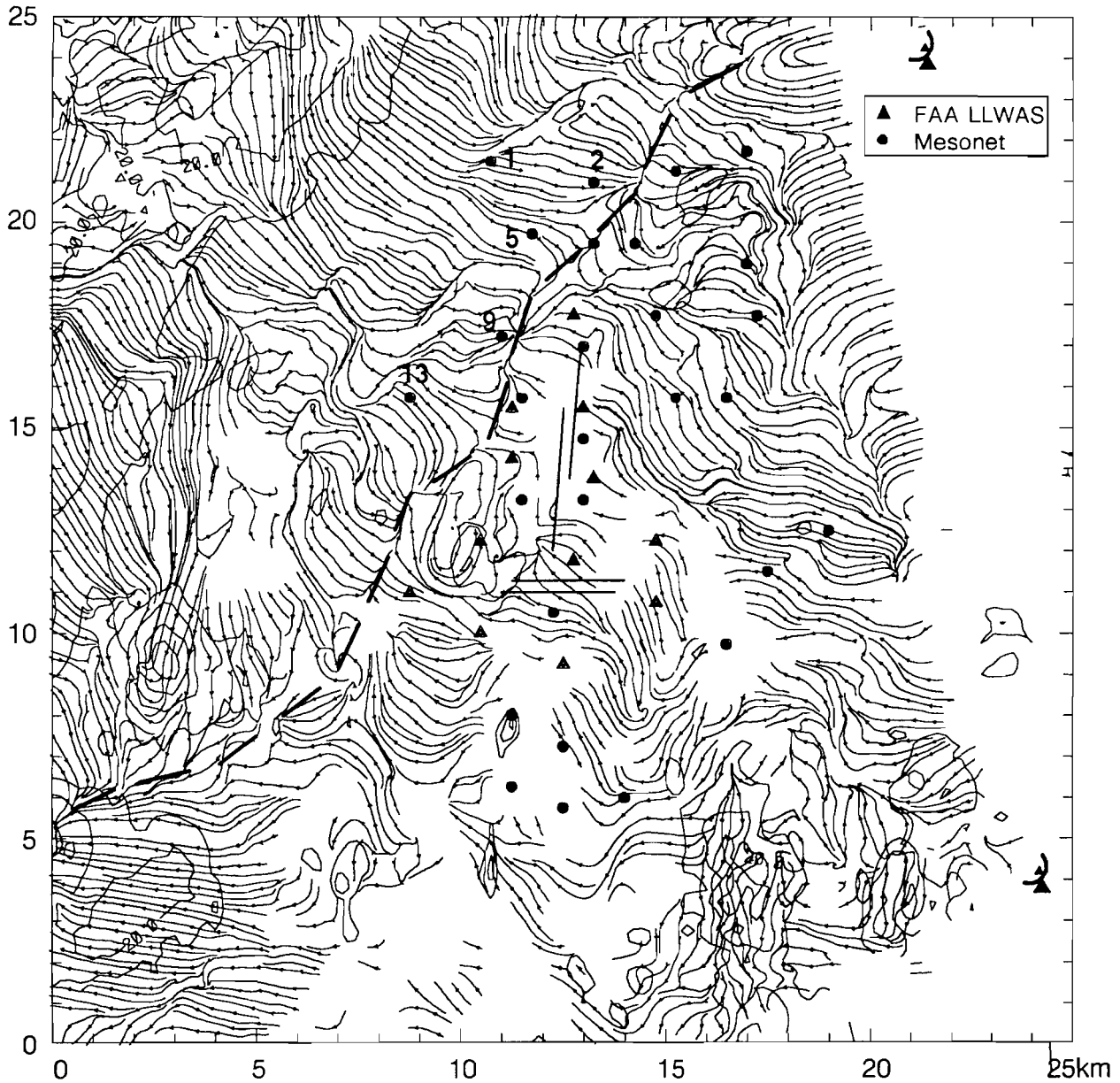

Figure V-6b. Dual Doppler plot of the streamline and reflectivity field at 2204:47 UTC on 21 August 1987. The dashed outline shows the leading edge of the gust front entering the network.

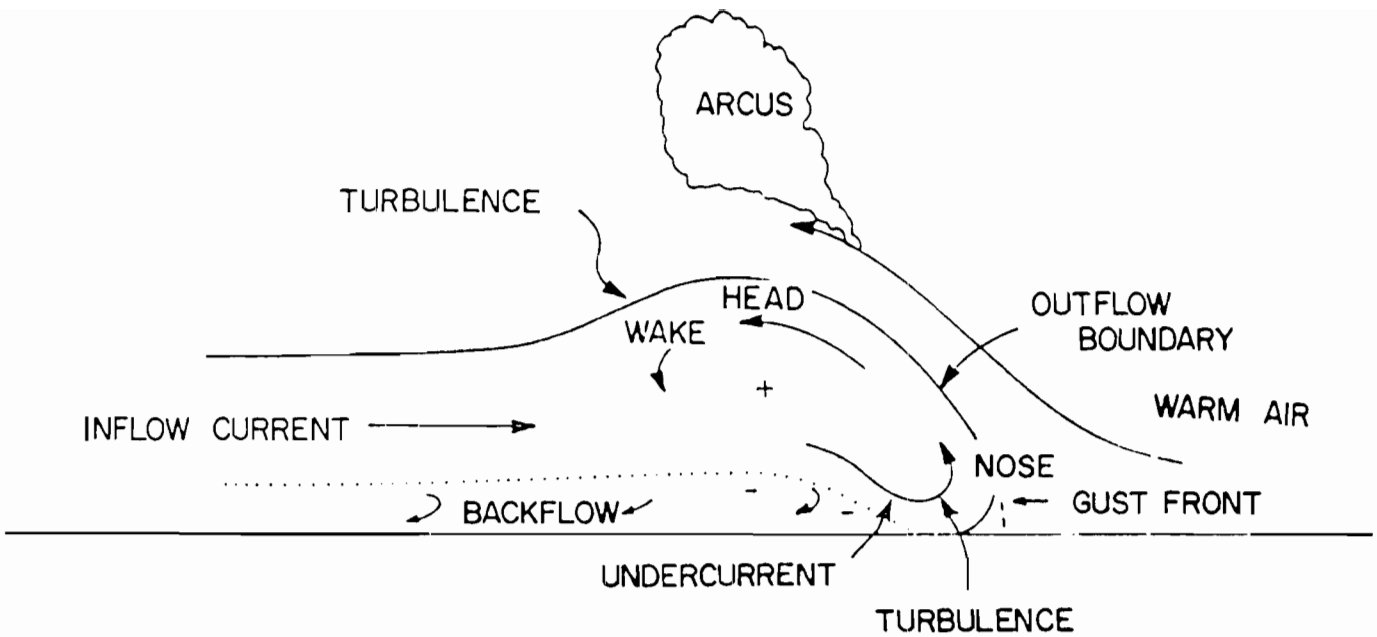

Figure V–7. A schematic diagram of the vertical cross section of a thunderstorm outflow. Structures within the outflow are identified; such as the head, nose, and gust front. (Adapted from Goff, 1976).

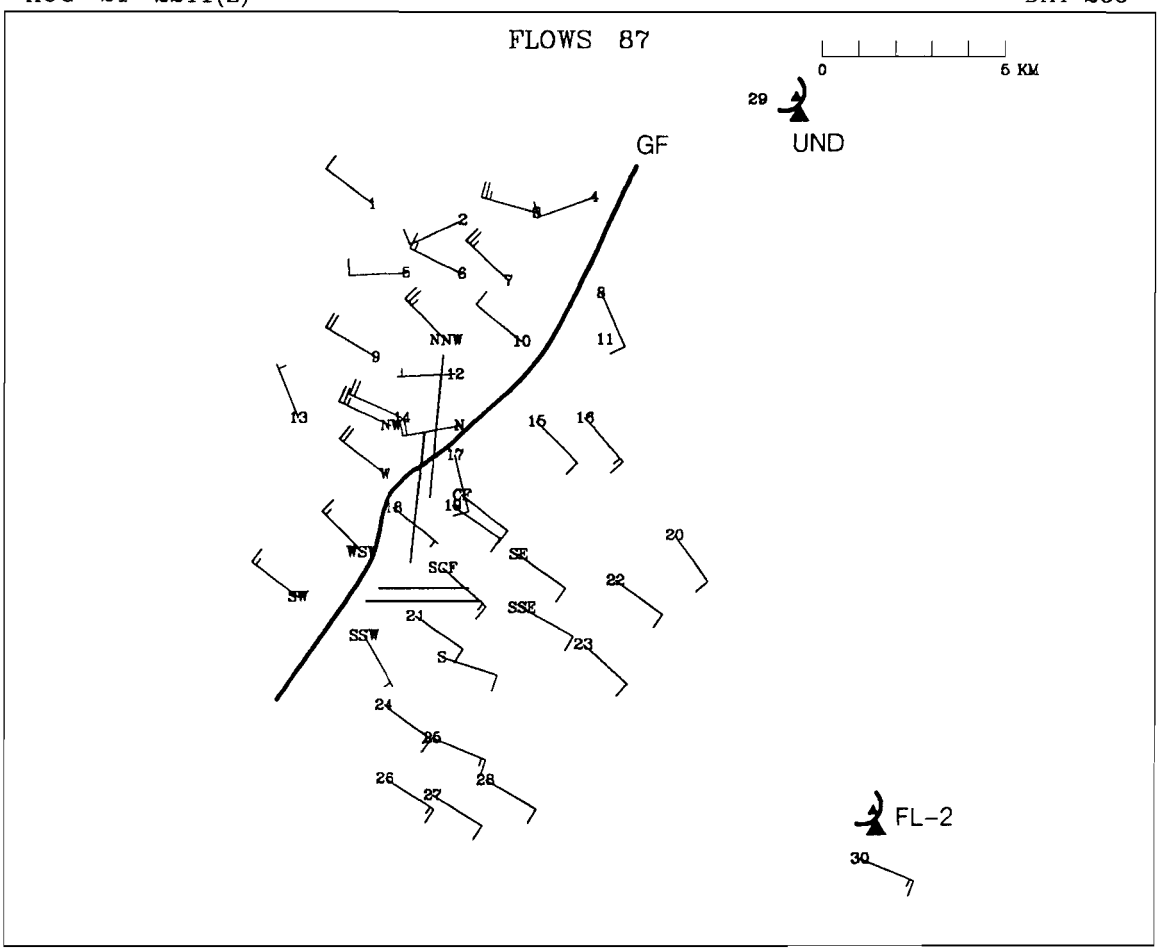

Figure V–8. Mesonet/LLWAS winds at 2211 UTC on 21 August 1987. Gust front (GF) is now centered over the network. A wind shift from the southeast to the northwest at moderate speeds delineates the leading edge of the gust front boundary.

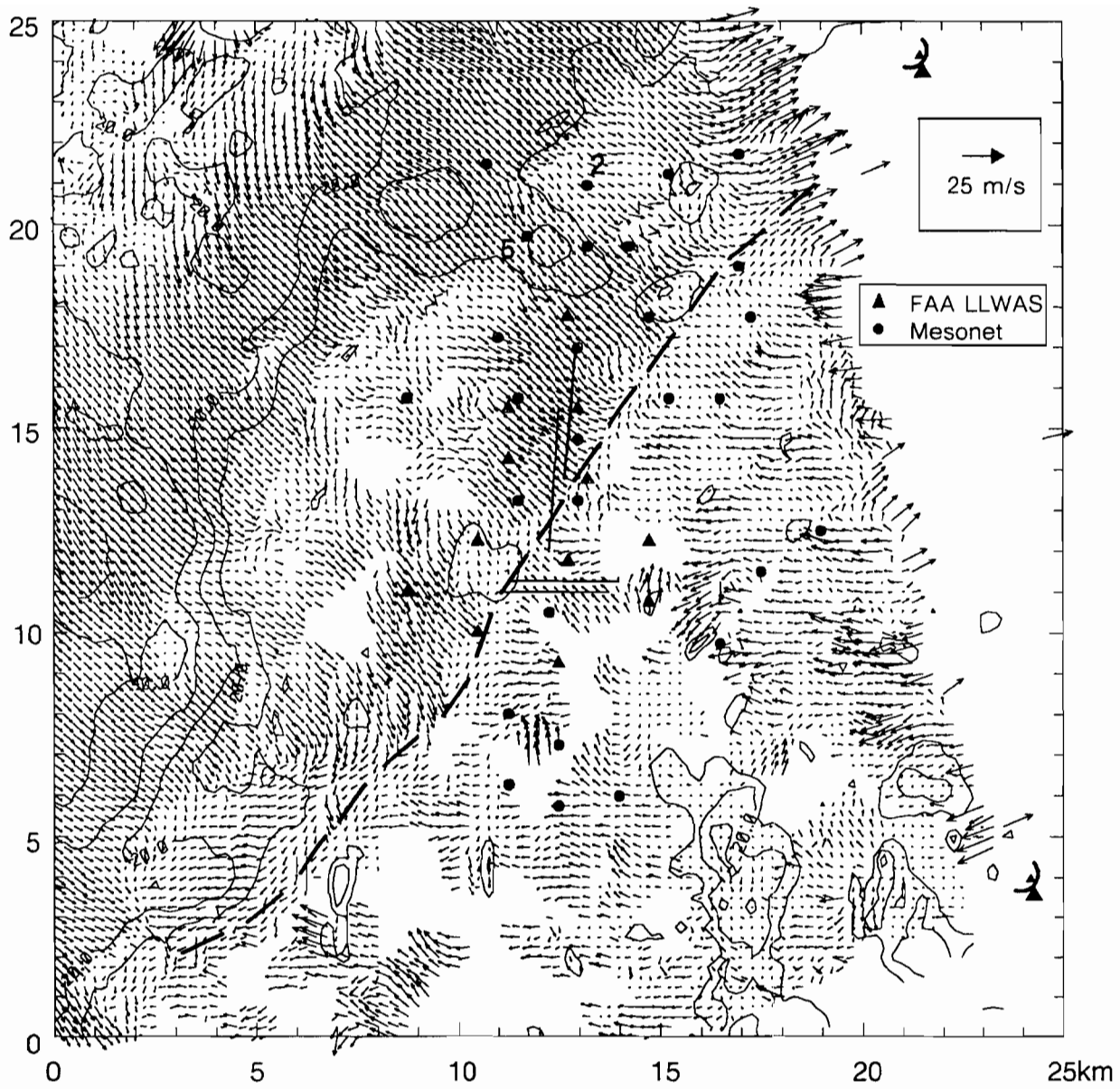

Figure V-9a. Dual Doppler plot of the wind and reflectivity field at 2211:51 UTC on 21 August 1987. The dashed outline shows the leading edge of the gust front.

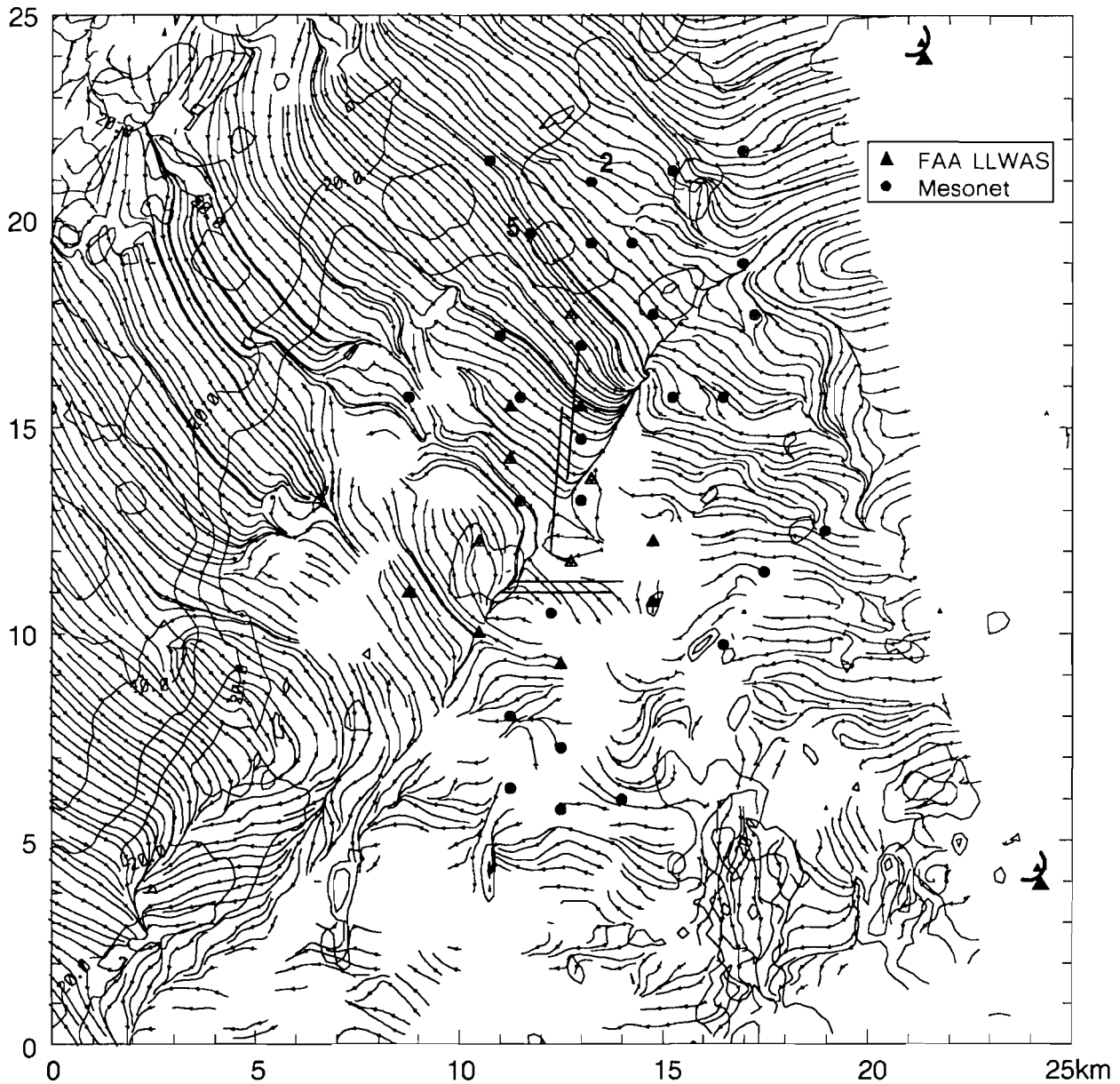

Figure V–9b. Dual Doppler plot of the streamline and reflectivity field at 2211:51 UTC on 21 August 1987. Gust front is clearly shown passing over the center of the runways.

detect. Otherwise, the mesonet/LLWAS and dual Doppler winds agree well. The streamline analysis in Fig. V-9b clearly shows the position of the gust front.

The gust front continued to progress southeastward, and had crossed the airport by 2219 UTC. Winds from the northwest were peaking at 15 m/s (Fig. V-10). Figure V-11 shows the leading edge of the outflow air at the east edge of the airport. Another push of outflow air near the east edge of the reflectivity region (west of the airport) can also be seen. This line of echoes, 6 km west of the mesonet at 2211, had moved 3-5 km eastward by this time. The layered single Doppler FL-2 data at 2219:56, (Fig. V-12) show these echoes very clearly*. A thin reflectivity line (0-10 dBZ) associated with the gust front is clearly revealed in the southeastern portion of the network. By 2245 (not shown), the northwest flow had subsided considerably and some light reflectivity echoes (10-20 dBZ) had begun to reach the western edge of the mesonet.

* The small reflectivity region with values up to 50 dBZ between 20 and 25 km range (reflectivity plot in Fig. V-12) is associated with a region of 0 m/s Doppler velocity (velocity plot in Fig. V-12). This region is not weather; it is the ground clutter return from the tall buildings in downtown Denver.

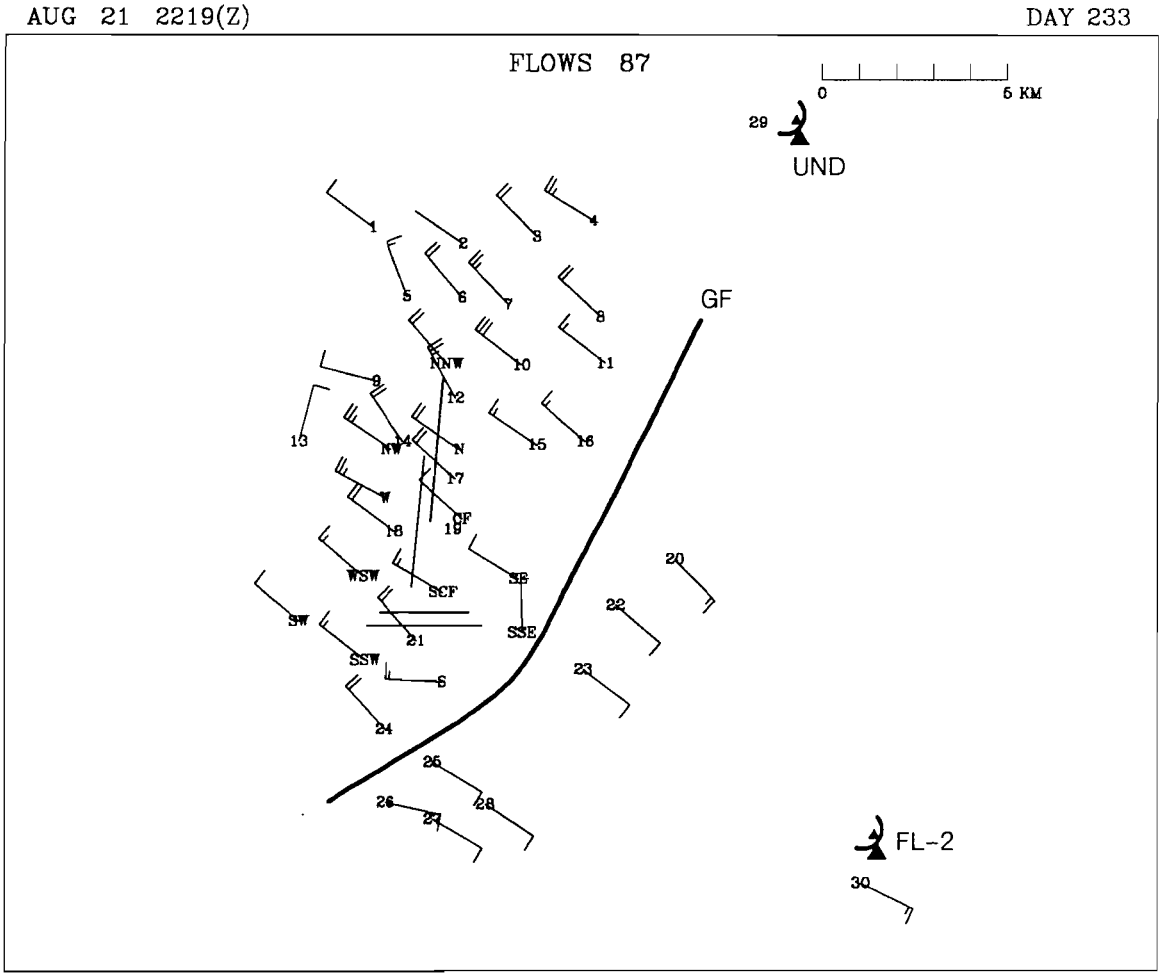

Figure V-10. Mesonet/LLWAS winds at 2219 UTC on 21 August 1987. Gust front (GF) is now moving through the eastern portion of the network.

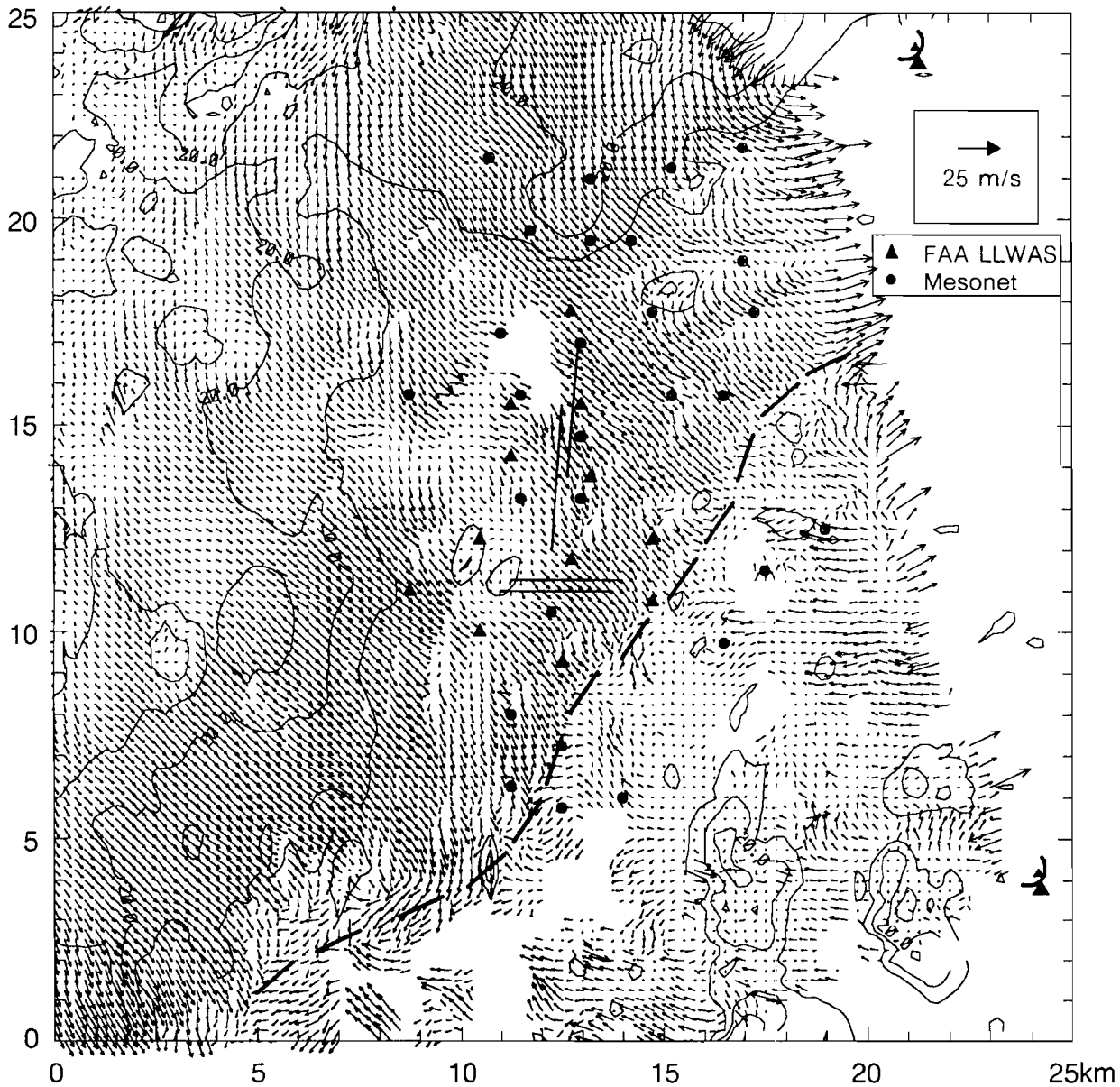

Figure V-11a. Dual Doppler plot of the wind and reflectivity field at 2219:56 UTC on 21 August 1987. Gust frontal winds are overspreading much of the network. The dashed outline represents the leading edge of the gust front.

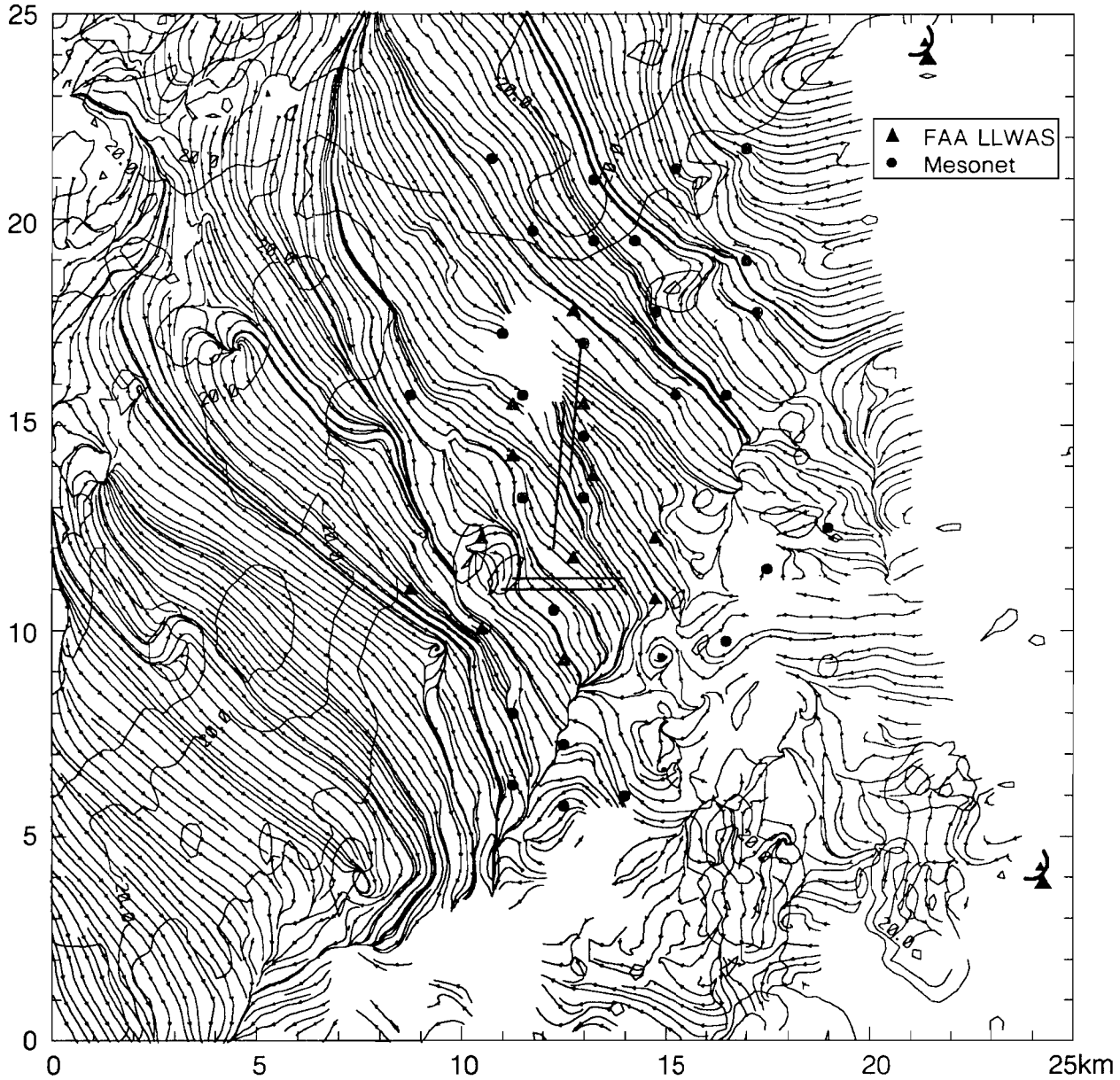

Figure V-11b. Dual Doppler plot of the streamline and reflectivity field at 2219:56 UTC on 21 August 1987.

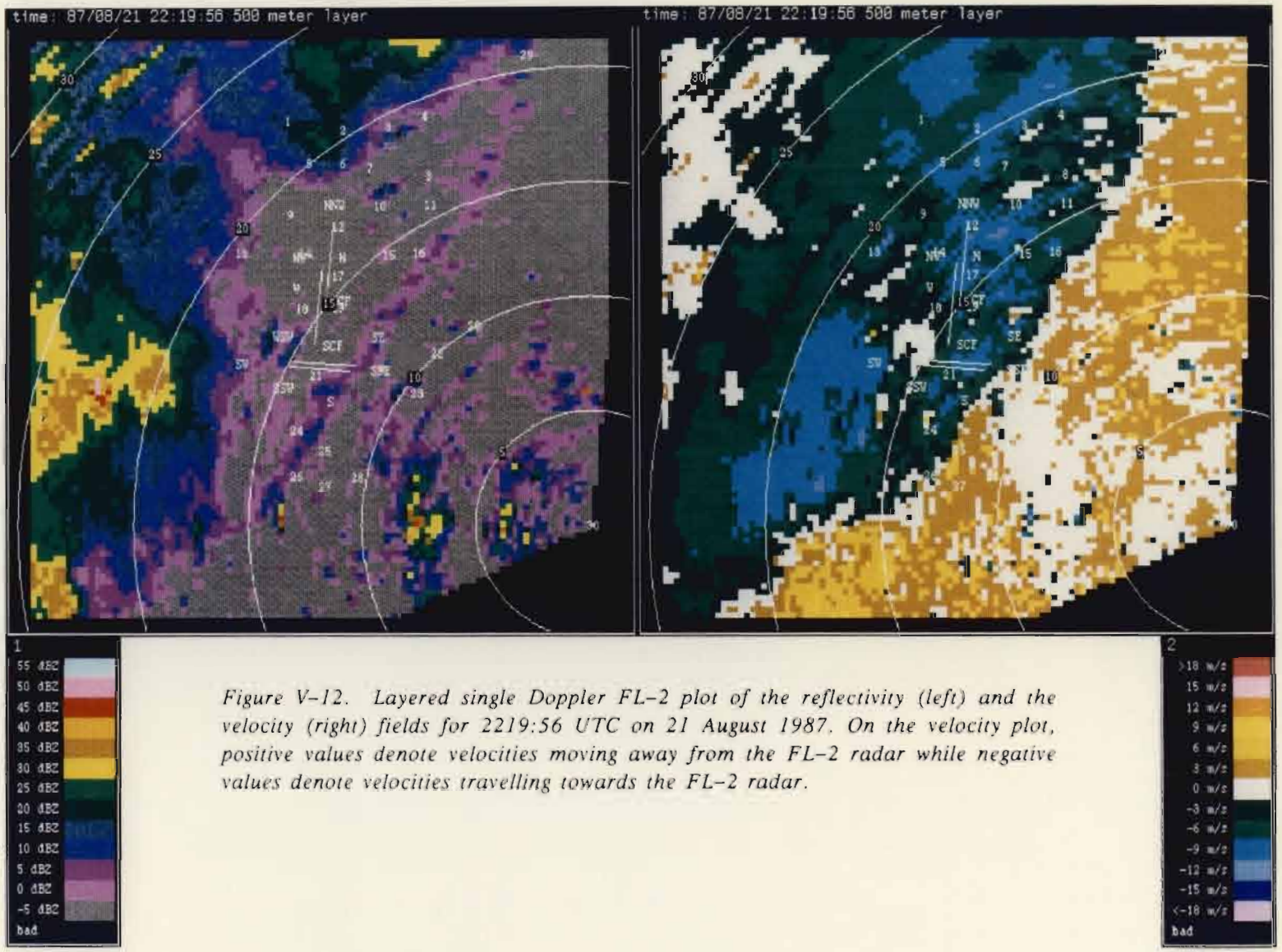

Figure V–12. Layered single Doppler FL–2 plot of the reflectivity (left) and the velocity (right) fields for 2219:56 UTC on 21 August 1987. On the velocity plot, positive values denote velocities moving away from the FL–2 radar while negative values denote velocities travelling towards the FL–2 radar.

VI. 26 AUGUST 1987

A microburst/divergent line (MB/div line) moving across Stapleton airport from the northwest was the predominant wind shear event for the day. This MB/div line, which was preceded by a strong gust front, had weakened by the time it moved across the airport.

A. Available Data

Mesonet, LLWAS, and FL-2 single Doppler data were provided for the period 0000 to 0055 UTC. It was possible to perform dual Doppler analyses for this same time period, at one minute intervals. The FL-2 and UND radar scan times, and the difference between these scan times, for each dual Doppler analysis are given below in Table VI-1.

Table VI-1. FL-2 and UND scan times used for 26 August 1987 dual Doppler analyses.

Dual Doppler Pair	FL-2 time (UTC)	UND time (UTC)	Time diff. (sec)
1	0000:53	0000:56	3
2	0001:51	0001:57	6
3	0002:50	0002:54	4
4	0003:48	0003:57	9
5	0004:54	0005:00	6
6	0005:56	0006:01	5
7	0006:54	0007:02	8
8	0007:54	0008:00	6
9	0008:52	0009:02	10
10	0009:58	0010:05	7
11	0011:00	0011:06	6
12	0011:59	0012:08	9
13	0012:58	0013:05	7
14	0013:56	0014:07	11
15	0015:02	0015:11	9
16	0016:05	0016:12	7
17	0017:03	0017:13	10
18	0018:02	0018:10	8
19	0019:01	0019:12	11
20	0020:06	0020:16	10
21	0021:09	0021:16	7
22	0022:07	0022:17	10
23	0023:07	0023:14	7
24	0024:05	0024:17	12

25	0025:11	0025:20	9
26	0026:14	0026:21	7
27	0027:12	0027:22	10
28	0028:12	0028:19	7
29	0029:10	0029:22	12
30	0030:16	0030:25	9
31	0031:18	0031:26	8
32	0032:16	0032:27	11
33	0033:16	0033:25	9
34	0034:14	0034:27	13
35	0035:20	0035:30	10
36	0036:22	0036:31	9
37	0037:21	0037:32	11
38	0038:20	0038:29	9
39	0039:18	0039:32	14
40	0040:24	0040:35	11
41	0041:27	0041:35	8
42	0042:26	0042:36	10
43	0043:26	0043:34	8
44	0044:24	0044:36	12
45	0045:31	0045:39	8
46	0046:33	0046:40	7
47	0047:32	0047:41	9
48	0048:33	0048:39	6
49	0049:30	0049:41	11
50	0050:36	0050:45	9
51	0051:40	0051:46	6
52	0052:38	0052:47	9
53	0053:38	0053:44	6
54	0054:36	0054:47	11
55	0055:41	0055:50	9

B. Synoptic Situation

At noon (1800 UTC), a line of moderate intensity echoes had developed over the mountains. The anvil from these storms covered the plains and produced only weak surface shear. The strongest of these cells moved to the south of FL-2 at a distance of 50 km. By late afternoon (2334 UTC), a line of echoes formed west of Stapleton. Convergence was noted at mid-levels in these cells. Two outflows (microburst and macroburst) were scanned in a dual Doppler mode, beginning at 0000 UTC.

At 0000 UTC, most weather observation sites in western Colorado were reporting cloudy skies with northwest winds at 10 m/s. However, surface winds in eastern and southeastern CO were southwesterly at 10 m/s. Surface temperatures throughout the state were in the 50's and low 60's (°F). In addition, showers and thundershowers were present in the region west of the airport. The long range reflectivity map from FL-2 at 0032 UTC (half-way through the dual Doppler scanning period) exhibited a large region of 35-45 dBZ echoes approximately 42 km to the north-northeast of the FL-2 radar (Fig. VI-1). The cloud tops of these strong cells were measured by the National Weather Service radar to be 33,000 ft. with cell movement towards the southeast at 10 m/s. Another smaller region of cells with reflectivity up to 40 dBZ can be seen approximately 12 km to the northwest of FL-2. These cells are associated with the gust front that has just exited, and the microburst line that is just entering Stapleton airport.

Figure VI-2 shows the upper level winds observed over Colorado at 1200 UTC on 26 August. On that date, a deep trough was present in most levels of the atmosphere over the eastern part of the state. This trough was the result of a deepening low pressure cell over northern Montana. The upper level winds from the southwest (13 m/s or 25 knots), in advance of a surface frontal system from the west, acted as a catalyst for the wind shear events which occurred at the beginning of the day.

The visible satellite image (Fig. VI-3) taken at 2331 UTC on 25 August, one half hour before dual Doppler scanning, shows the higher cloud tops from Mexico to Wyoming streaming northeastward as a result of the upper level wind direction. Another noticeable feature in this figure is the large billowing cumulonimbus clouds stretching north-northeastward from Texas to Nebraska. This convective activity was associated with a strong cold front at the surface. An infrared satellite image taken one hour later (Fig. VI-4; 0031 UTC on 26 August 1987), illustrates cloud conditions just prior to the MB/div line impacting the mesonet/LLWAS sensors. This figure displays a band of colder and consequently taller cloud tops a short distance northwest of Denver. These cells appear to be the thundershowers which impacted Denver at 0100 UTC.

C. Wind Shear Events

i. Wind Shear Summary

During the time period of interest (0000 to 0055 UTC), a gust front moved east-southeastward ahead of a developing microburst line. At the beginning of this period (0000 UTC), uniform winds were blowing from the southeast with an average speed of 5 to 10 m/s over the entire mesonet. By 0010, a couple of microbursts formed close together creating a divergent outflow line pattern 15 km northwest of Stapleton airport. This MB/div line moved southeastward and was preceded by a gust front (the leading edge of the outflow from the MB/div line). The gust front was centered over the airport at 0020 UTC. As the gust front exited Stapleton airport,

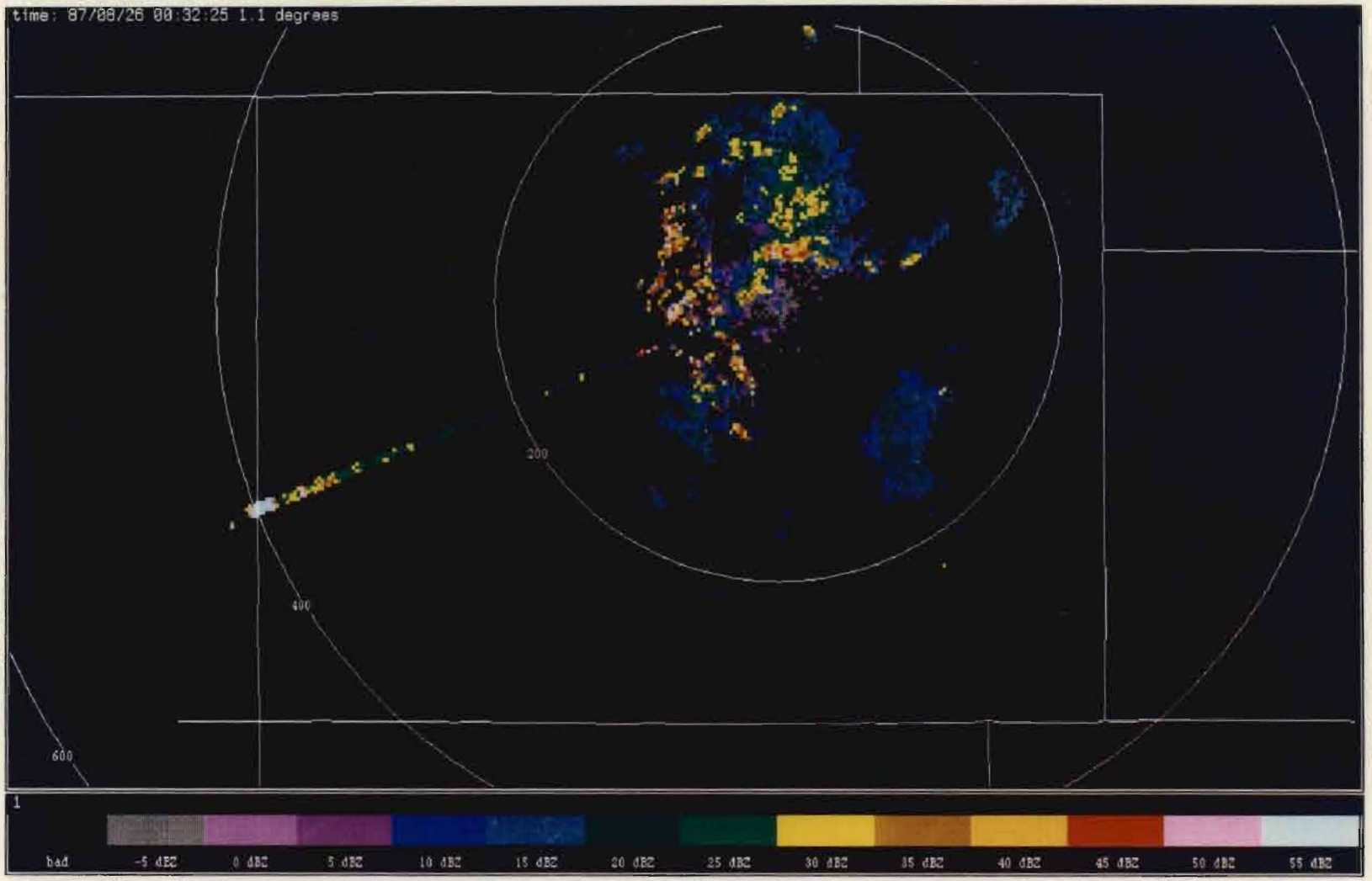

Figure VI-1. Long range reflectivity map from FL-2 at 0032:25 UTC on 26 August 1987. Weak echo returns are found over the mesonet/LLWAS network while stronger echoes (20-40 dBZ) are detected northeast of FL-2. The radial of data extending out beyond the 400 km range ring (in southwestern Colorado) is erroneous.

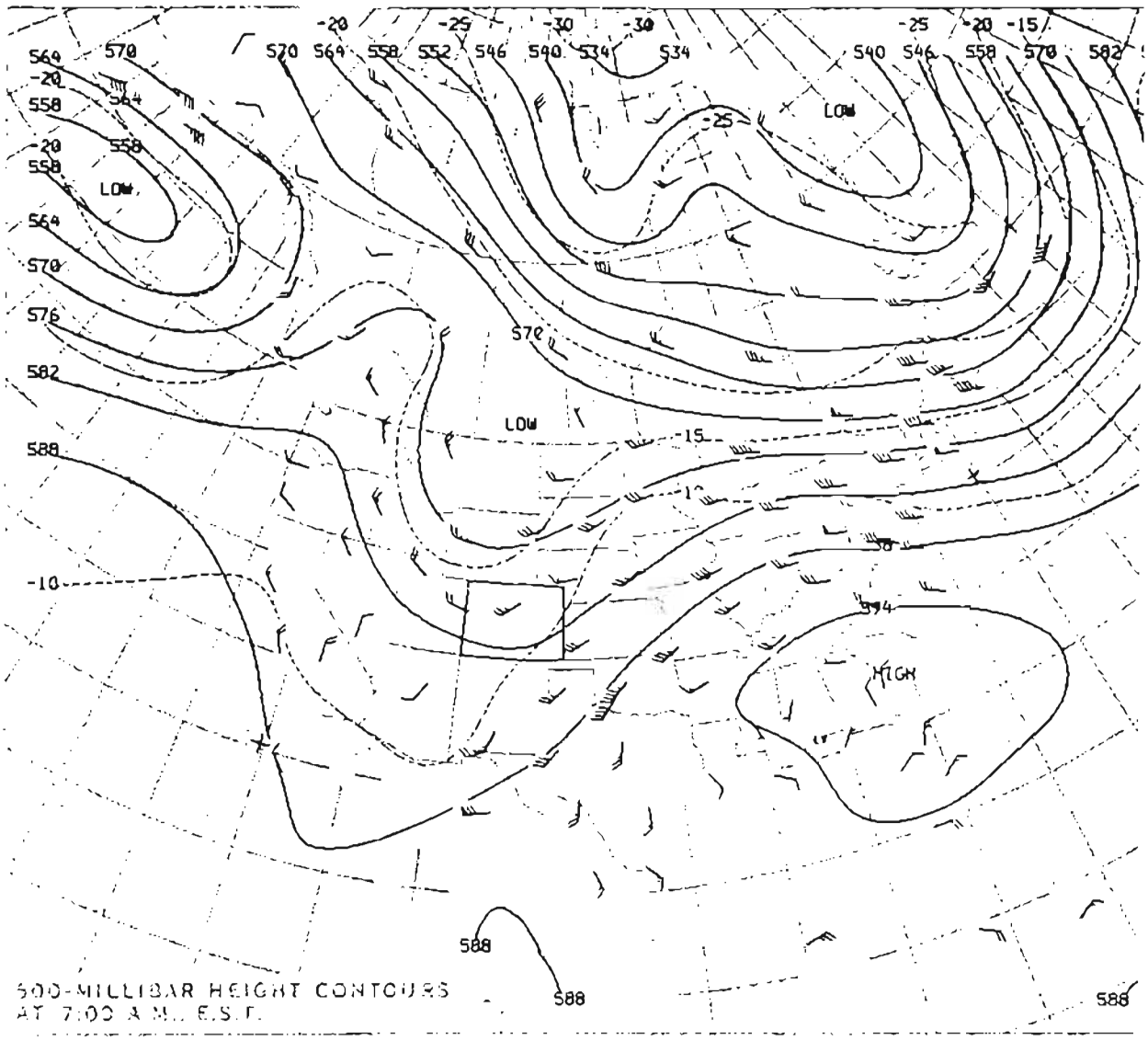

Figure VI–2. 500 mb heights/winds representing 1200 UTC observations on 26 August 1987. Map represents upper level conditions 12 hours after the start of dual Doppler scanning.

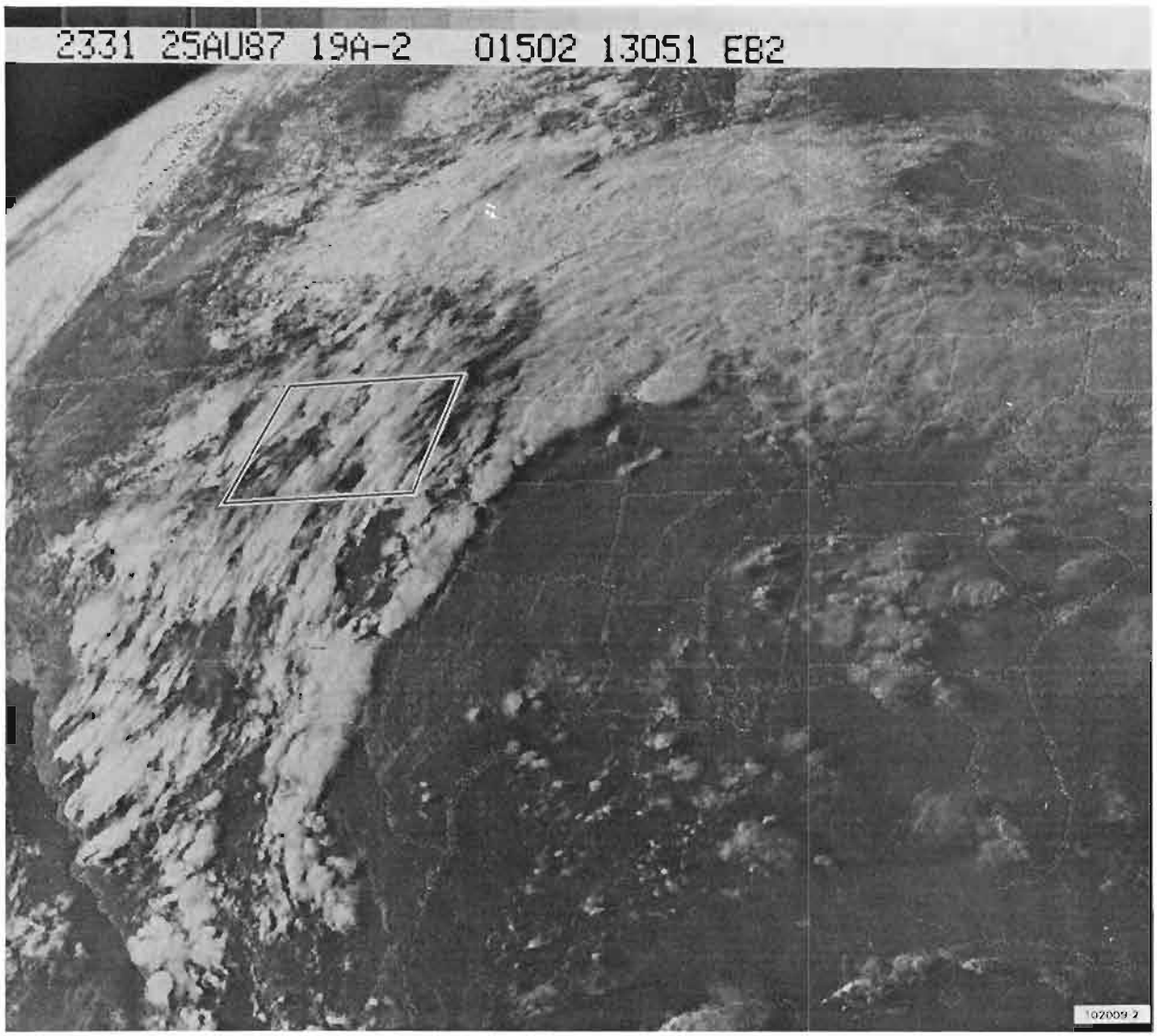

Figure VI-3. Visible satellite image of the central U.S. taken at 2331 UTC on 25 August 1987. Image represents conditions prior to the gust front and microburst events at Stapleton Airport.

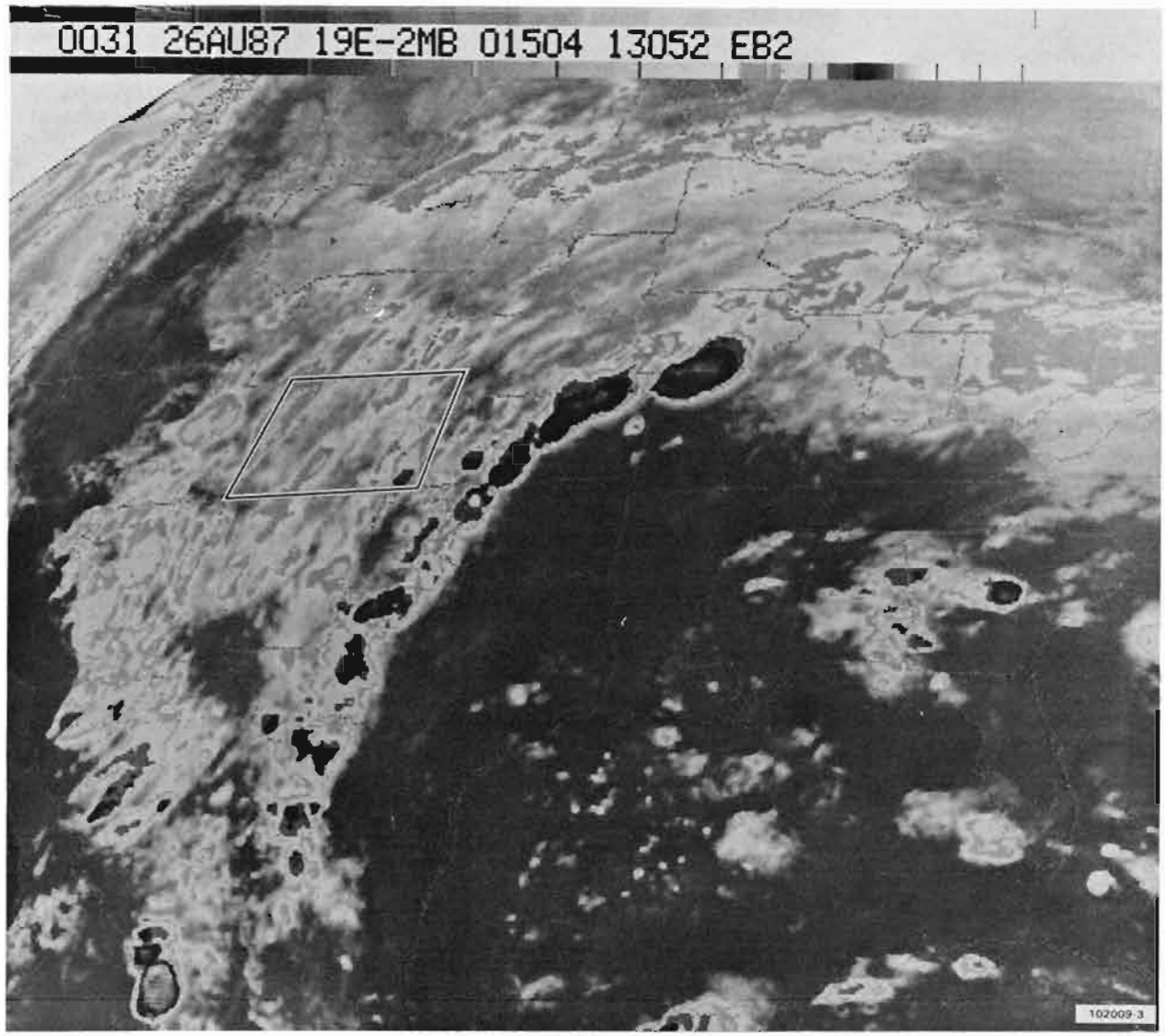

Figure VI-4. Infrared satellite image of the central U.S. taken at 0031 UTC on 26 August 1987. A microburst was occurring near Stapleton Airport at the same time this image was produced. See Fig. V-3 caption for description of the cloud temperature grey scale used here.

the MB/div line began to affect the western portion of the mesonet/LLWAS network. However, individual microburst centers to the north and south of the airport began to take control, leaving a very complicated wind flow pattern over the runways. Figure VI-5a shows the progression of the gust front (at 5 min. intervals). Figure VI-5b shows the progression of the MB/div line (at 5 min. intervals) based on dual Doppler data.

ii. Wind Shear Examples

By 0026, the leading edge of the gust front was approaching mesonet stations No. 20, 22 and 23. Behind the gust front, fairly strong westerly winds influenced the remainder of the network (Fig VI-6). The dual Doppler plots show similar wind conditions over the network (Fig. VI-7), as well as the MB/div line located about 5 km west-northwest of the network. The only disagreement worth noting between the dual Doppler and mesonet data is in the exact position of the gust front. A light (2.5 m/s) south-southwesterly peak wind was observed at stations Nos. 20, 22, and 23 (Fig. VI-6) indicating that the gust front was very close by. However, the dual Doppler wind vector image (Fig.VI-7a) shows moderate (approximately 5-7.5 m/s) winds from the southeast at these stations. This represents a 0.75-1.5 km discrepancy, with the mesonet feeling the presence of the gust front first. This may again be related to the vertical shape of the leading edge, or nose, of the gust front (see Fig. V-7).

The edge of the reflectivity echoes associated with the MB/div line was positioned along the eastern-most portion of the mesonet, coincident with the gust front (Fig. VI-8). The bulk of the larger echoes (40-50 dBZ) were impacting the southwest corner of the mesonet. Figure VI-8 also shows that the strongest core of radial wind velocities was centered over the runways at 0026:14 UTC. The largest velocity value detected is 18 m/s at LLWAS station WSW. A few minutes later (at 0028 and 0032 UTC), the wind speed gusted to 17 m/s at LLWAS station CF.

By 0044 UTC, the MB/div line had entered the mesonet/LLWAS network and began to impinge on the airport. According to the mesonet/LLWAS wind plot in Fig. VI-9, the MB/div line is oriented south-southwest to north-northeast through a portion of the network. The dual Doppler wind field in Fig. VI-10a shows the gust front, and associated strong winds, approaching the FL-2 radar. It is difficult to pick out the MB/div line in this plot, but its location is clearly revealed by the streamline analysis in Fig. VI-10b.

The 0044 UTC dual Doppler analysis is largely consistent with the mesonet/LLWAS surface wind field regarding the placement of the MB/div line. The only significant difference observed is in the northern portion of the network. The surface wind field (Fig. VI-9) reveals divergent winds between mesonet station Nos. 2 and 3. However, dual Doppler indicates that the divergent line is somewhat further west.

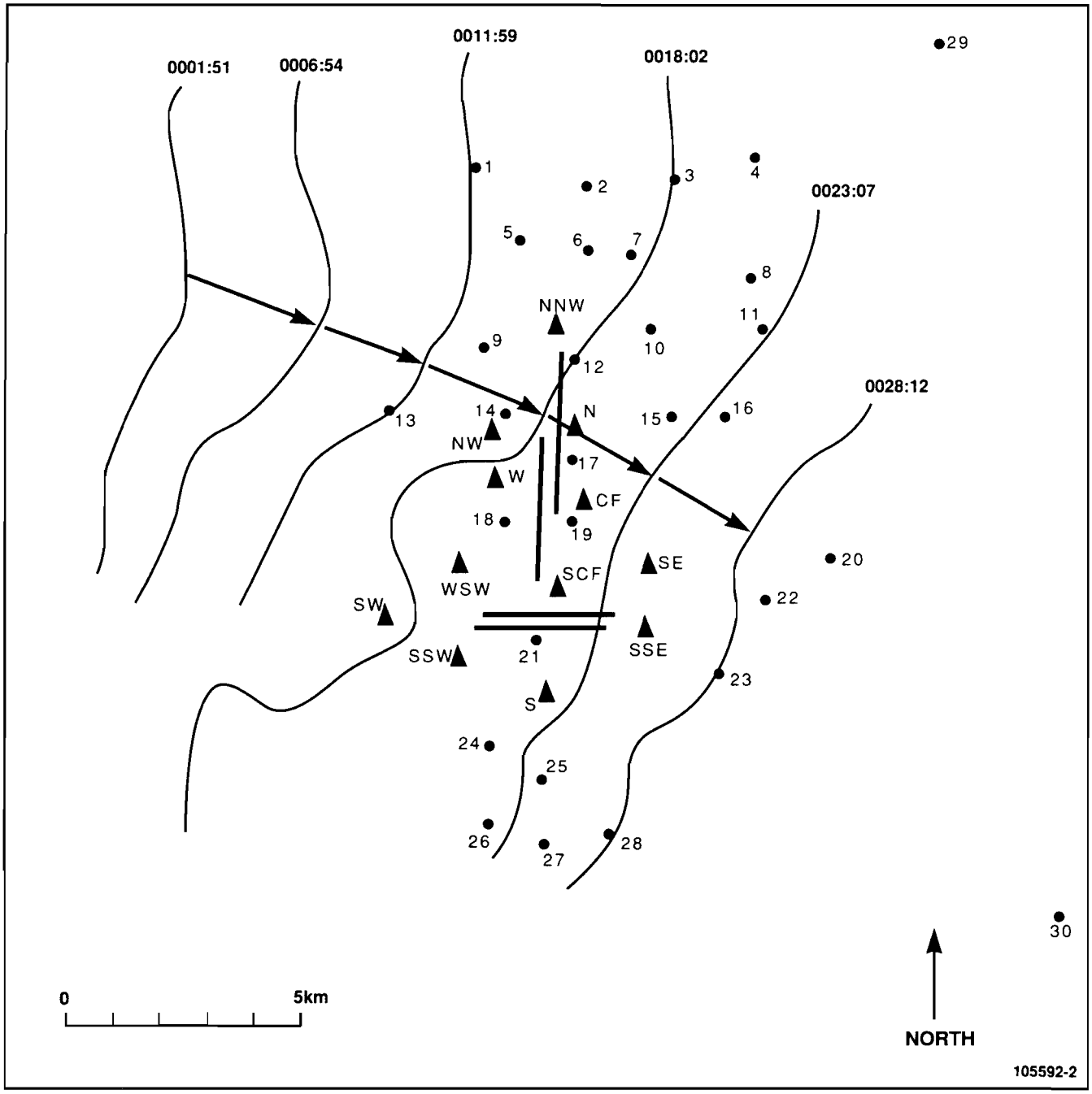

Figure VI–5a. Map representing the progression of the gust front during the 0000–0055 UTC time period for 26 August 1987. Map is based on dual Doppler data. Solid lines show the progression of the gust front moving from the northwest toward the southeast.

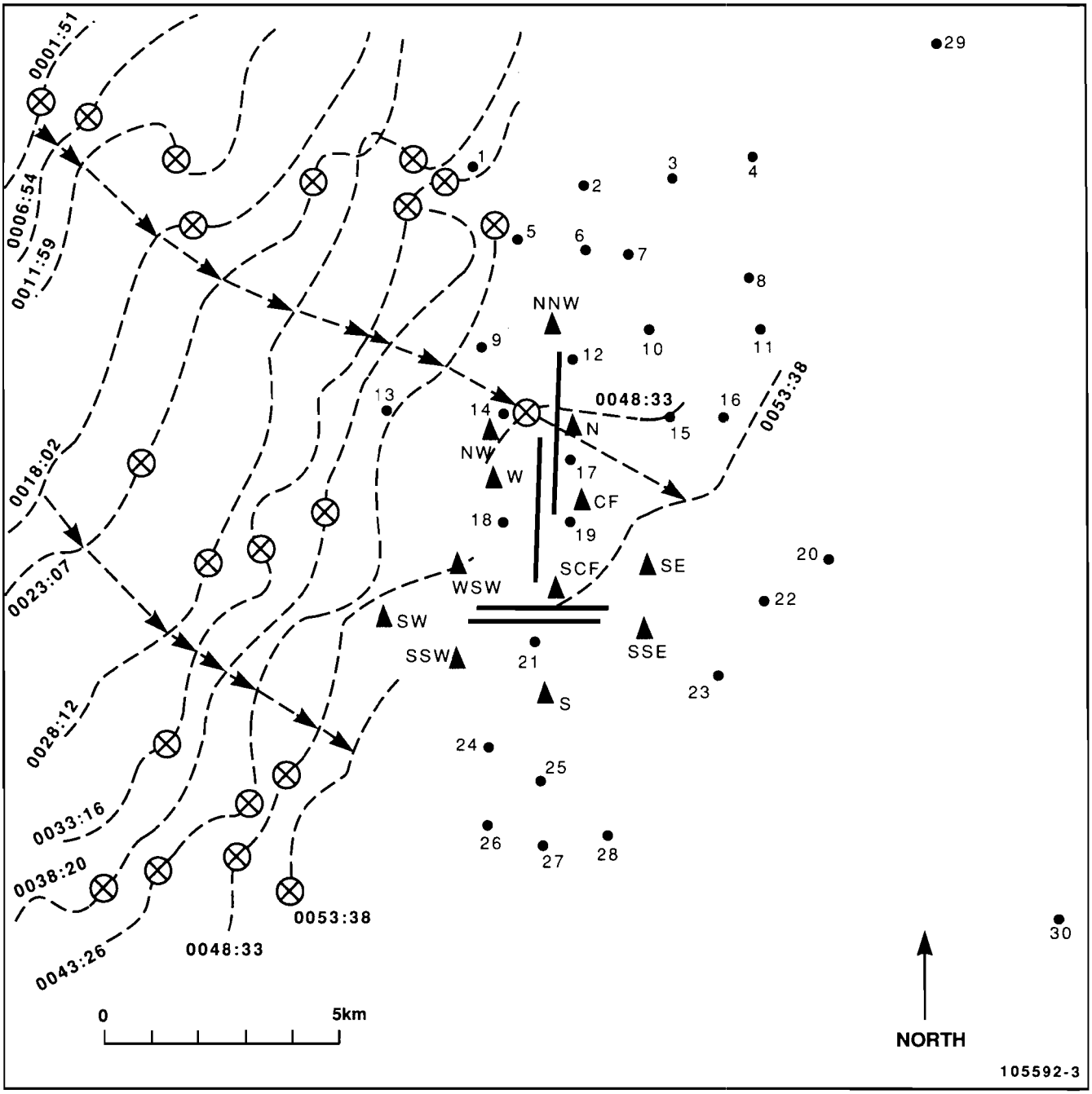

Figure VI-5b. Map representing the progression of the MB/div line during the 0000–0055 UTC time period for 26 August 1987. Map is based on dual Doppler data. Dashed lines show the progression of the MB/div line moving toward the southeast, and x's enclosed with circles show the locations of the parent cells along the MB/div line.

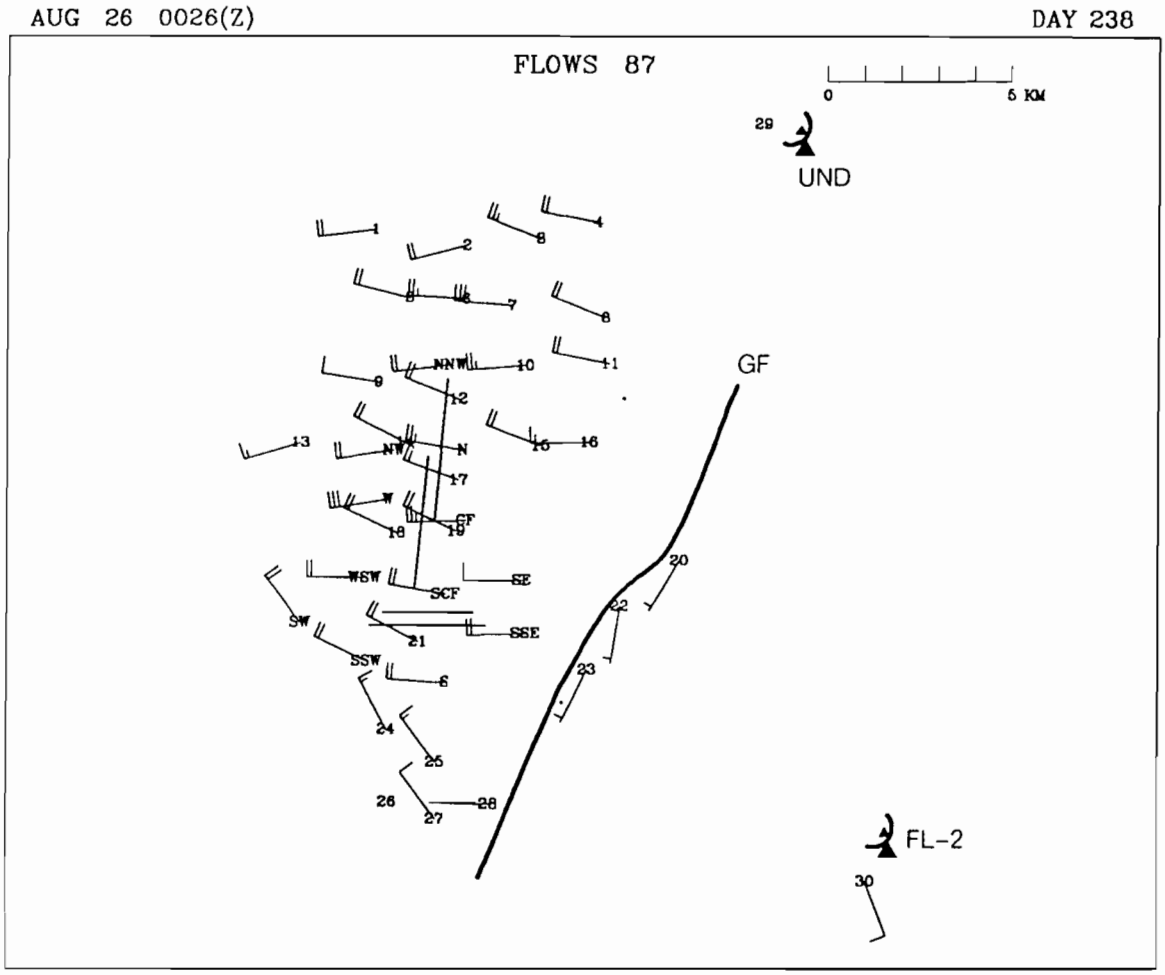

Figure VI-6. Mesonet/LLWAS winds at 0026 UTC on 26 August 1987. A gust front (GF) has recently passed through the network and a MB/div line (cannot be seen at this time) is approaching the network from the west. A full barb on the wind direction arrow represents 5 m/s and a half barb represents 2.5 m/s.

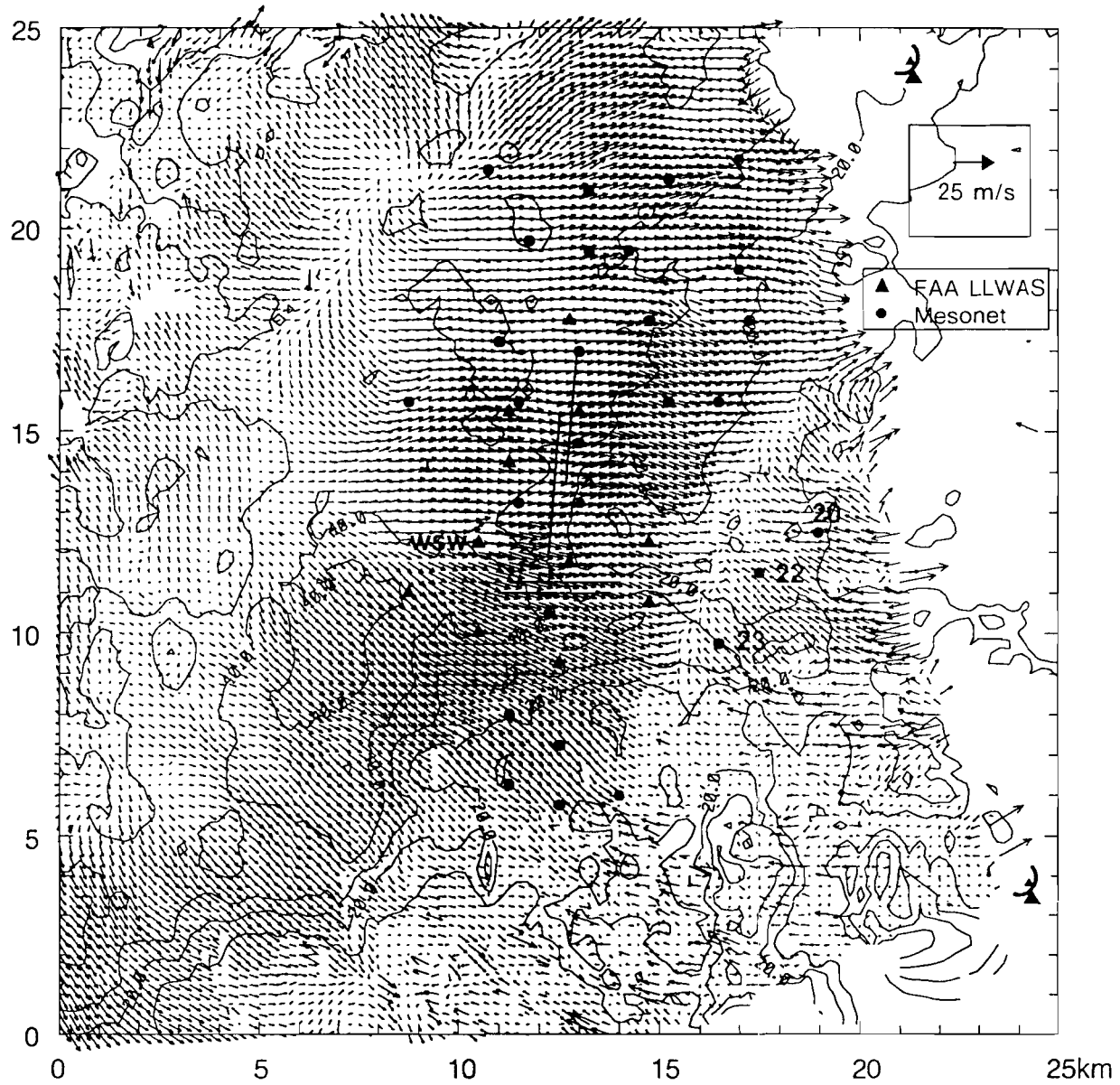

Figure VI-7a. Dual Doppler plot of the wind and reflectivity field at 0026:14 UTC on 26 August 1987. A MB/div line can be seen approaching the network from the northwest while the gust front, at the leading edge of the outflow, is about 1 km west of station Nos. 20, 22, and 23.

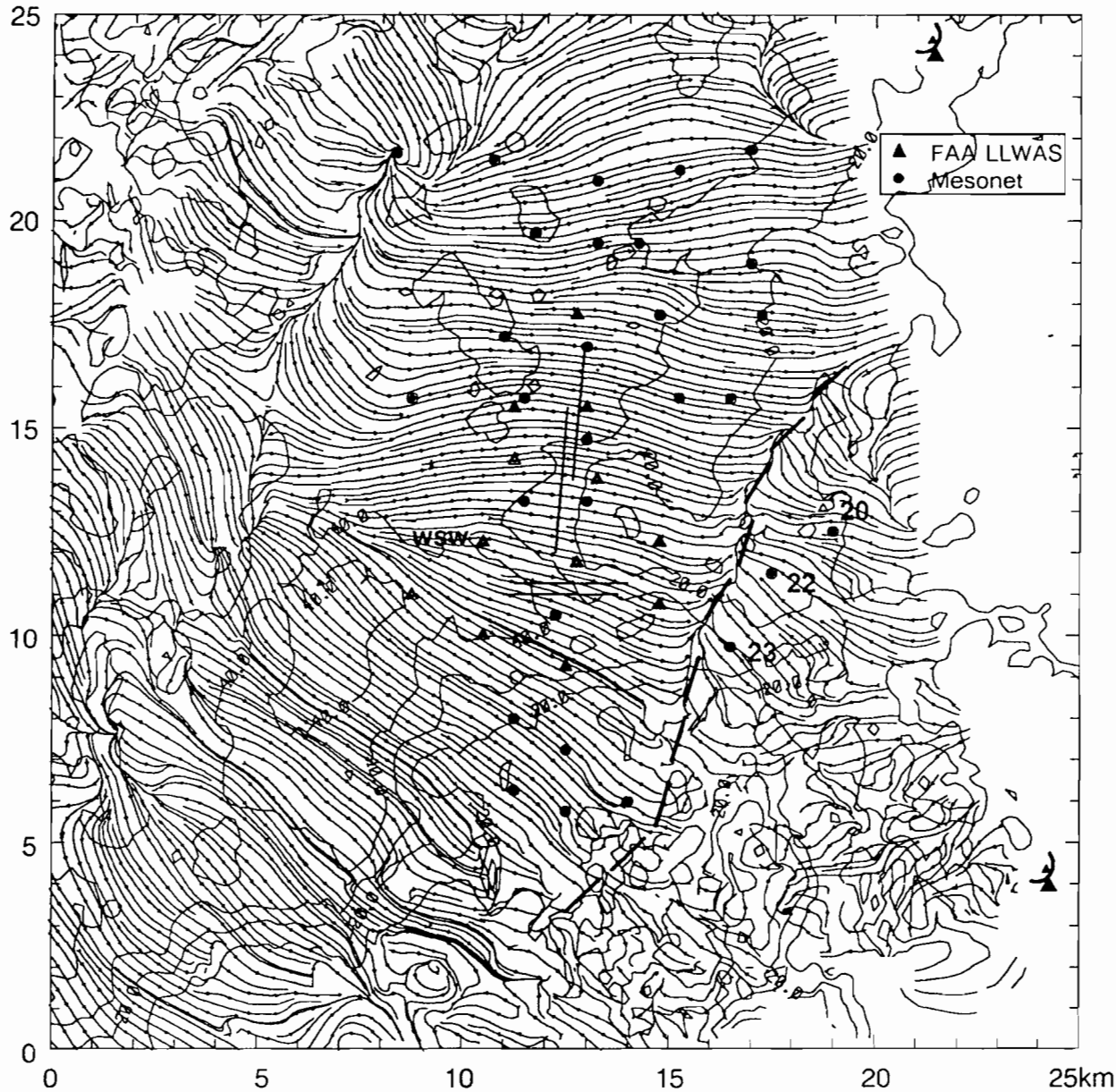

Figure VI-7b. Dual Doppler plot of the streamline and reflectivity field at 0026:14 UTC on 26 August 1987. The MB/div line is clearly evident in the northwest quadrant and the dashed line denotes the gust front boundary. Both of these wind shear lines are moving from the northwest toward the southeast.

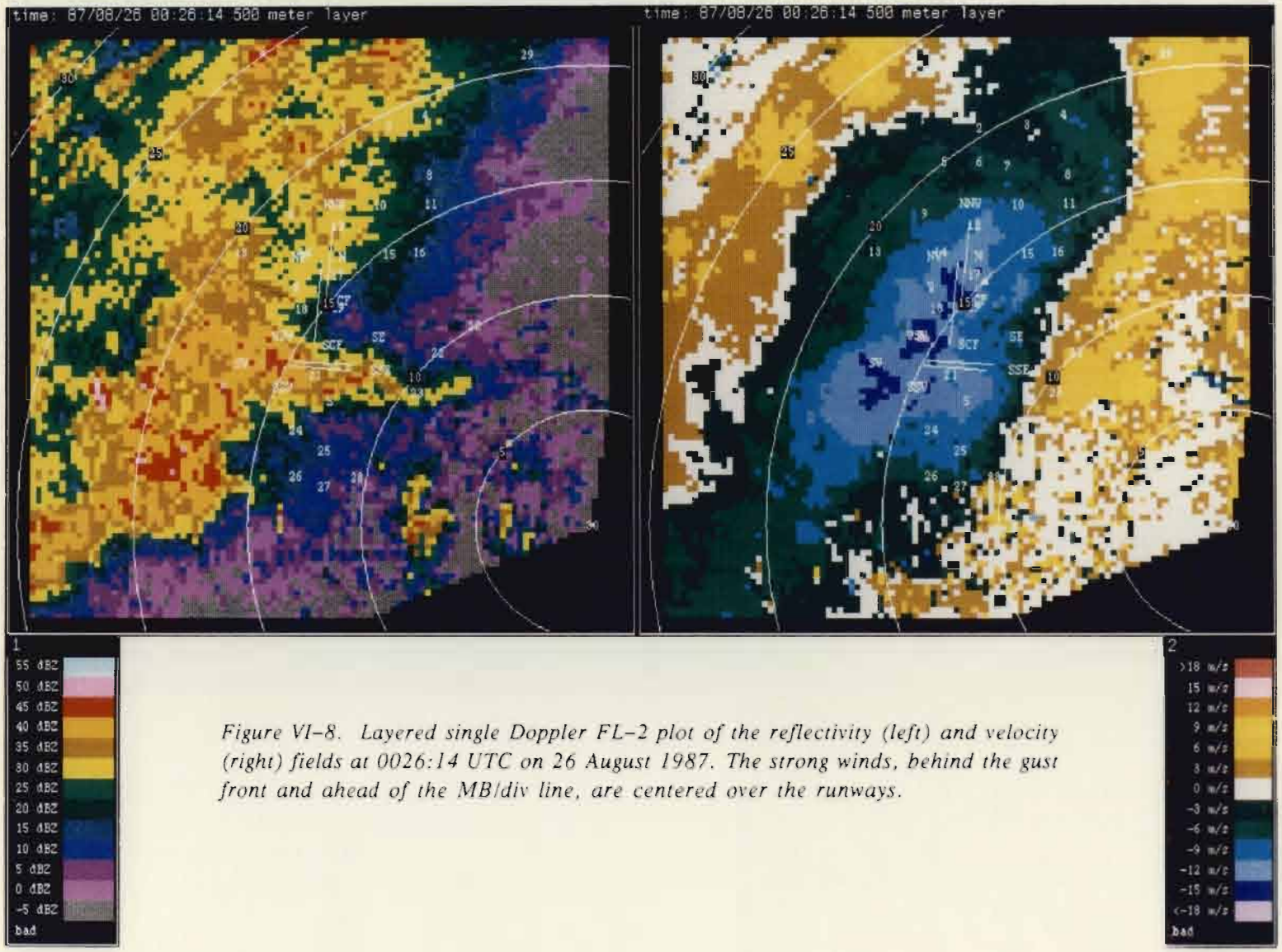

Figure VI-8. Layered single Doppler FL-2 plot of the reflectivity (left) and velocity (right) fields at 0026:14 UTC on 26 August 1987. The strong winds, behind the gust front and ahead of the MB/div line, are centered over the runways.

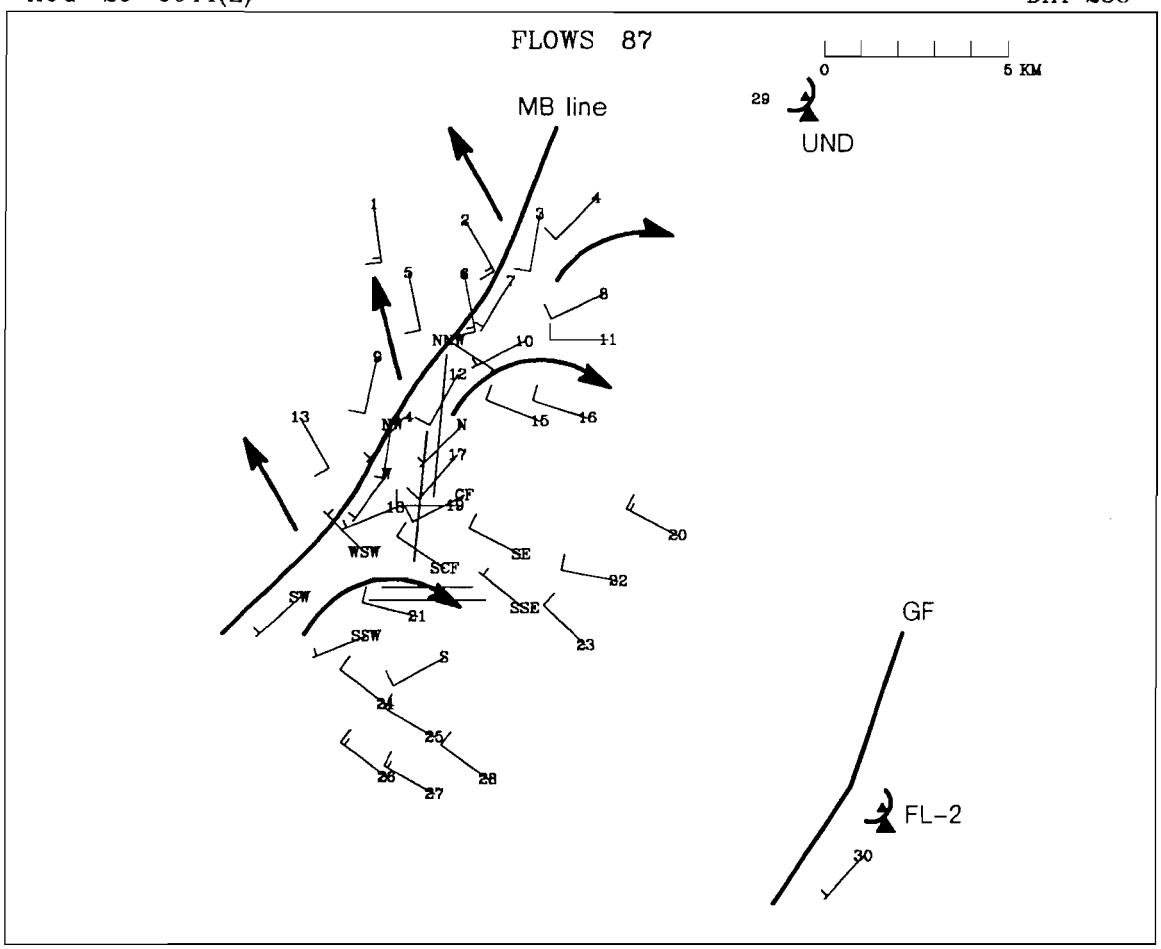

Figure VI–9. Mesonet/LLWAS winds at 0044 UTC on 26 August 1987. Microburst/divergent line is positioned very close to the runways but is disorganized at this time. Divergence along this MB/div line is clear in the northern portion of the network but in the southern portion of the network the actual location of the divergence is ambiguous. Bold arrows indicate the direction from which the wind is moving.

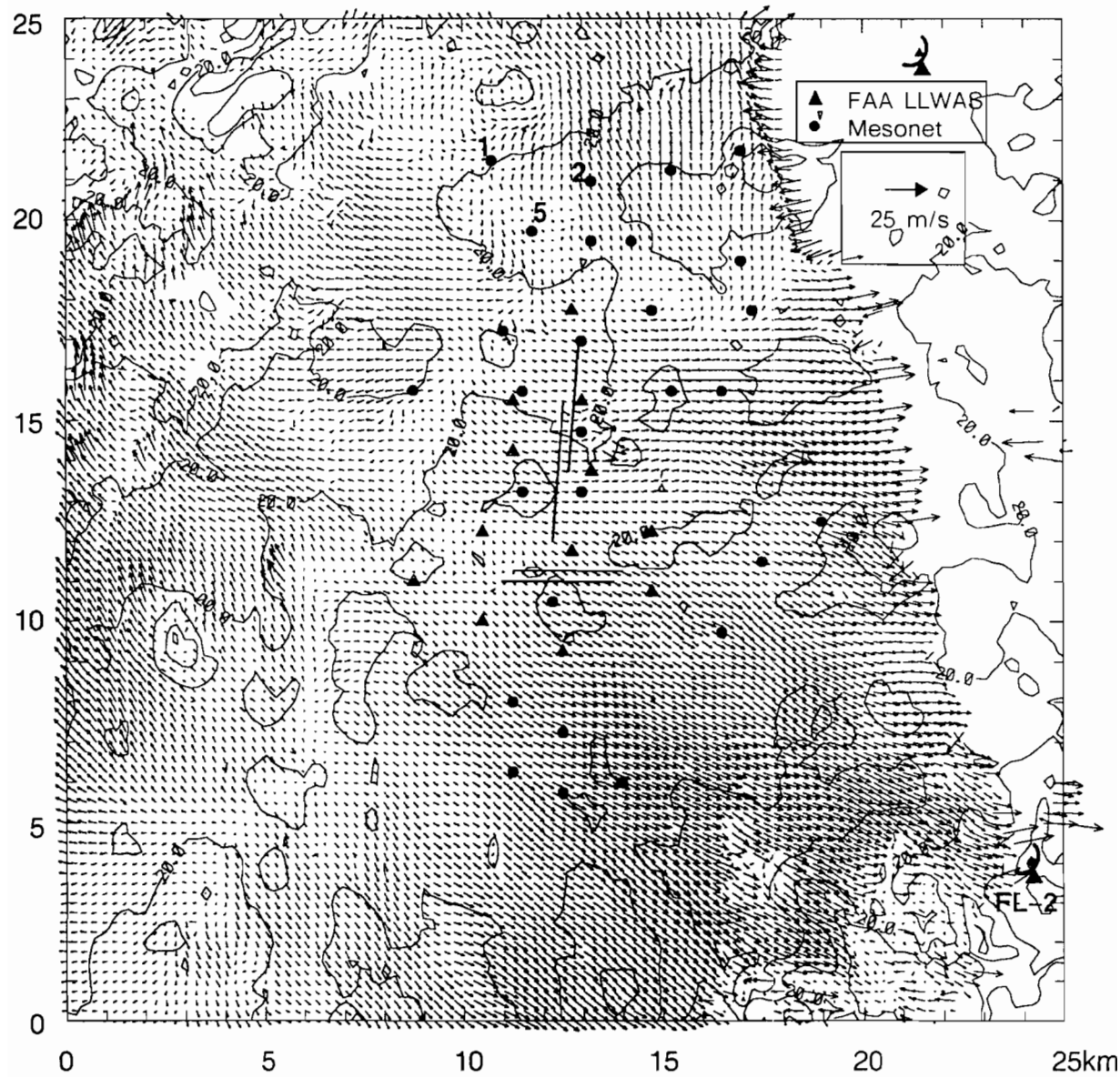

Figure VI-10a. Dual Doppler plot of the wind and reflectivity field at 0044:24 UTC on 26 August 1987.

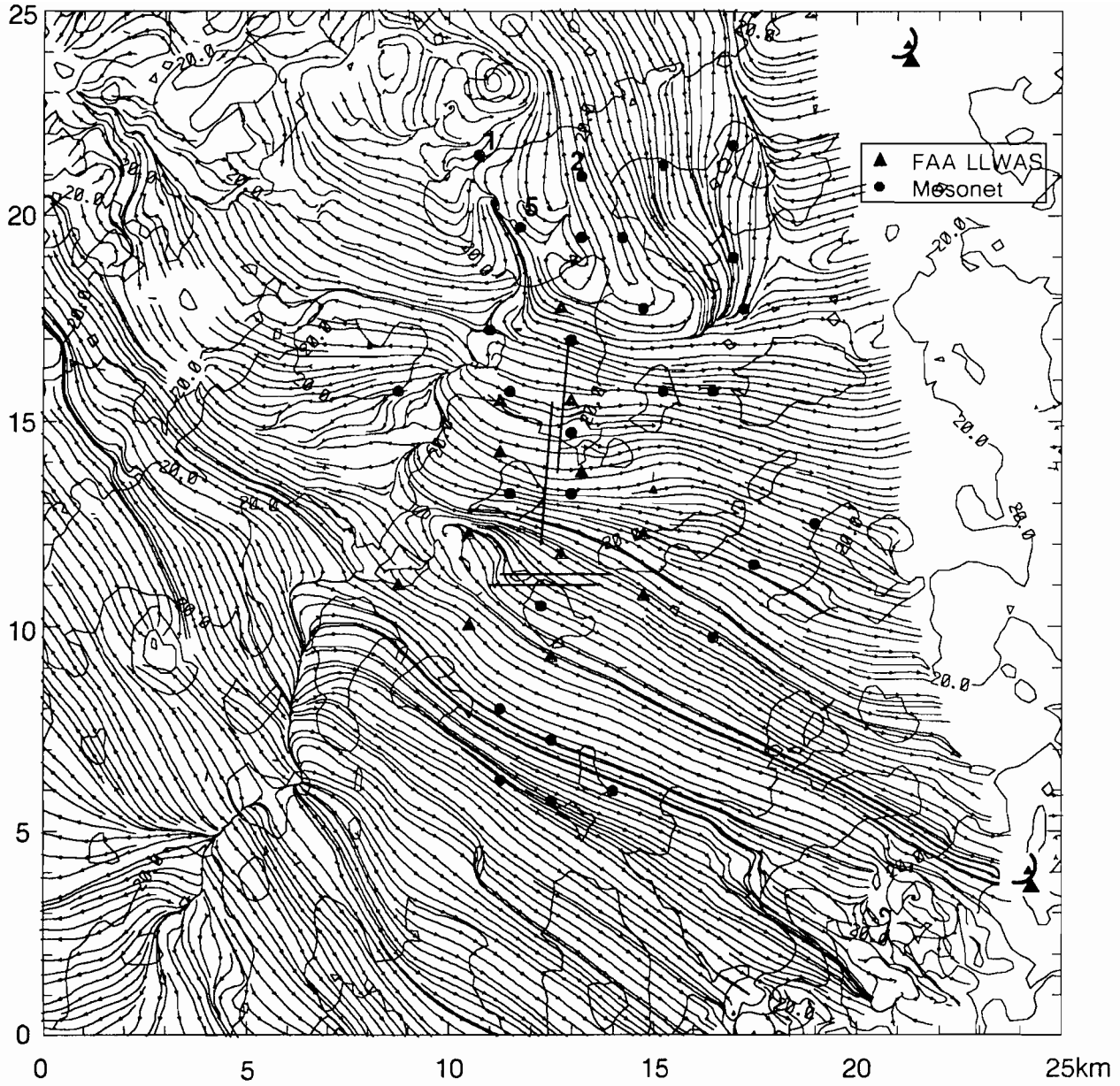

Figure VI-10b. Dual Doppler plot of the streamline and reflectivity field at 0044:24 UTC on 26 August 1987. This image clearly displays the divergent flow present at this time.

Upon further analysis, it was found that the surface divergent outflow associated with the MB/div line in the northern portion of the network was very shallow. The FL-2 surface scans from 0034-0055 UTC (not shown) indicated Doppler velocities approaching the radar, because they were contaminated with the approaching velocites occurring aloft. At the same time the mesonet reported wind directions from the south-southeast (receding velocities from the FL-2 radar). It can be concluded that the mesonet/LLWAS measurements more accurately depict the surface winds than do the dual Doppler analyses regarding the placement of the MB/div line in the northern portion of the network.

As the MB/div line moved across the mesonet, two microburst cells became evident. One cell, located in the northern portion of the network, continued to move eastward, while the second cell moved from west to east across the airport. This second microburst showed a distinct anti-cyclonic (clockwise) circulation as it crossed the airport.

At 0049 UTC, towards the end of this event, the weakening MB/div line was centered over the mesonet/LLWAS network. Figure VI-11 illustrates how weak the wind speeds were at this time. Winds were blowing from the southeast over the western mesonet stations and from the northwest over southeastern stations. Wind speeds had subsided considerably and reflectivity echoes were approximately 20-30 dBZ over the entire network. The only exception was the 17 m/s peak wind speed recorded at mesonet station No. 10. No evidence of this strong wind could be found in the Doppler radar data. Two minutes later, station No. 10 and all surrounding stations showed no sign of any strong winds (Fig. VI-12).

Figure VI-13a depicts the dual Doppler wind and reflectivity plot for 0051 UTC. Except for some anomalously strong velocity vectors, which are located near the center of the north-south runways, this dual Doppler wind field is quite consistent with the surface measured wind field identified in Fig. VI-12. The strong winds blowing away from the FL-2 radar, associated with an anomalous point target in the reflectivity field, were the result of contamination of the Doppler velocity data by aircraft; the stronger winds blowing in the opposite direction (toward the radar) were part of the circulation discussed in the following paragraph. Another anomalous point target (aircraft) with associated large Doppler velocities can be seen just inside the 15 km range ring, northeast of LLWAS station CF.

Another feature worth mentioning, which is clearly identified in the streamline image (Fig. VI-13b), is the anticyclonic circulation (clockwise rotation at stations 19 and CF) which developed along the MB/div line. This phenomenon also shows up quite clearly over the north-south runways in the FL-2 single Doppler velocity plot (Fig. VI-14). The small circulation moved eastward and dissipated a few minutes later.

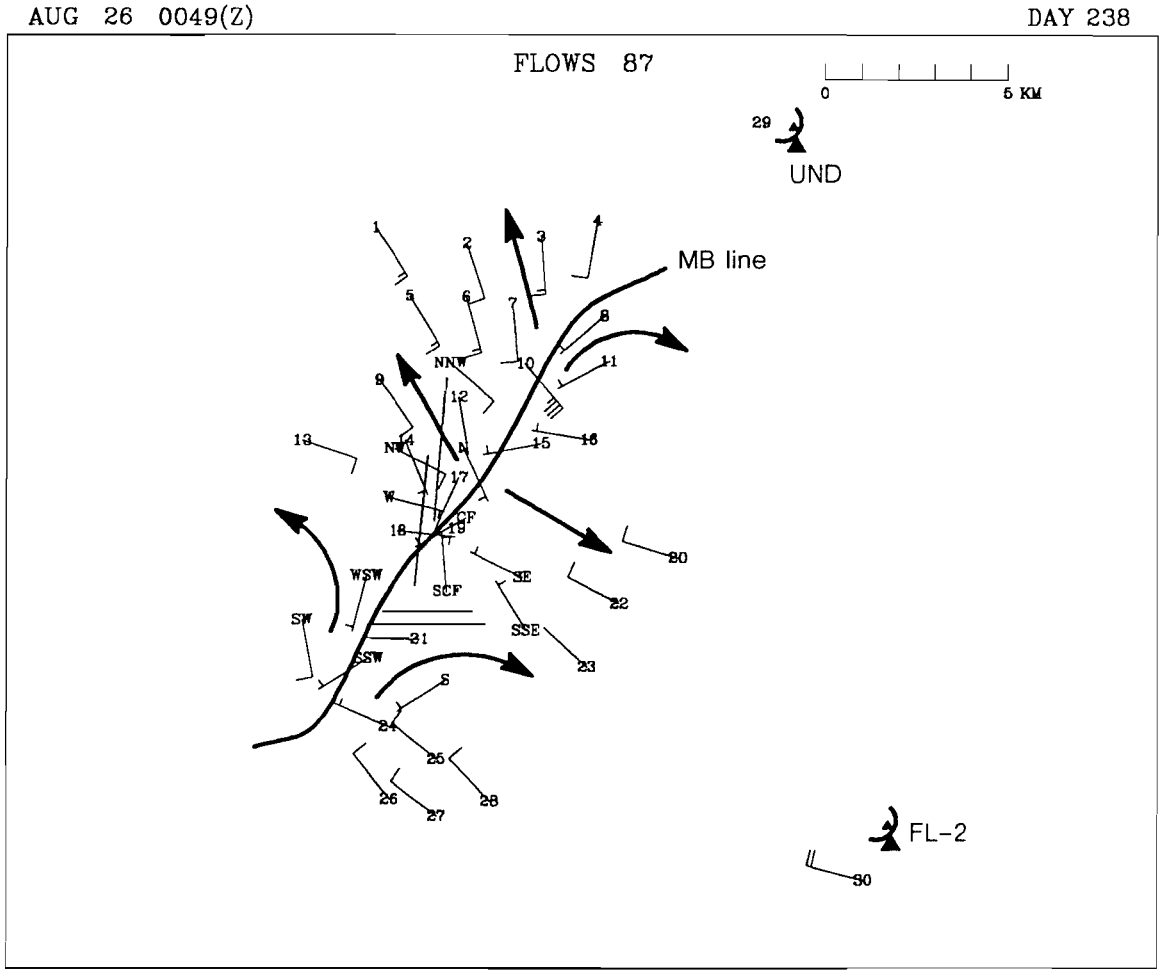

Figure VI-11. Mesonet/LLWAS winds at 0049 on 26 August 1987. The weak MB/div line is now centered over the runways. All stations are recording light winds except for station No. 10, where a 17 m/s peak wind speed is detected.

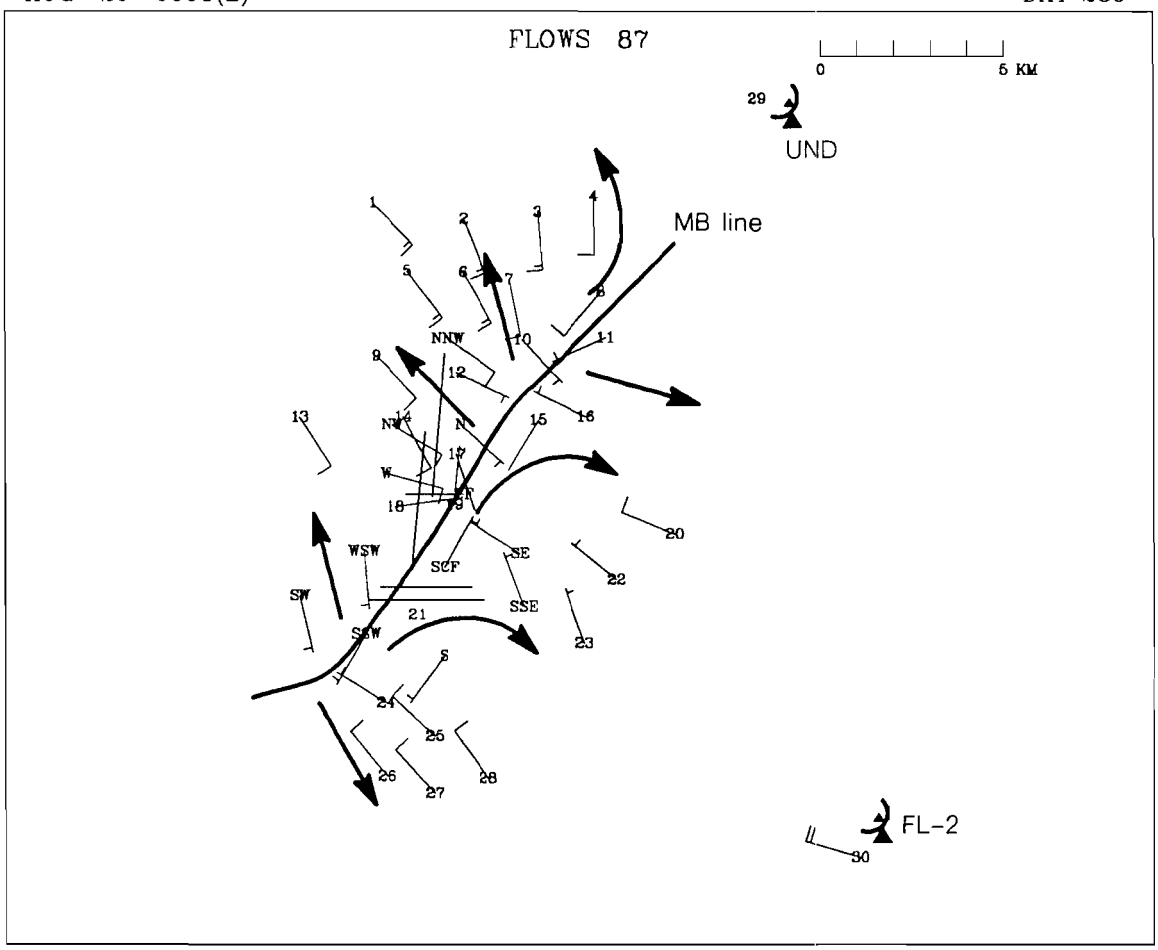

Figure VI–12. Mesonet/LLWAS winds at 0051 UTC on 26 August 1987. Conditions are the same as the previous mesonet/LLWAS plot (Fig. VI–11) except with station No. 10 now recording a much lighter wind flow.

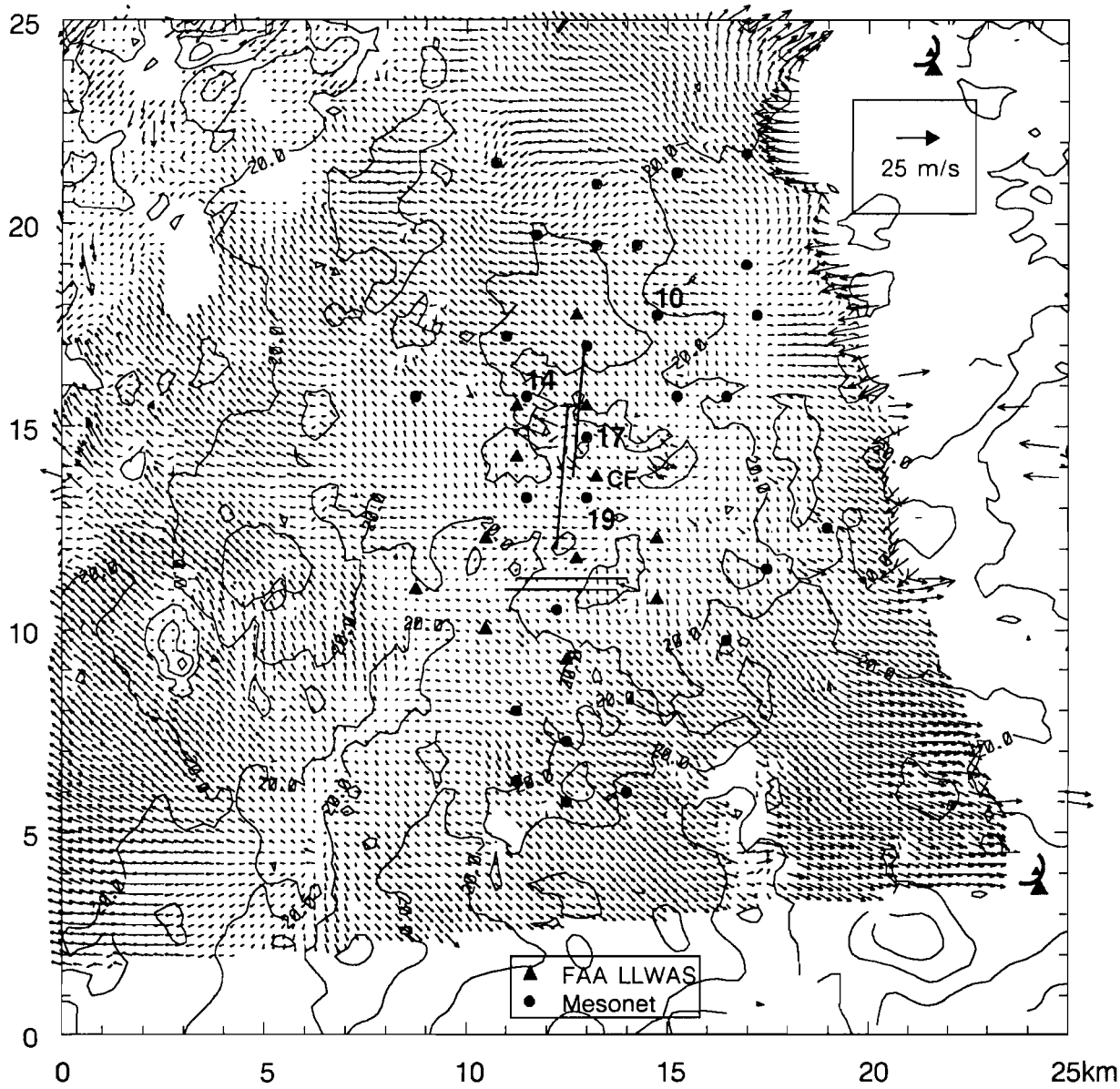

Figure VI-13a. Dual Doppler plot of the wind and reflectivity field at 0051:40 UTC on 26 August 1987. The divergent line is very disorganized, and a small clockwise rotation, located over the runways, has developed in its wake. A few long wind vectors (15-20 m/s) are present between mesonet station Nos. 14 and 17 but most winds near and over these stations are not that strong.

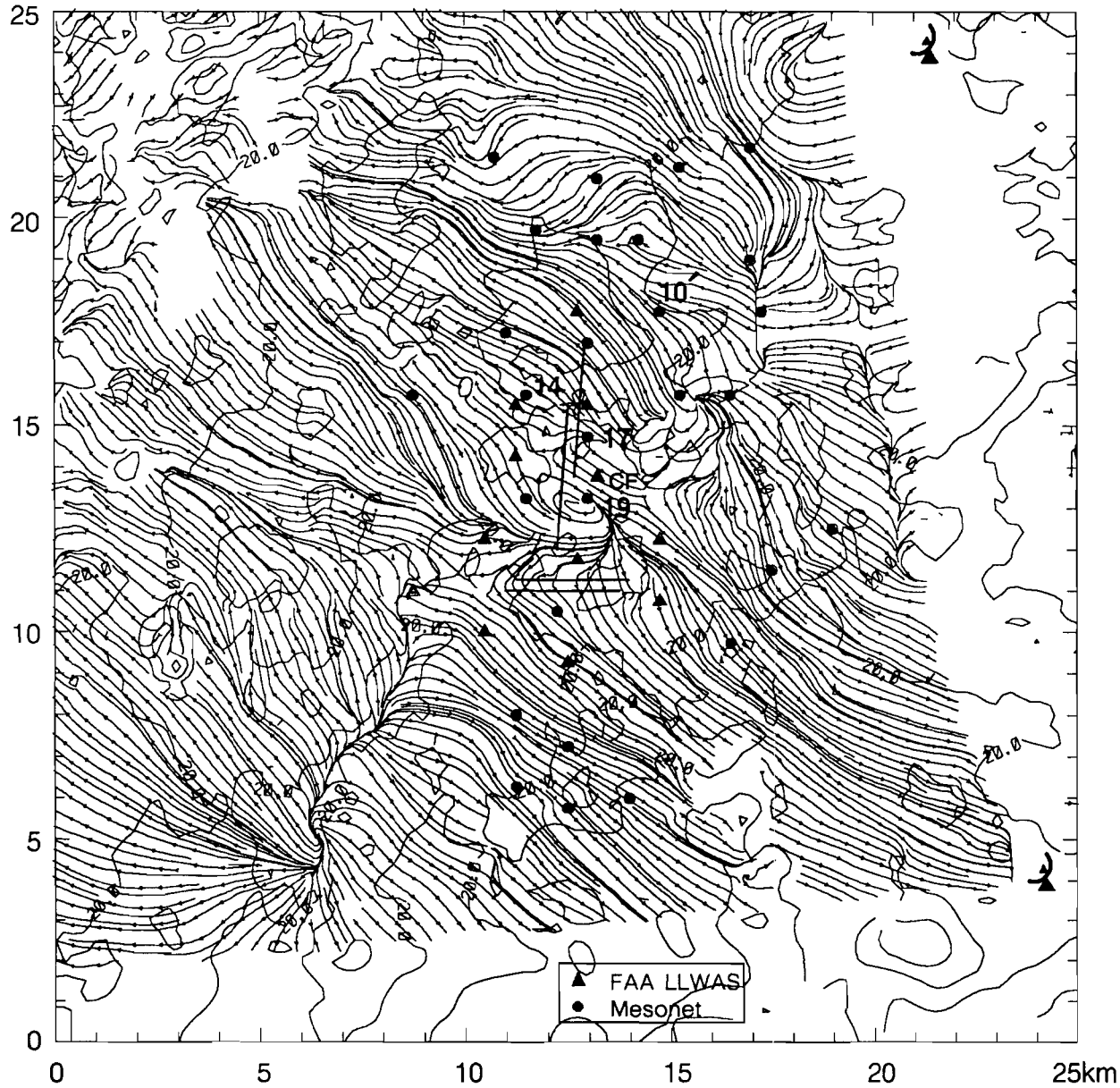

Figure VI-13b. Dual Doppler plot of the streamline and reflectivity field at 0051:40 UTC on 26 August 1987. Note how clearly a clockwise rotation shows up on this image (centered over the runways).

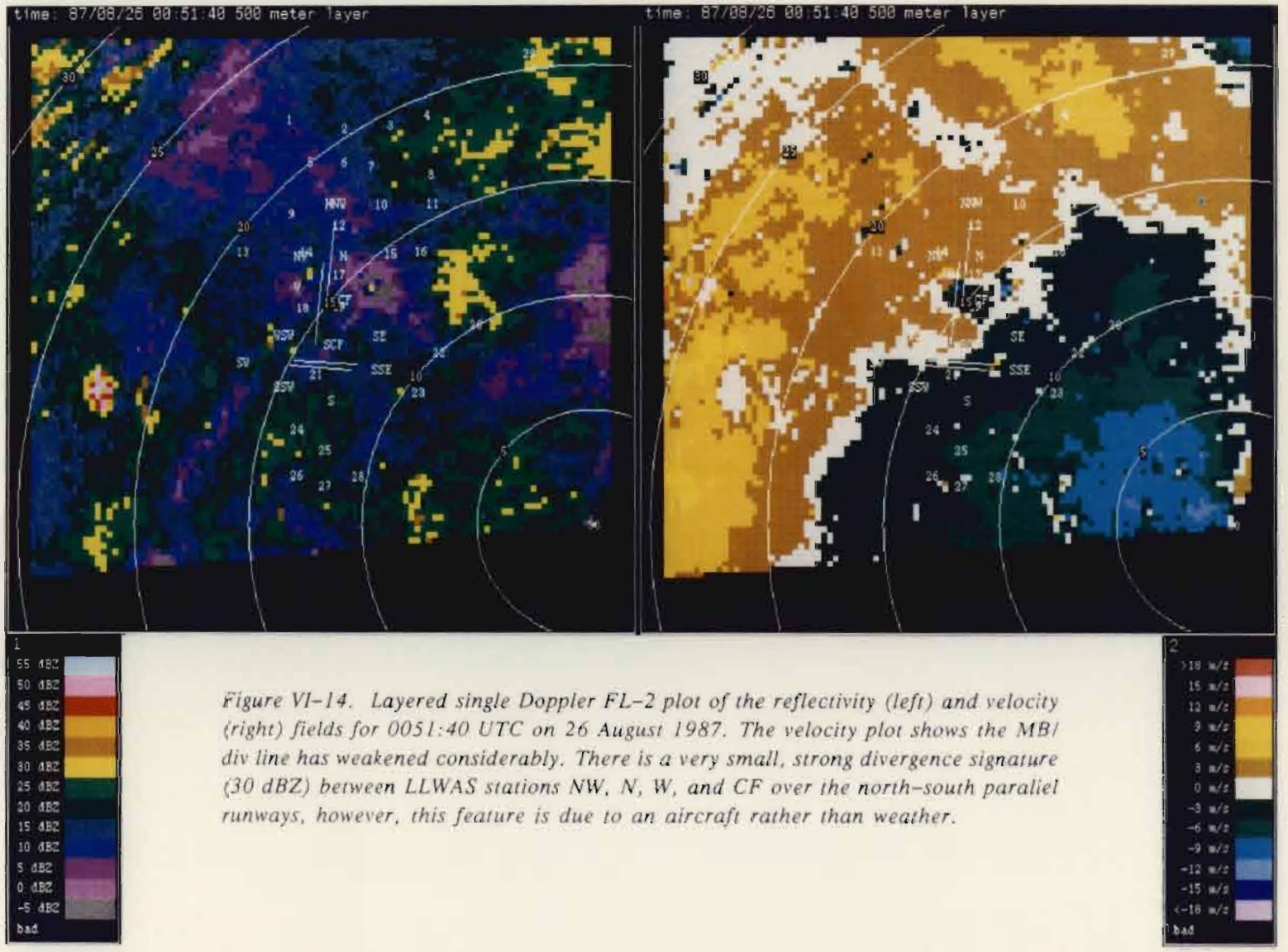

Figure VI-14. Layered single Doppler FL-2 plot of the reflectivity (left) and velocity (right) fields for 0051:40 UTC on 26 August 1987. The velocity plot shows the MB/ div line has weakened considerably. There is a very small, strong divergence signature (30 dBZ) between LLWAS stations NW, N, W, and CF over the north-south parallel runways, however, this feature is due to an aircraft rather than weather.

VII. 28 AUGUST 1987

The predominant feature of the day was a gust front which tracked eastward from the Rocky Mountains across Stapleton airport. This gust front, associated with a developing thin reflectivity line, did not produce much of a wind direction shift over the airport; instead a much stronger wind flow from the northwest resulted from its passage.

A. Available Data

The time period of interest was originally 2200–2300 UTC. This was later revised to cover only the first half hour. Mesonet, LLWAS, and FL–2 single Doppler data were provided for the period 2205 to 2235 UTC. The FL–2 and UND radar scan times, and the differences between these scan times, for each dual Doppler analysis are given below in Table VII–1.

Table VII–1. FL–2 and UND scan times used for 28 August 1987 dual Doppler analyses.

Dual Doppler Pair	FL–2 time (UTC)	UND time (UTC)	Time diff. (sec)
1	2205:10	2205:57	47
2	2205:56	2205:57	1
3	2207:03	2207:00	3
4	2208:05	2208:01	4
5	2209:04	2209:02	2
6	2210:03	2209:59	4
7	2211:02	2211:02	0
8	2212:09	2212:05	4
9	2213:11	2213:06	5
10	2214:10	2214:07	3
11	2215:08	2215:04	4
12	2216:07	2216:07	0
13	2217:14	2217:10	4
14	2218:16	2218:11	5
15	2219:15	2219:12	3
16	2220:15	2220:09	6
17	2221:14	2221:12	2
18	2222:21	2222:15	6
19	2223:23	2223:16	7
20	2224:22	2224:17	5
21	2225:21	2225:14	7
22	2226:20	2226:17	3
23	2227:27	2227:20	7

24	2228:29	2228:21	8
25	2229:28	2229:22	6
26	2230:27	2230:19	8
27	2231:26	2231:22	4
28	2232:33	2232:25	8
29	2233:35	2233:26	9
30	2234:34	2234:27	7
31	2235:33	2235:24	9

B. Synoptic Situation

The wind shear activity for the day was initiated when a line of storms developed south of FL-2 during the afternoon. This activity tracked eastward without entering the region around Stapleton airport. Later in the day (2200 UTC), a line of storms which initially developed over the mountains, did move across the airport. The gust front at their leading edge was scanned in a dual Doppler mode.

At 2100, one hour before dual Doppler scanning began over Stapleton, conditions over Colorado were mostly cloudy in central and western sections and mainly clear in eastern sections. Winds were from the northwest in western CO and from the southeast in eastern CO. The air was relatively dry with most weather observation sites reporting dewpoints in the 30's and 40's (°F) when the gust front moved over the center of the mesonet/LLWAS network.

The long range reflectivity map fom FL-2 at 2224 UTC exhibited a narrow line of very weak (10-20 dBZ) echoes in the vicinity of the airport (Fig. VII-1). The strongest portion of the reflectivity line was located in central CO (well south of FL-2), where 40 to 50 dBZ echoes were detected. The line movement was to the southeast at 5 m/s while the individual cell movement was to the east-northeast at 7.5 m/s.

Figure VII-2 shows the cloud conditions over the state of CO at 2231 UTC. By this time, the gust front had passed through most of the network. This figure was taken seven minutes after the long range reflectivity map shown in the previous figure. Most of the clouds have blossomed vertically, especially the cells to the south of FL-2. The cloud tops are grouped in a line just east of Denver (over the mesonet/LLWAS network). These are the tops of the storms that produced the gust front that tracked across the airport.

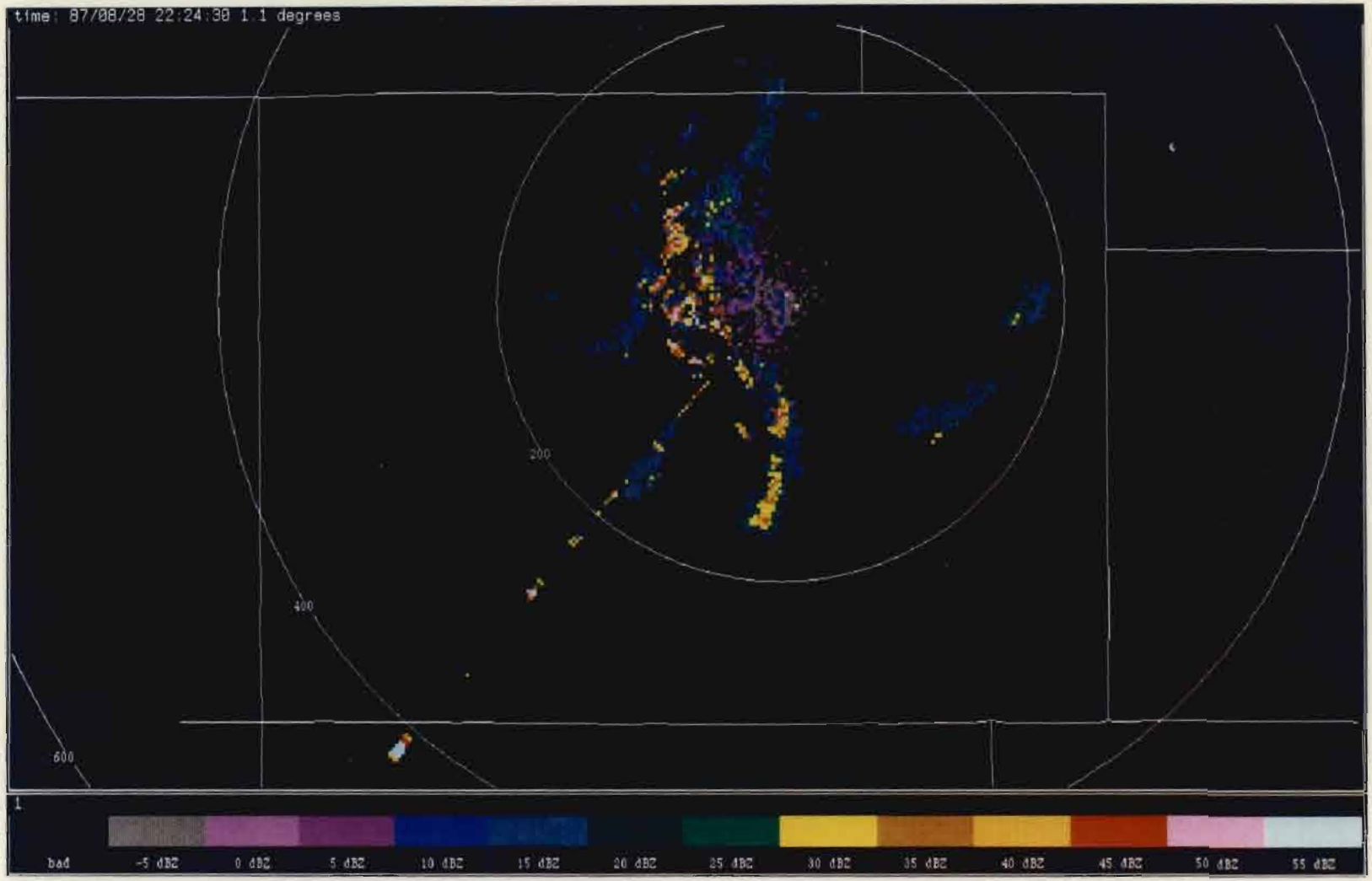

Figure VII-1. Long range reflectivity map from FL-2 at 2224:30 UTC on 28 August 1987. A thin reflectivity line is shown passing through the mesonet/LLWAS network. The stronger echoes (45-50 dBZ) associated with this line are located 50-150 km south of FL-2. The radial of data extending out beyond the 400 km range ring (in southwestern Colorado) is erroneous.

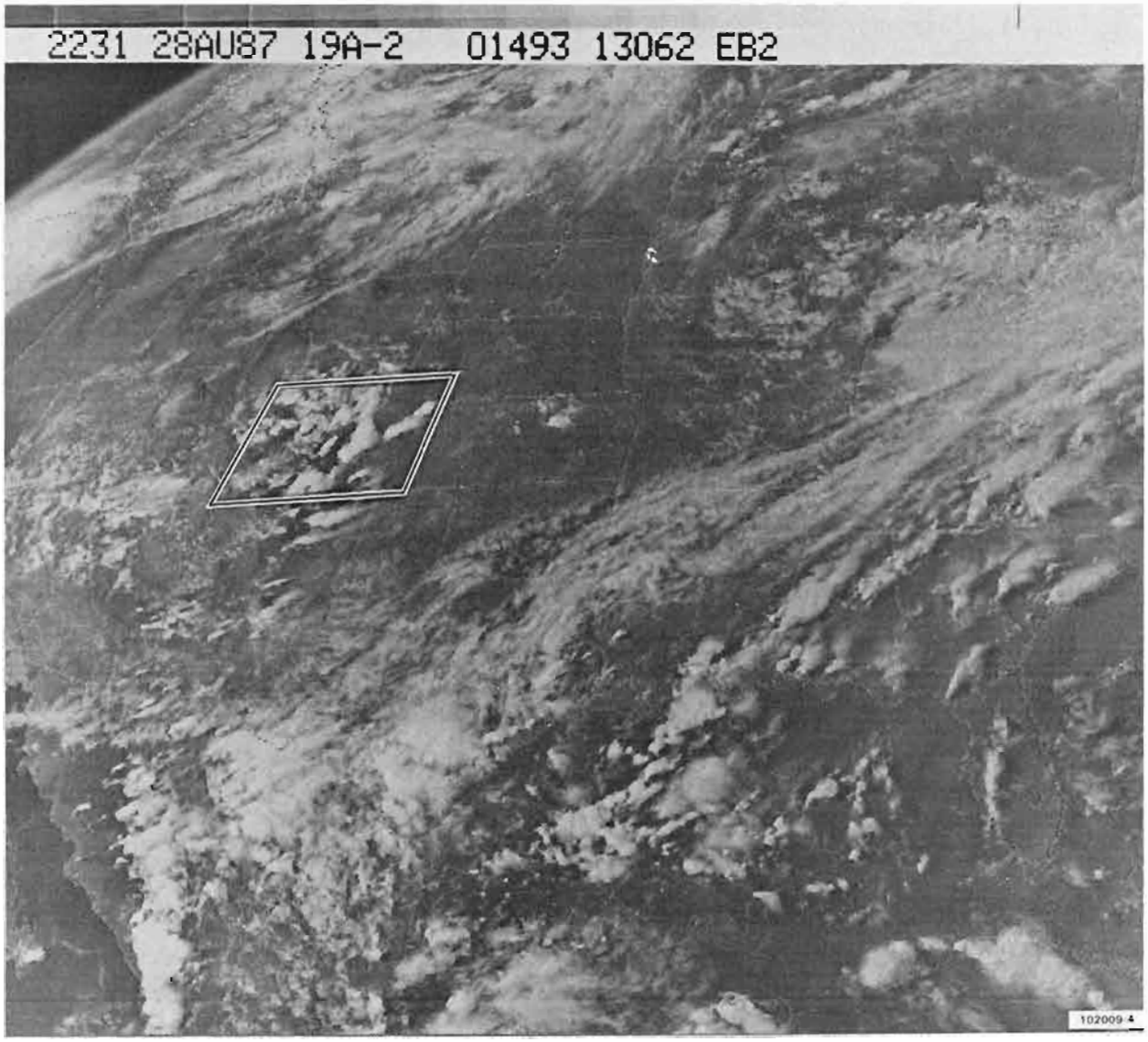

Figure VII-2. Visible satellite image of the central U.S. taken at 2231 UTC on 28 August 1987. This image represents conditions just after the gust front had passed through Stapleton Airport.

C. Wind Shear Event

i. Wind Shear Summary

During the period from 2205 to 2235 UTC, a gust front travelling from west to east brought moderate to strong northwesterly winds and little if any precipitation to the mesonet/LLWAS network. At the beginning of this time period, the entire network was reporting light (2.5 m/s or less) and variable winds, with wind directions mostly from the north. A couple of minutes later (2213 UTC), the gust front moved into dual Doppler range from the northwest. By 2221 UTC, the gust front was centered over the runways. It did not begin to exit the network until 2235 UTC. Figure VII-3 shows the progression of the gust front, for the time period of interest, based on dual Doppler data.

ii. Wind Shear Examples

By 2218 UTC, the gust front had just entered the network area, and was influencing the winds at station No. 13 (Fig. VII-4). All other stations were reporting light peak speeds during the minute. The dual Doppler wind and streamline plots for the 2218:16 UTC analysis (Fig. VII-5) are shown for comparison. As can be seen in Fig. VII-5a, the reflectivity line, the leading edge of which corresponds well to the gust front, has passed over station Nos. 1, 9, and 13. Moderate ($\sim$ 7.5 m/s) winds were detected over station Nos. 1, 5, 9, 13, and NW. Although their wind directions agree well with those indicated by dual Doppler, the mesonet peak wind speeds at these stations were considerably slower (Fig. VII-4). Here again a discrepancy exists between the mesonet and radar data. In this case, though, it appears as if the mesonet data is lagging (in either space or time) the radar data. In the streamline analysis (Fig. VII-5b), the gust front can only be located by the thin reflectivity line (10-20 dBZ) and a slight "kink" in the streamlines, since the wind direction does not change much across the front. At 2220, northwest winds with speeds up to 13 m/s began to impact the western edge of the surface network.

Two minutes later (2222 UTC), a thin reflectivity line associated with the gust front was moving through Stapleton airport. Figure VII-6 illustrates an average peak wind speed of 10 m/s behind the gust front. The gust front boundary can be detected by the division between the weaker and stronger northwesterly winds. A separate, weaker wind shift line may be present ahead of the gust front in the southern part of the network. The dual Doppler wind analysis (Fig. VII-7a) agrees closely with the mesonet plot in the location of the gust front.

The FL-2 single Doppler reflectivity image (Fig. VII-8) clearly shows the thin line associated with the gust front. Maximum echoes of 30 to 40 dBZ are detected in some areas along the reflectivity line. The reflectivity levels are higher in Fig. VII-8 than in Fig. VII-7 because the reflectivity fields from FL-2 and UND were averaged in the dual Doppler analyses. The UND radar measured considerably lower reflec-

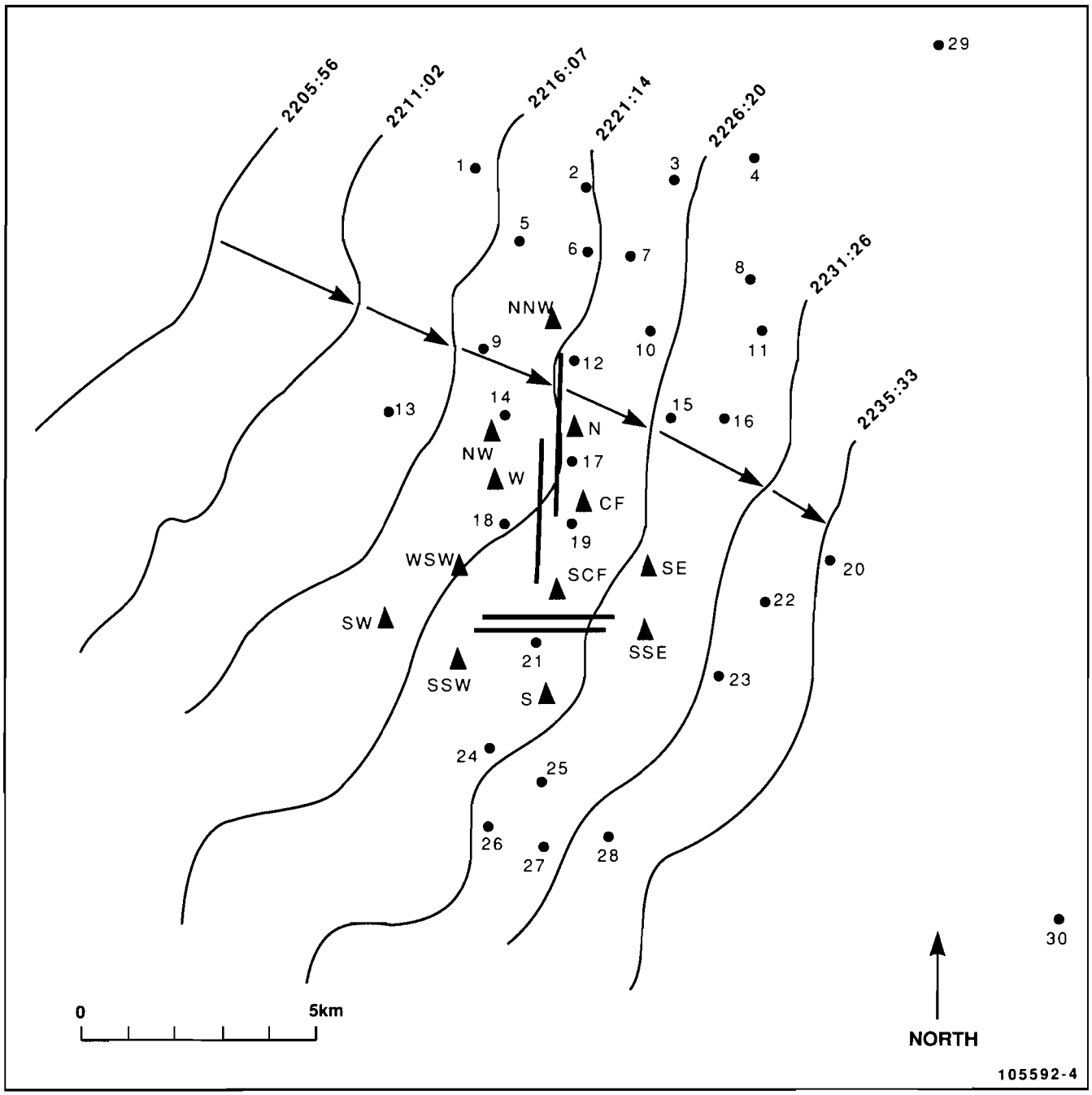

Figure VII–3. Map representing the progression of the gust front during the 2205–2235 UTC time period for 28 August 1987. Map is based on dual Doppler data. Solid lines show the progression of the gust front moving from the northwest toward the southeast at roughly 5 min. intervals.

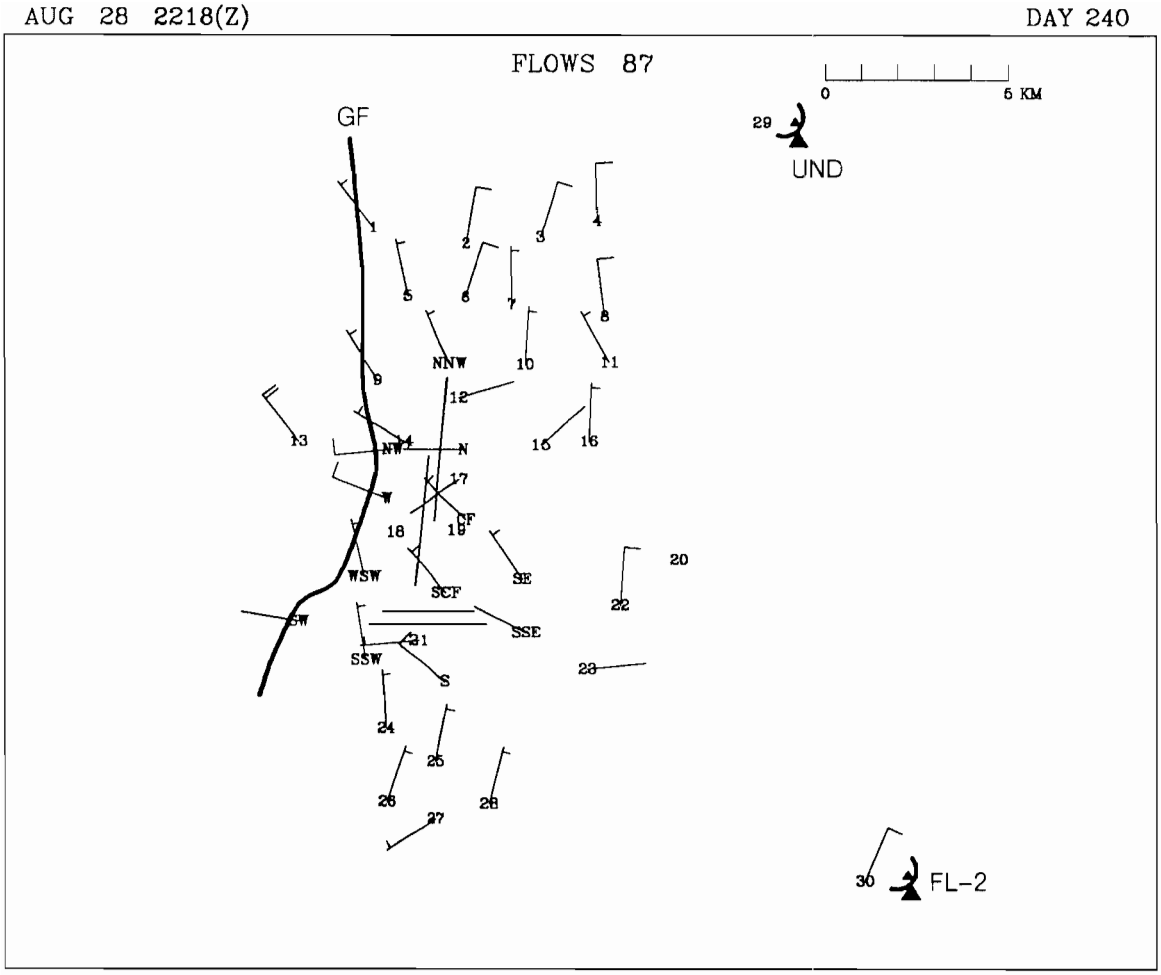

Figure VII-4. Mesonet/LLWAS winds at 2218 UTC on 28 August 1987. Station No. 13 is the only station which has been impacted by the approaching gust front (GF). A full barb on the wind direction arrow represents 5 m/s and a half barb represents 2.5 m/s.

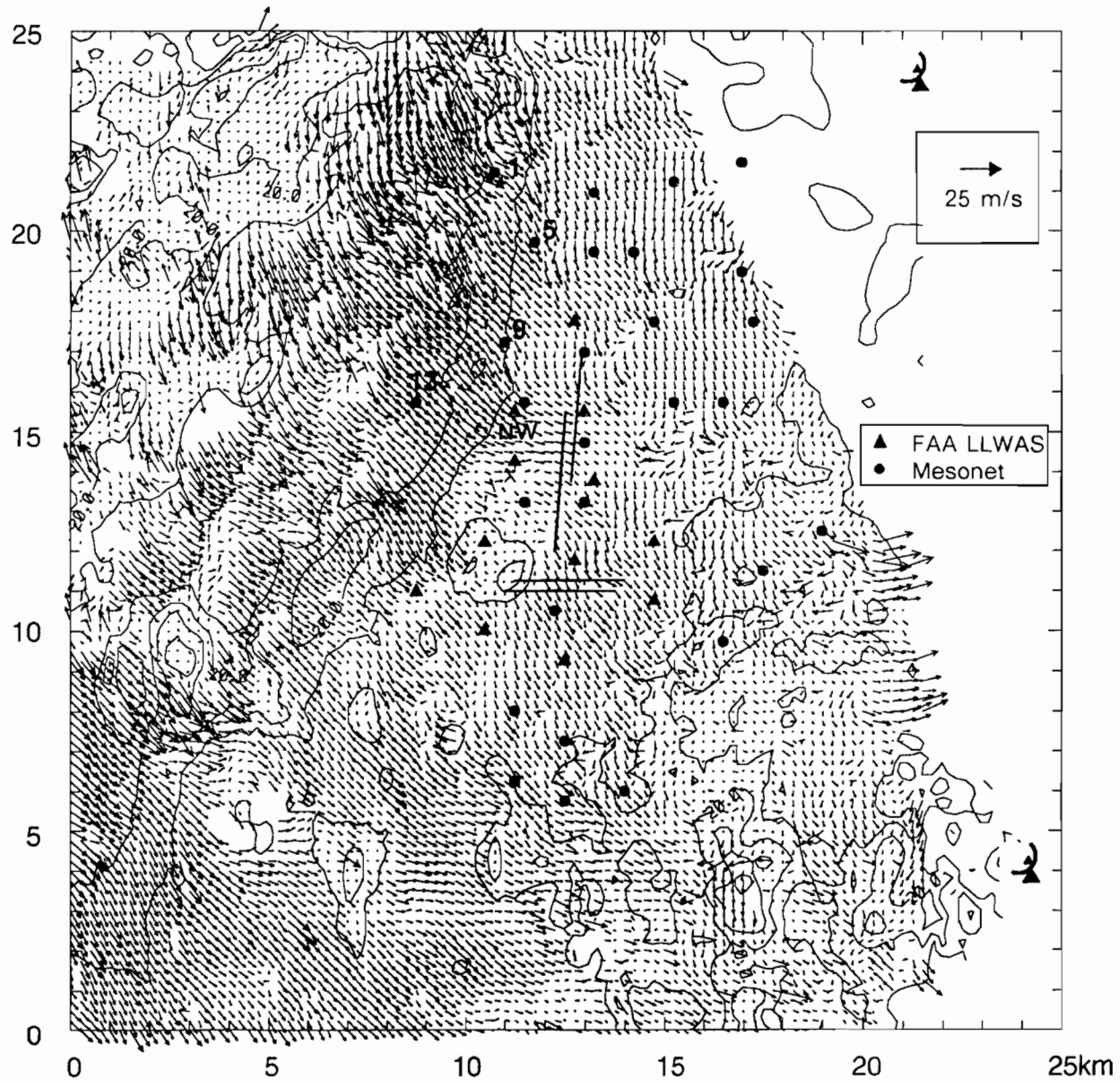

Figure VII-5a. Dual Doppler plot of the wind and reflectivity field at 2218:16 UTC on 28 August 1987. The gust front, which is now entering the western portion of the network, is located along the thin reflectivity line.

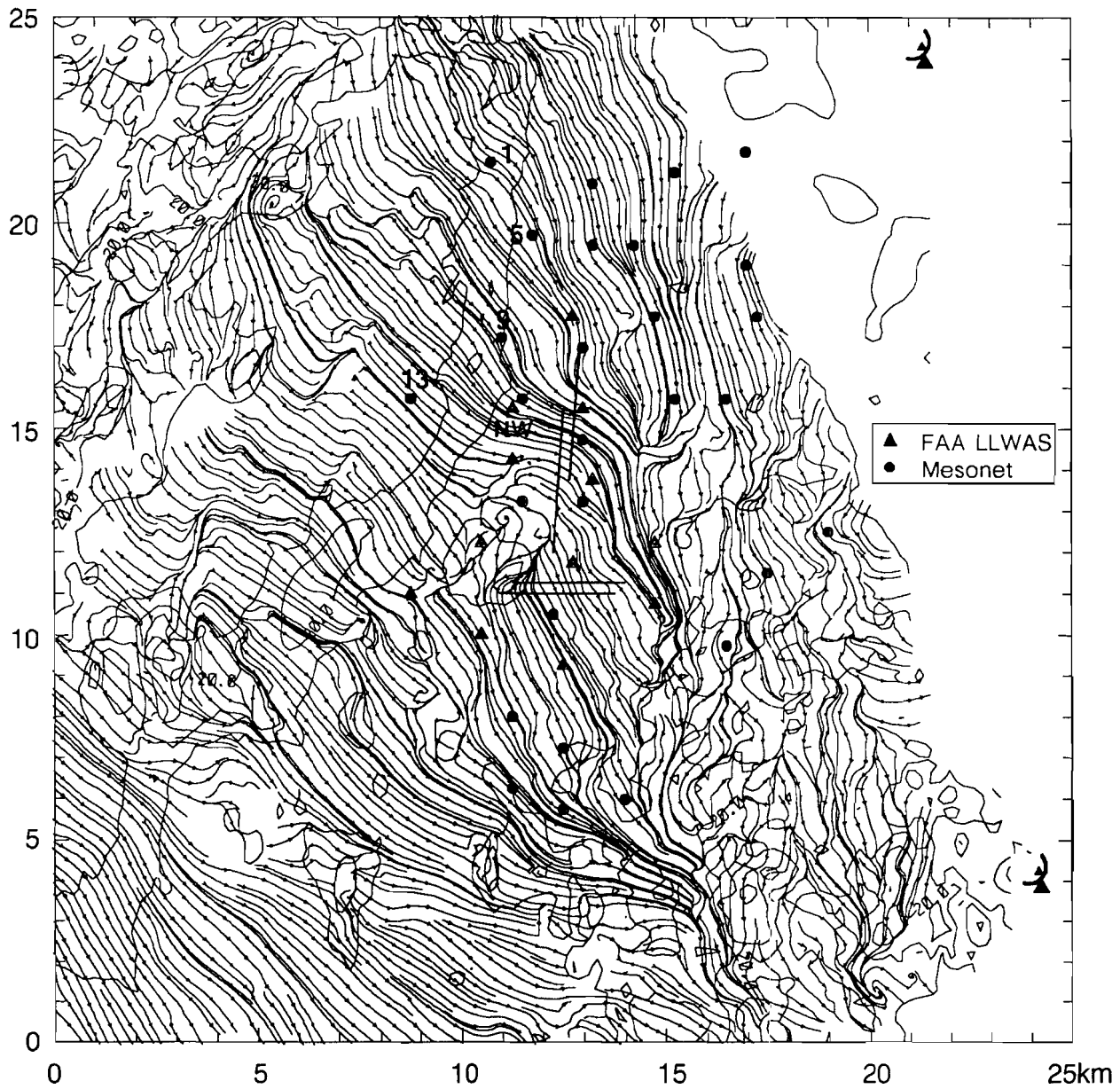

Figure VII-5b. Dual Doppler plot of the streamline and reflectivity field at 2218:16 UTC on 28 August 1987.

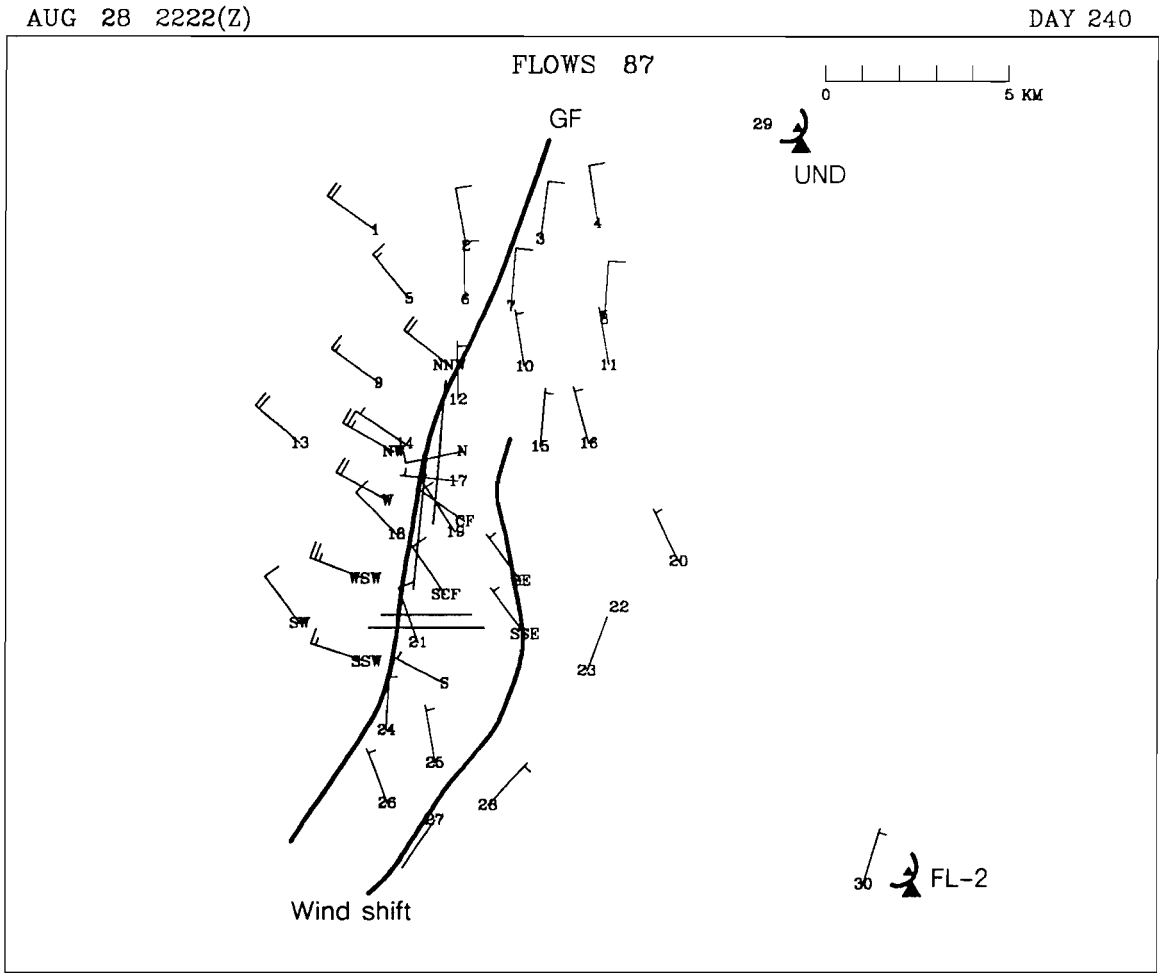

Figure VII-6. Mesonet/LLWAS winds at 2222 UTC on 28 August 1987. The division between light and strong northwesterly winds signifies the location of the gust front (GF). It appears as though there may be a separate, weaker wind shift line ahead of the gust front in the southern part of the network.

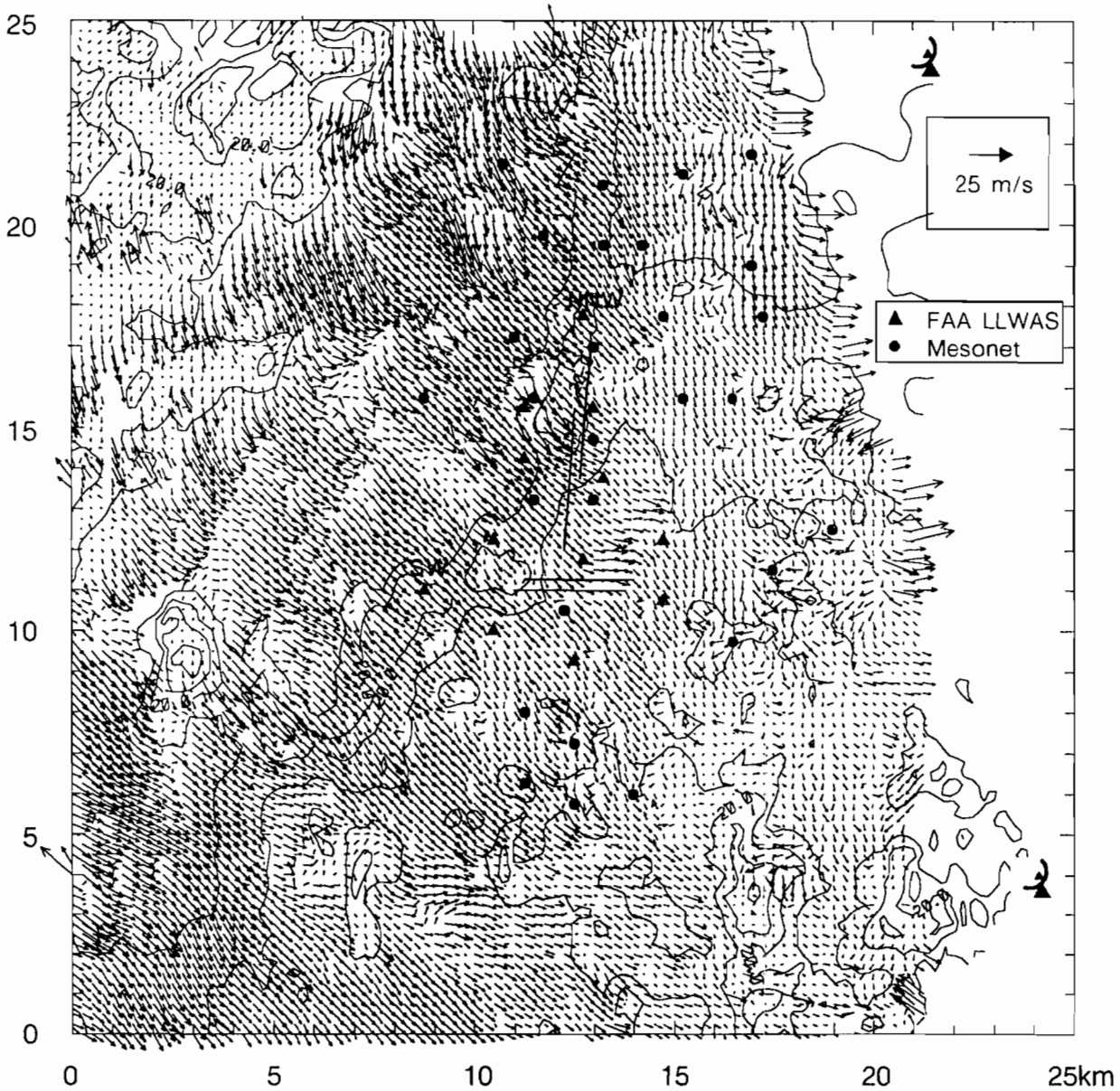

Figure VII–7a. Dual Doppler plot of the wind and reflectivity field at 2222:21 UTC on 28 August 1987. The gust front is now centered over the runways.

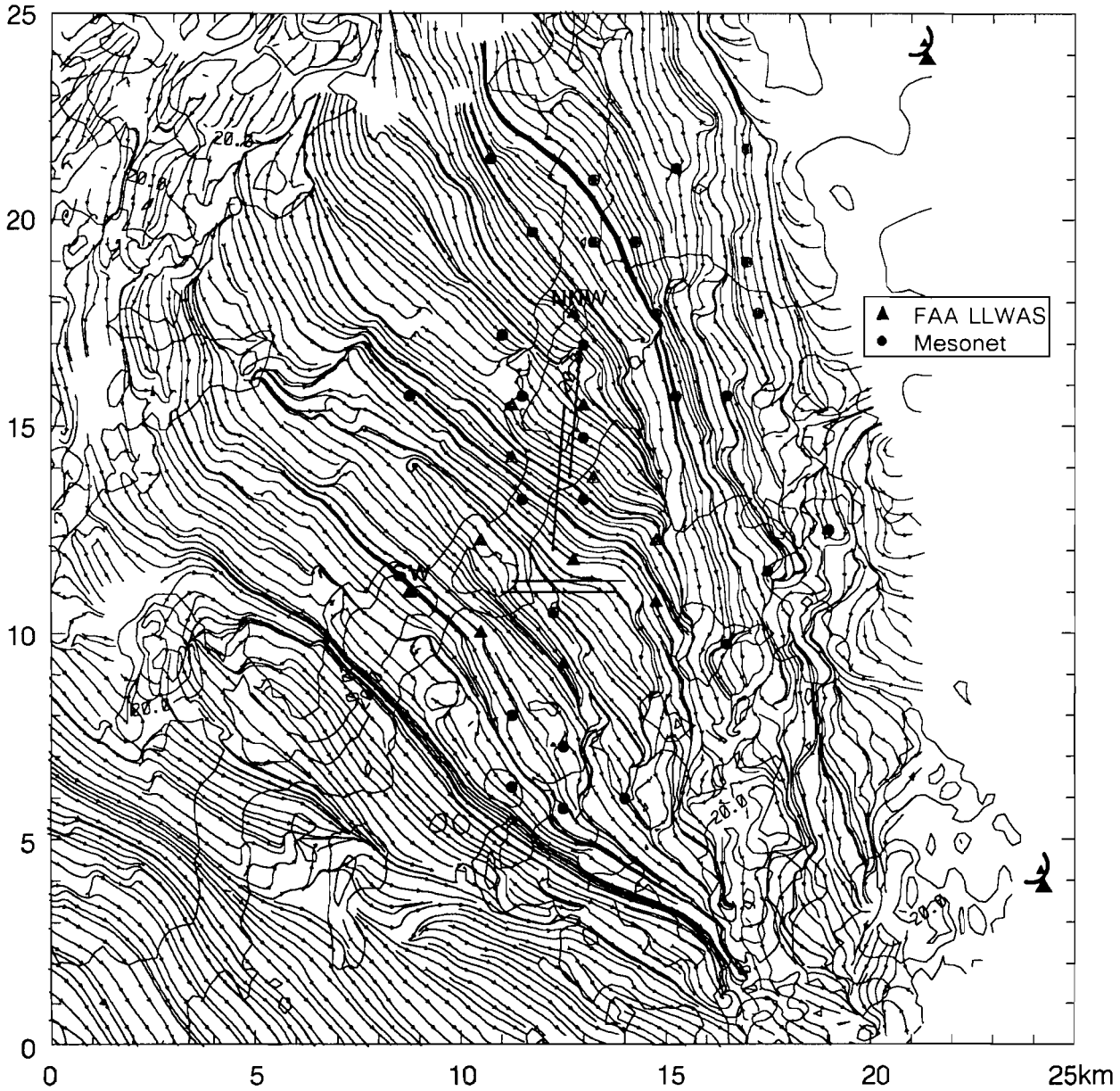

Figure VII-7b. Dual Doppler plot of the streamline and reflectivity field at 2222:21 UTC on 28 August 1987. Even though the streamlines would seem to detect a gust front approaching FL-2; the reflectivity line, in the center of the image, is the true location of the gust front.

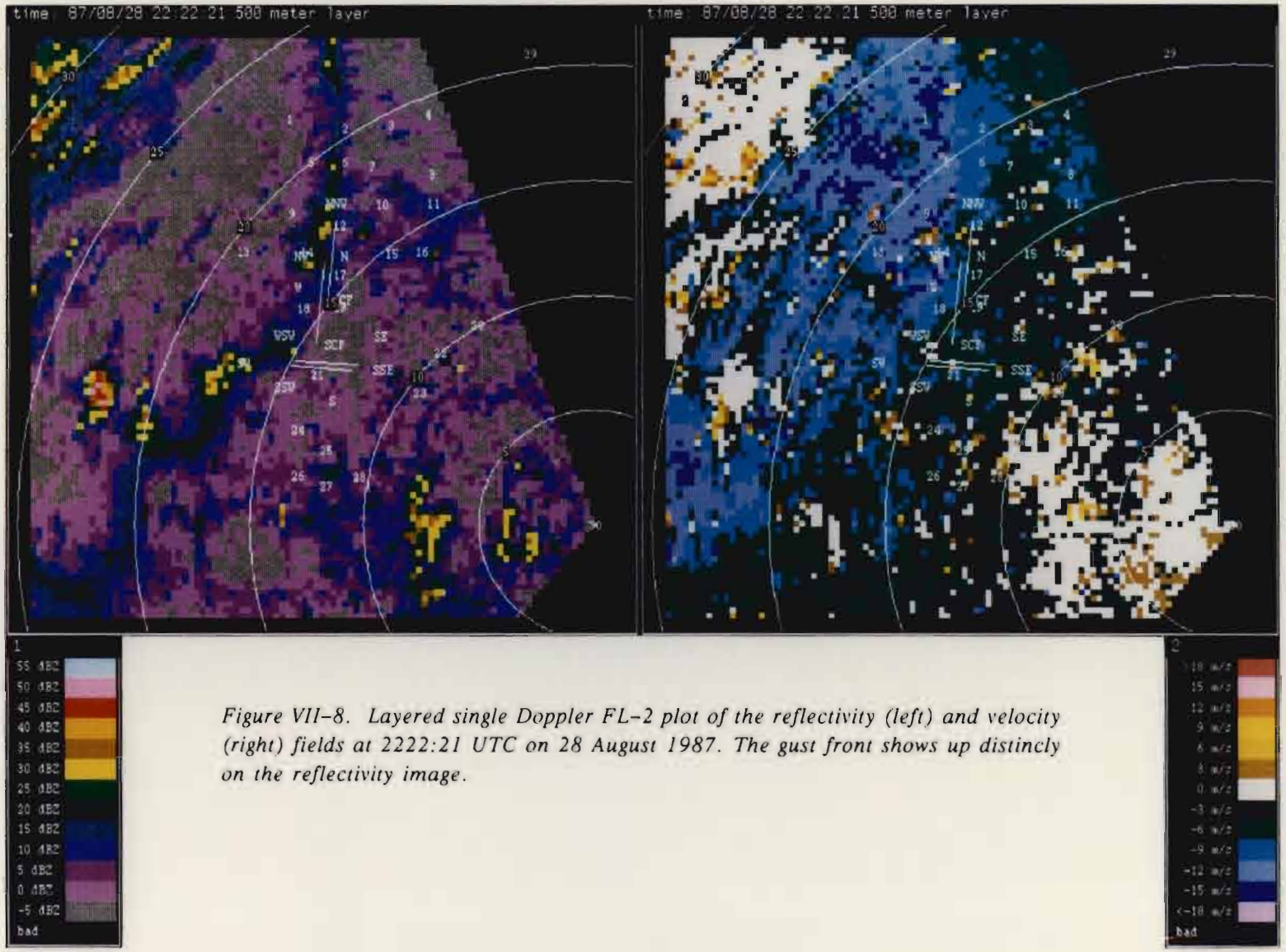

Figure VII-8. Layered single Doppler FL-2 plot of the reflectivity (left) and velocity (right) fields at 2222:21 UTC on 28 August 1987. The gust front shows up distincly on the reflectivity image.

tivity values than did FL–2 in the region of the thin line. The Doppler velocity pattern shown in Fig. VII–8 agrees well with the dual Doppler wind analysis, because the true wind direction was very close to the radial wind direction with respect to FL–2.

As the gust front continued to push further east, the reflectivity line became more organized and consequently stronger echoes developed, particularly northeast of the runways. By late in the period (2227 UTC), the FL–2 radar was detecting velocities of 17.4 m/s in a few small areas near the airport runways (not shown).

VIII. 2 SEPTEMBER 1987

Several microbursts, some moving across the mesonet/LLWAS network from the northwest and some developing right over the network, were the principal wind shear events during the day. Also, a gust front located in the southern part of the network moved toward the north, at the same time another gust front, located near the UND radar, moved toward the south. The two gust fronts collided just north of the runways before moving eastward. All of these wind shear events were captured in a dual Doppler mode.

A. Available Data

The time period of interest was 2200–2315 UTC. This was later revised to include an additional 15 minutes. Mesonet, LLWAS, and FL–2 single Doppler data were provided for the period 2200 to 2330 UTC. It was possible to perform dual Doppler analyses for this same time period, at roughly one minute intervals. The FL–2 and UND radar scan times, and the differences between these scan times, for each dual Doppler analysis are given below in Table VIII–1.

Only 5 different UND surface scans were available during the first 25 minutes of the requested time period. Each of these scans was paired with 3–4 unique FL–2 scans to produce the first 16 dual Doppler analyses. Pair Nos. 2, 5, 8, 12, and 16 have the smallest time differences between the FL–2 and UND scan times, and are thus the most accurate analyses; other analyses in this time period should be used for qualitative purposes only.

Table VIII–1. FL–2 and UND scan times used for 2 September 1987 dual Doppler analyses.

Dual Doppler Pair	FL–2 time (UTC)	UND time (UTC)	Time diff. (sec)
1	2200:48	2201:41	53
2	2201:47	2201:41	**6**
3	2202:54	2201:41	73
4	2203:57	2205:19	82
5	2204:55	2205:19	**24**
6	2205:53	2205:19	34
7	2215:14	2216:14	60
8	2216:16	2216:14	**2**
9	2217:15	2216:14	61
10	2218:14	2219:52	98
11	2219:13	2219:52	39
12	2220:20	2219:52	**28**
13	2221:22	2219:52	90

14	2222:20	2223:57	97
15	2223:19	2223:57	38
16	2223:58	2223:57	**1**
17	2225:04	2225:00	4
18	2226:06	2226:00	6
19	2227:05	2227:01	4
20	2228:03	2227:58	5
21	2229:02	2229:00	2
22	2230:08	2230:03	5
23	2231:10	2231:03	7
24	2232:09	2232:04	5
25	2233:07	2233:01	6
26	2234:06	2234:03	3
27	2235:12	2235:05	7
28	2236:14	2236:06	8
29	2237:13	2237:07	6
30	2238:11	2238:04	7
31	2239:10	2239:06	4
32	2240:16	2240:10	6
33	2241:18	2241:10	8
34	2242:17	2242:11	6
35	2243:15	2243:08	7
36	2244:13	2244:10	3
37	2245:20	2245:13	7
38	2246:22	2246:13	9
39	2247:20	2247:14	6
40	2248:18	2248:10	8
41	2249:17	2249:12	5
42	2250:24	2250:15	9
43	2251:25	2251:16	9
44	2252:24	2252:17	7
45	2253:22	2253:14	8
46	2254:21	2254:15	6
47	2255:27	2255:19	8
48	2256:29	2256:19	10
49	2257:27	2257:20	7
50	2258:25	2258:17	8
51	2259:24	2259:19	5
52	2300:30	2300:22	8
53	2301:31	2301:22	9
54	2302:30	2302:23	7
55	2303:28	2303:19	9
56	2304:27	2304:22	5

57	2305:33	2305:25	8
58	2306:35	2306:25	10
59	2307:33	2307:26	7
60	2308:31	2308:23	8
61	2309:30	2309:24	6
62	2310:36	2310:28	8
63	2311:38	2311:28	10
64	2312:37	2312:29	8
65	2313:35	2313:26	9
66	2314:33	2314:28	5
67	2315:40	2315:30	10
68	2316:41	2316:31	10
69	2317:40	2317:31	9
70	2318:38	2318:28	10
71	2319:36	2319:30	6
72	2320:42	2320:33	9
73	2321:44	2321:34	10
74	2322:42	2322:34	8
75	2323:40	2323:31	9
76	2324:39	2324:34	5
77	2325:45	2325:37	8
78	2326:47	2326:37	10
79	2327:45	2327:38	7
80	2328:43	2328:35	8
81	2329:41	2329:37	4
82	2330:48	2330:40	8

B. Synoptic Situation

By noon, a line of thundershowers extended along the front range of the Rocky Mountains. Several microburst scale outflows were detected over the mountains, but they did not enter the mesonet area. At 1850 UTC, a gust front was scanned west of Stapleton airport. The gust front boundary only impacted the southern-most LLWAS sensor (S). Later in the day (2130 UTC), strong cells formed along a boundary north of the UND radar. As the boundary drifted southward, new cloud growth aloft was observed near Stapleton airport. As a result, a number of microburst outflows, all with similar radial velocity differentials, impacted regions in and around the mesonet/LLWAS network. The divergent outflows were captured by both radars during the period from 2230 to 2330 UTC.

At 2100 UTC, one hour before dual Doppler scanning began, surface temperatures were in the 80's and low 90's (°F). As in the previous wind shear event

studies, a dry air mass was present over much of the state, with surface dewpoints in the 40's (°F). Scattered thundershowers were present in the region north and northwest of the airport. At this time, many stations throughout the state were reporting light southwesterly winds.

Figure VIII-1 is an infrared satellite image of the cloud conditions over Colorado at 2201 UTC. Much of central CO is overspread with clouds. A few of the more developed clouds (denoted as the darker grey regions) appear to be positioned northwest and southwest of Stapleton airport. One hour later (Fig. VIII-2), these cells have become taller and more widespread (regions now contain black, denoting even colder cloud temperatures), and have moved slowly eastward. Figure VIII-2 was taken at a time when several microbursts had just dissipated over the mesonet/LLWAS network.

The long range reflectivity map from FL-2 at 2302 UTC (Fig. VIII-3) exhibited a small area of very weak echoes (5-15 dBZ) in the vicinity of the airport, as well as many isolated cells that were scattered throughout the state. This image agrees closely with Fig. VIII-2 in the placement of the large cell, 42 km to the northeast of FL-2. Maximum reflectivity echoes from this cell, which contained hail, were 55 dBZ. The echo tops were measured by the National Weather Service radar to be 38,000 feet. Movement of all of these cells was eastward at $\sim$ 5 m/s.

C. Wind Shear Events

i. Wind Shear Summary and Examples

Several microbursts and two gust fronts impacted the mesonet/LLWAS network during the hour from 2200 to 2300 UTC. Figure VIII-4 shows the progression of all of the wind shear events within the dual Doppler analysis region during the time period of interest.* At 2215 UTC, microburst A, detected as a 19 m/s radial velocity differential, moved into radar range from the west and continued to strengthen as it travelled toward the east.

At roughly the same time, microburst B, located 10 km north-northwest of Stapleton airport, developed and then moved westward, only to dissipate a few minutes later.

As microburst A entered the northwest region of the mesonet/LLWAS network (2240), the main divergent flow began to deteriorate, and transfer its energy to another divergent flow (microburst A′) which developed northeast of mesonet station No. 9 (2242). This cell (A′) began to breakup southeast of LLWAS station NNW at 2247, but pulsed into a third divergent flow (microburst A″) southwest of station No. 10 (2250). However, A″ was very weak and quickly dissipated. As the energy

* The mesonet and Doppler radar signatures of the microbursts in Fig. VIII-4 have been compared in detail by John DiStefano at Lincoln Laboratory (see DiStefano, 1988).

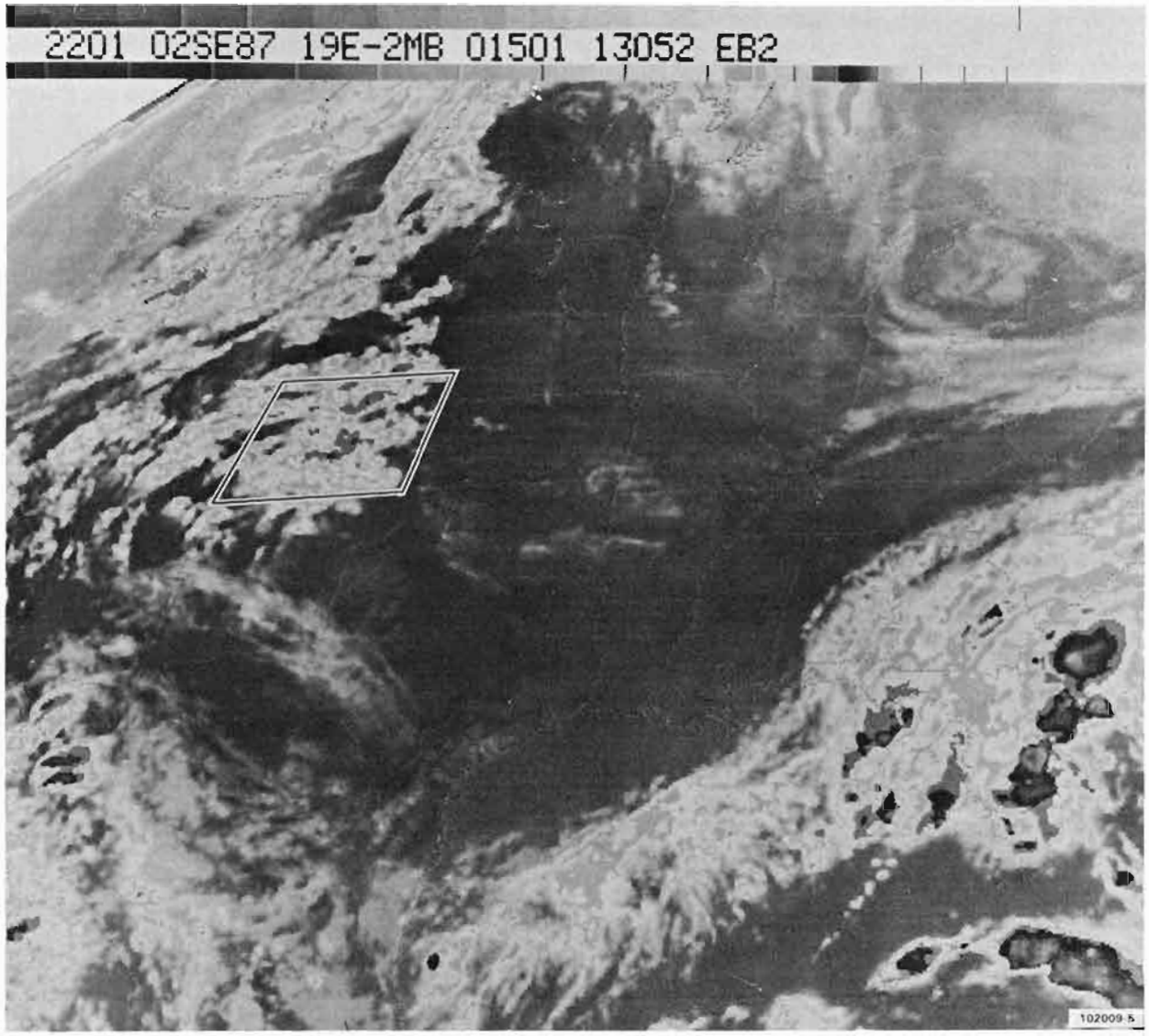

Figure VIII-1. Infrared satellite image of the central U.S. taken at 2201 UTC on 2 September 1987. This image represents cloud conditions 40 minutes before microbursts began to enter the mesonet/LLWAS network. See Fig. V-3 caption for description of the cloud temperature grey scale used here.

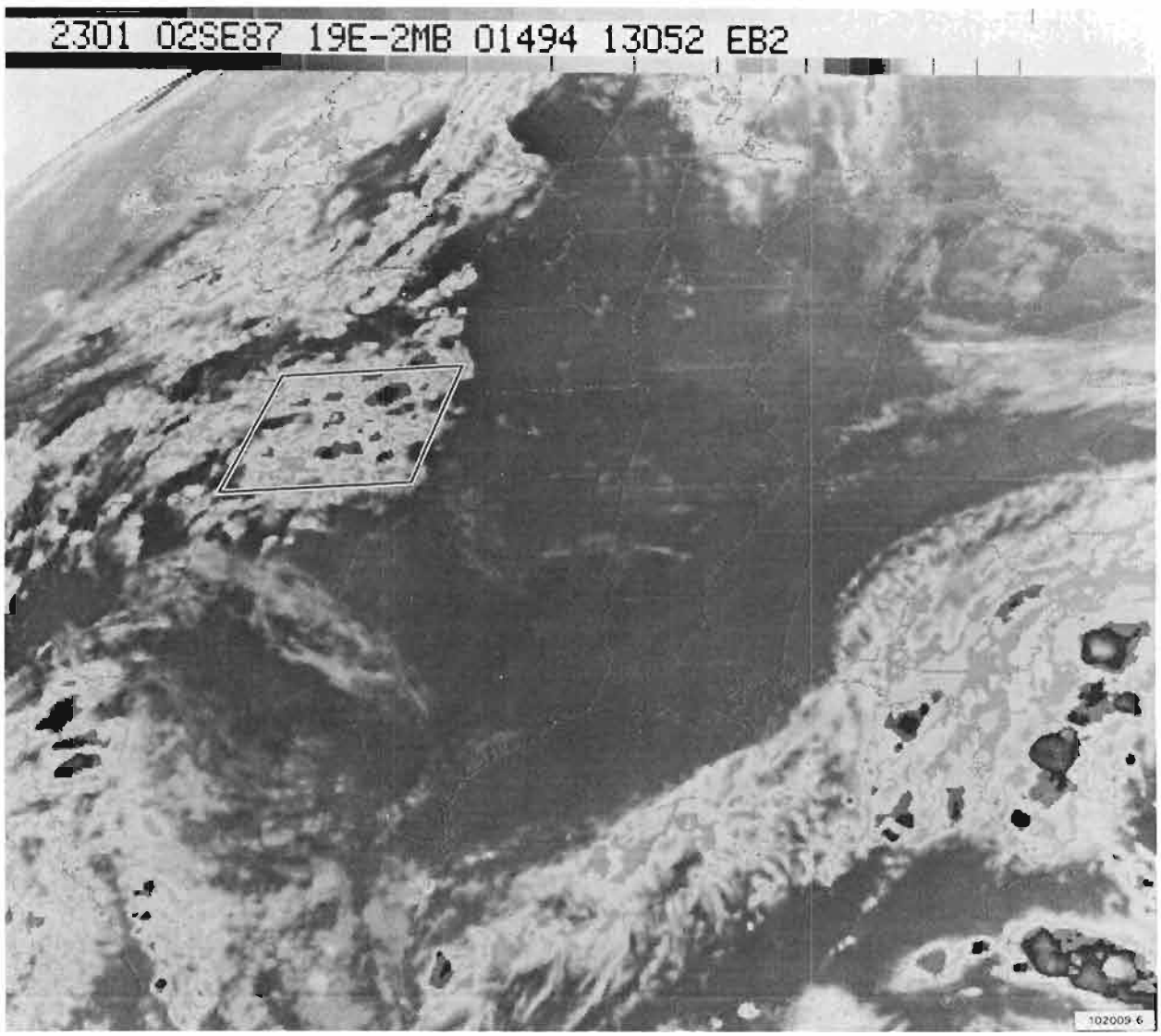

Figure VIII-2. Infrared satellite image of the central U.S. taken at 2301 UTC on 2 September 1987. Compared to the previous satellite image (Fig. VIII-1), the cells to the northeast and southwest of Stapleton airport have become taller (colder cloud temperatures) and more widespread.

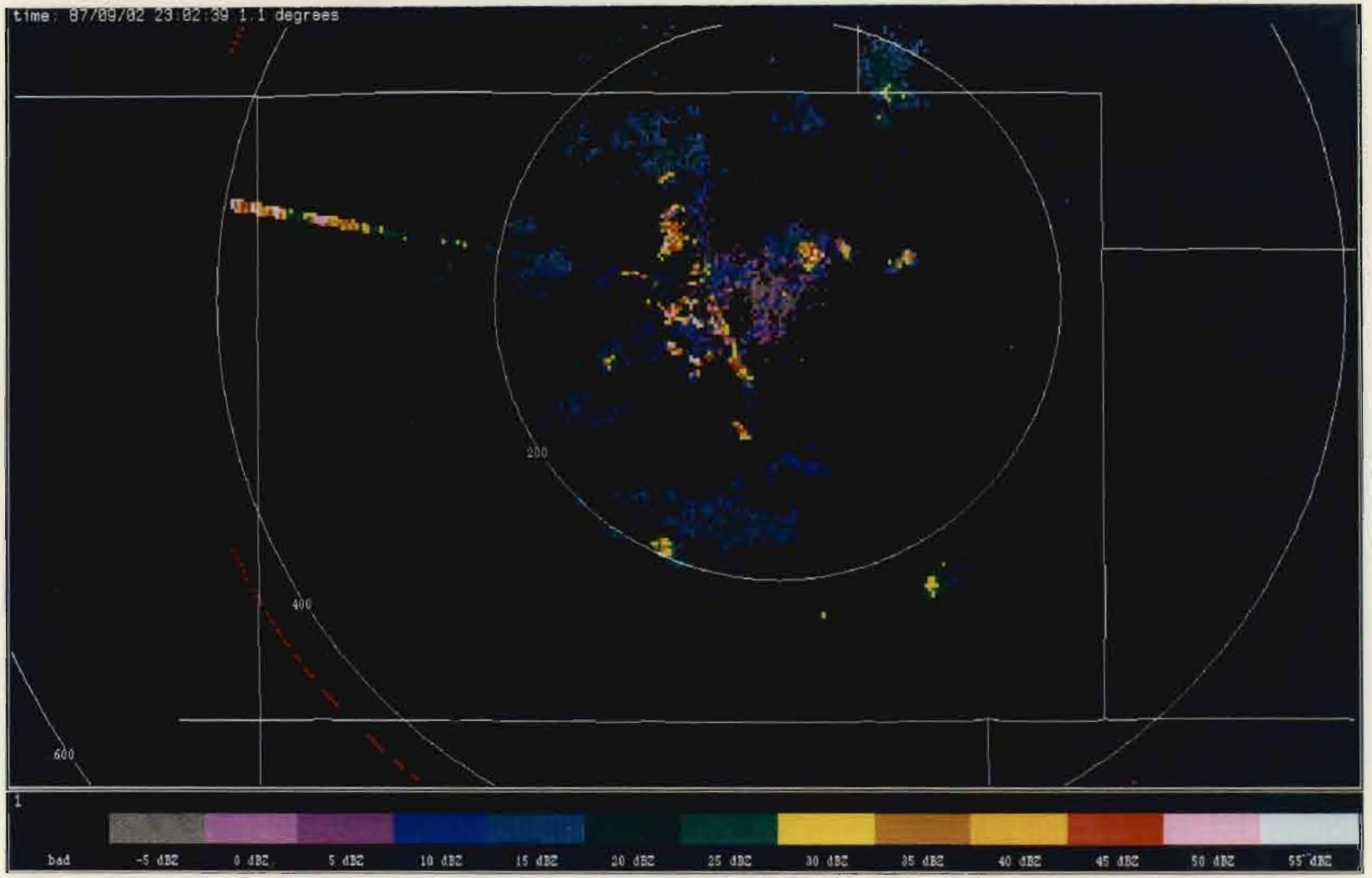

Figure VIII-3. Long range reflectivity map from FL-2 at 2302:39 UTC on 2 September 1987. Very small and weak echoes are detected over the mesonet/LLWAS network, indicating that the microbursts occurring on this day were dry. The radial of data extending out to 400 km (in northwestern Colorado) is erroneous.

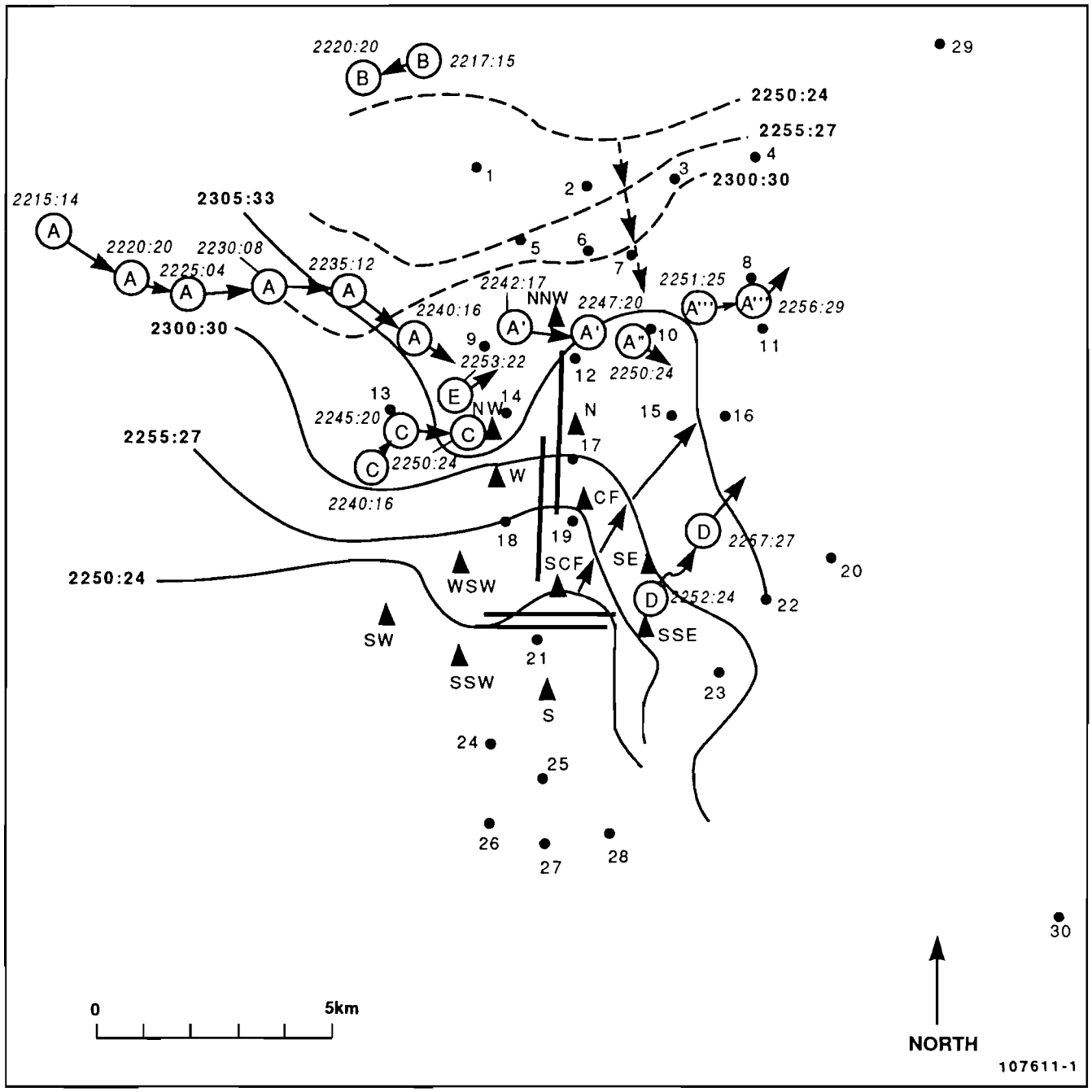

Figure VIII–4. Map representing the progression of the microbursts and gust fronts during the 2200–2330 UTC time period for 2 September 1987. Map is based on dual Doppler data. Solid lines show the progression of the gust fronts. Circled letters denote the progression of the microbursts. Microburst A continually pulsed along its west to east path; thus generating several cells from the original parent cell over the northern quadrant of the network.

from the original microburst continued to pulse along its west to east path, a fourth and rather strong (20 m/s radial velocity differential) divergent flow (microburst A′′′) formed northeast of station No. 10 (2251). This microburst moved between mesonet station Nos. 8 and 11 before it weakened at 2257 UTC.

At the same time microburst A began to weaken (2240), microburst C, with a surface outflow of 10 m/s (according to FL–2 single Doppler measurements), formed south of station No. 13. Figure VIII–5 shows the mesonet/LLWAS wind field, and Fig. VIII–6a shows the dual Doppler wind field at this time. The only evidence of a microburst signature in the mesonet wind field is the strong outflow at station Nos. 5, 9, 13, and NNW (No. 9 measured a peak wind speed of 20 m/s). The dual Doppler wind field, and especially the streamline analysis (Fig. VIII–6b), clearly reveal the divergent line of the eastward moving microburst A and the newly formed microburst C. In the dual Doppler analyses, station No. 13 appears to be exactly between these two events, but the mesonet winds (Fig. VIII–5) reveal that it was predominantly influenced by the outflow from microburst A.

In the following 5 minutes (from 2240 to 2245), microburst C moved northward toward station No. 13. According to mesonet/LLWAS wind plots (not shown) from 2246–2252 UTC, microburst C moved eastward and then dissipated. However, in the dual Doppler analyses (not shown) the outflow began to weaken at 2245, and by 2247 could no longer be classified as a microburst.

Microburst D then developed slightly north of LLWAS station SSE at 2252 UTC. This cell appeared to be one of the stronger surface outflows during this day. LLWAS stations SE and SSE observed a wind velocity differential of 15 m/s while FL–2 single Doppler radar detected a 19 m/s radial velocity outflow. The microburst moved northeastward and dissipated by 2300 UTC (see Fig. VIII–4).

The final microburst occurring within the time period (microburst E) developed southwest of station No. 9 at 2253, according to the surface mesonet/LLWAS data. Figure VIII–7 shows the four microbursts (A′′, A′′′, D, and E) and two gust fronts occurring simultaneously at this time. The first microburst (A′′) is situated between station Nos. 10, 15, and 16. The second microburst (A′′′) is located to the west of mesonet station Nos. 8 and 11. Both of these stations measured wind speeds in excess of 15 m/s. The third microburst (D), which had developed in the preceding minute, is located between stations SE and 22. A 15 m/s peak wind differential was recorded at that time. The fourth microburst (E), which had just developed, is impacting station Nos. 9 and 13. Microbursts A′′′, D, and E appear to be well defined by the dual Doppler wind and streamline plots in Figs. VIII–8a and VIII–8b, respectively, but the divergence associated with microburst A′′ appears to have diminished considerably.

The clear divergent signature of microburst E in the dual Doppler plot in Fig. VIII–8a was apparently enhanced by smoothing the UND velocity field before com-

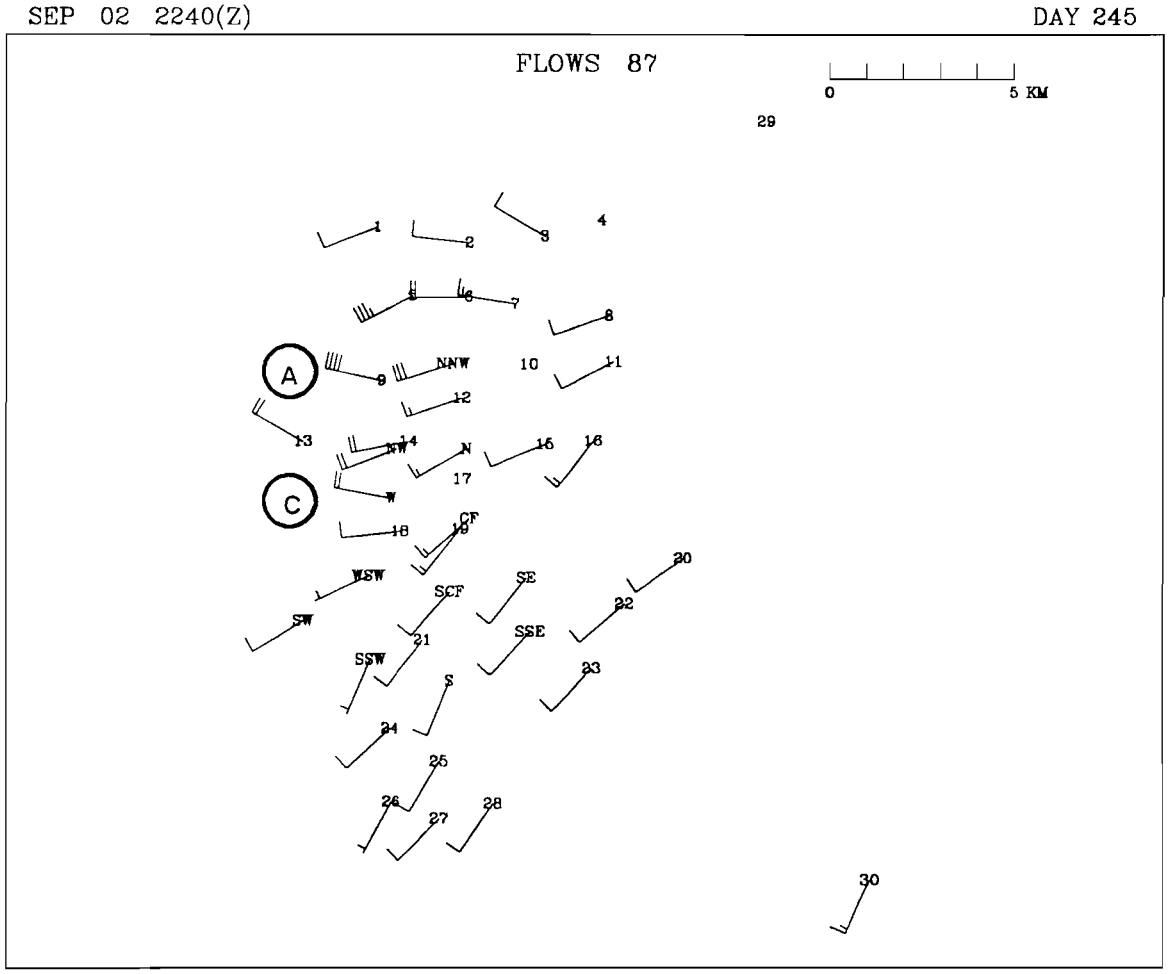

Figure VIII-5. Mesonet/LLWAS winds at 2240 UTC on 2 September 1987. Strong outflow winds are evident in the western quadrant of the network from microbursts located to the west of station No. 9 and south of station No. 13. A full barb on the wind direction arrow represents 5 m/s and a half barb represents 2.5 m/s.

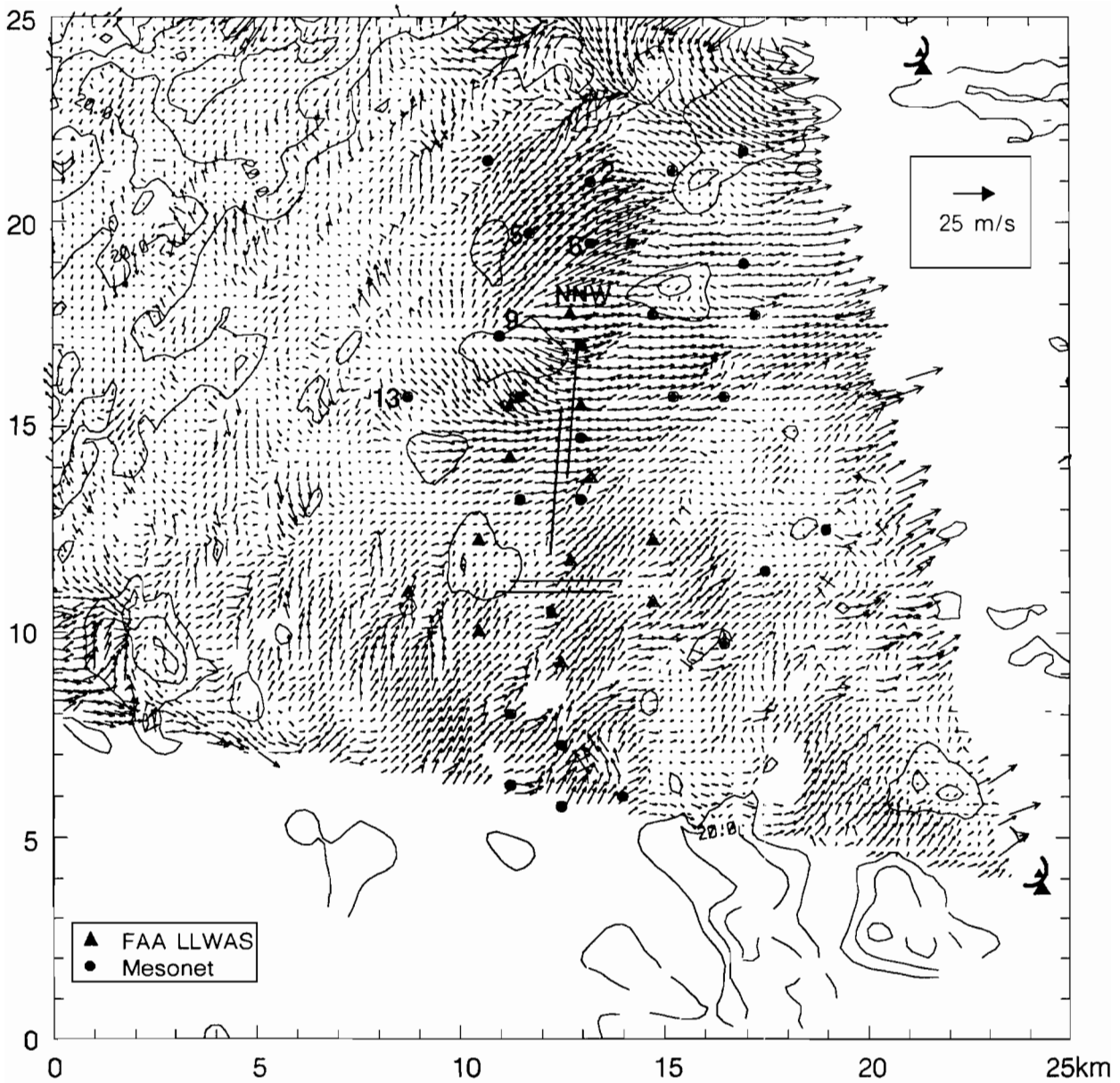

Figure VIII-6a. Dual Doppler plot of the wind and reflectivity field at 2240:16 UTC on 2 September 1987. Strong outflow winds, from the microburst to the west of station No. 9, can be seen impacting stations 2, 5, 6, and NNW.

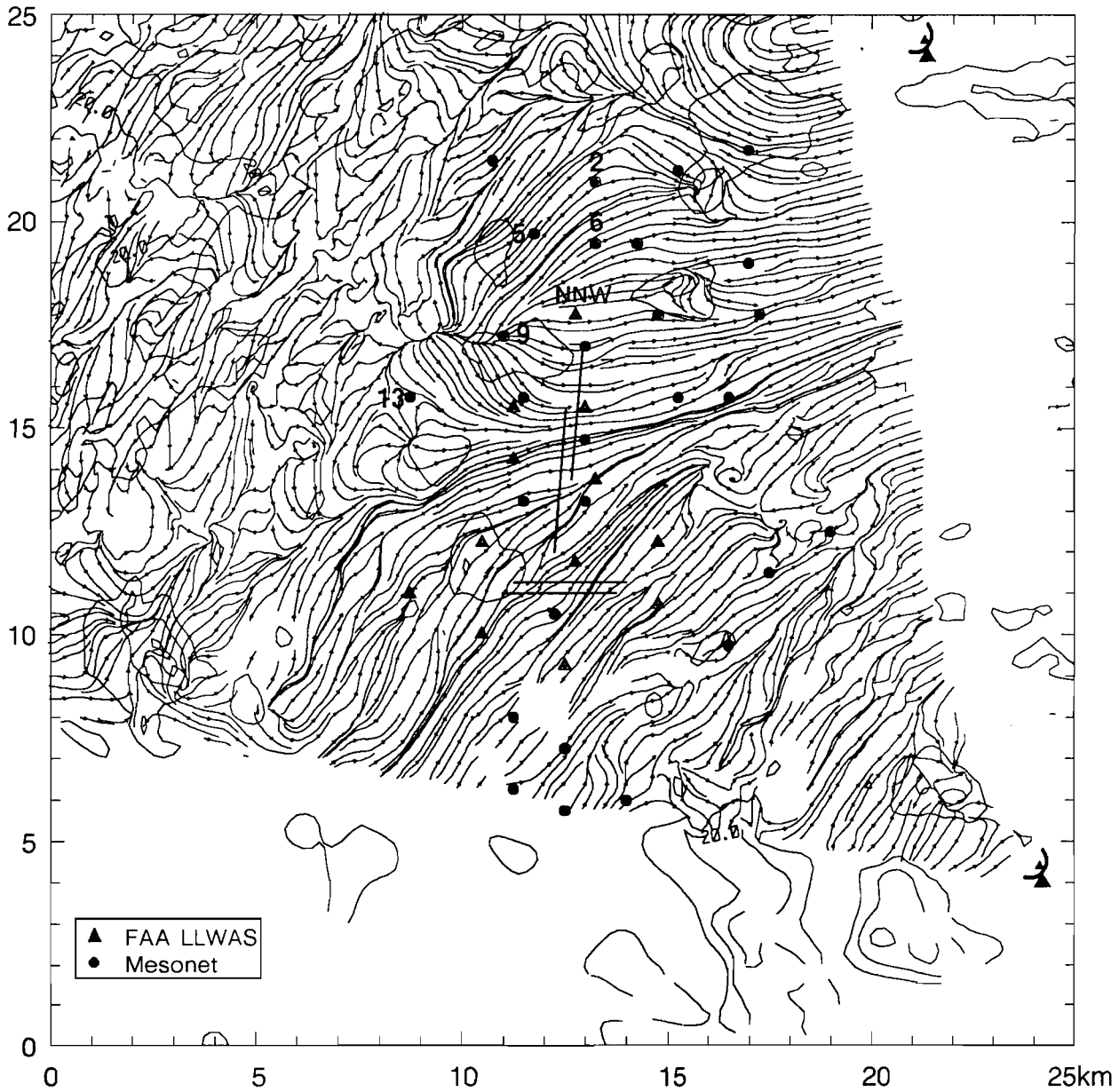

Figure VIII-6b. Dual Doppler plot of the streamline and reflectivity field at 2240:16 UTC on 2 September 1987. Two microburst signatures, located about 5 km west of the runways, show up clearly in this image.

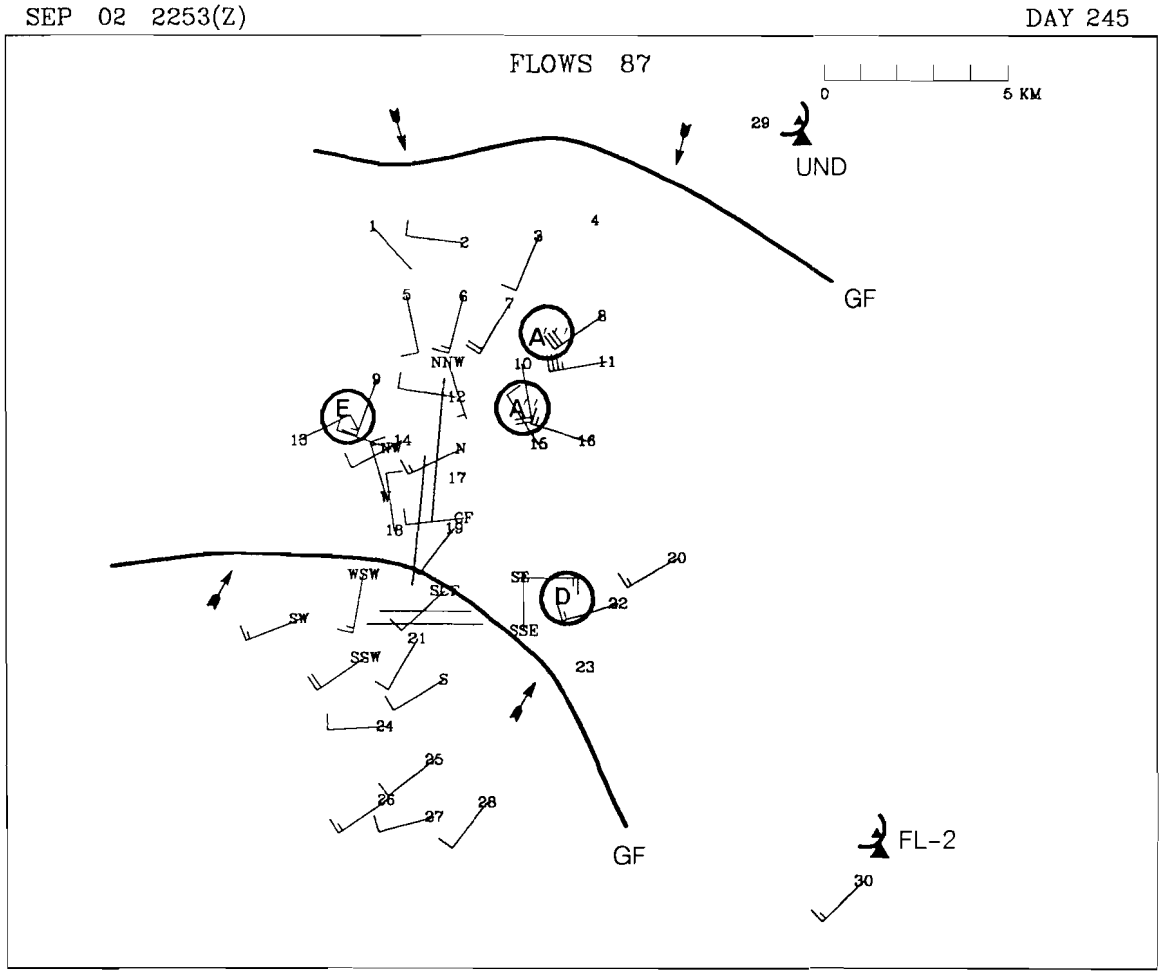

Figure VIII-7. Mesonet/LLWAS winds at 2253 UTC on 2 September 1987. The locations of four simultaneously occurring microbursts are denoted by the circled letters. Two gust fronts were also present at this time and the arrows behind each gust front indicate the direction of movement.

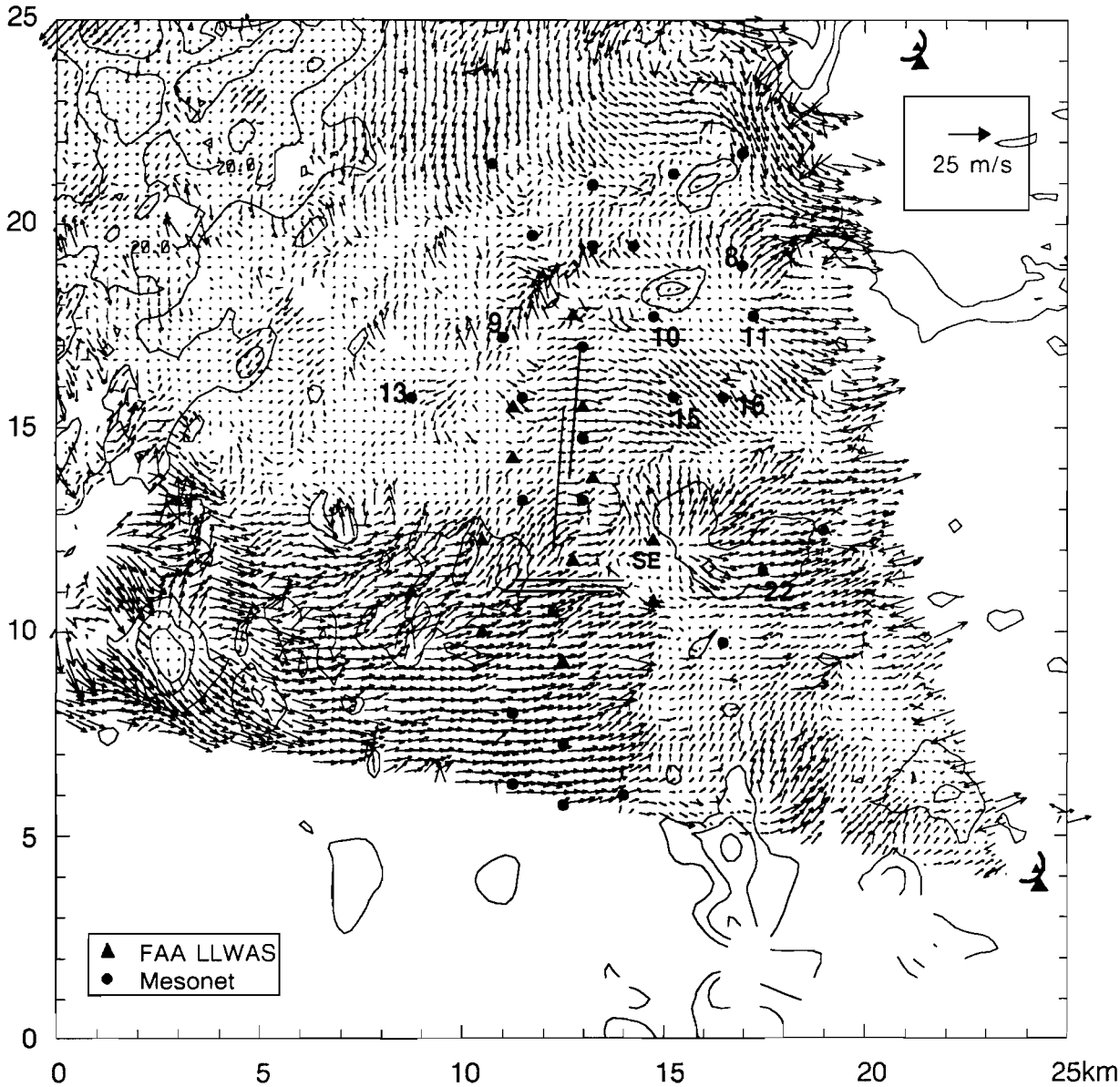

Figure VIII–8a. Dual Doppler plot of the wind and reflectivity field at 2253:22 UTC on 2 September 1987. A fourth, recently developed microburst, is located between station Nos. 9 and 13.

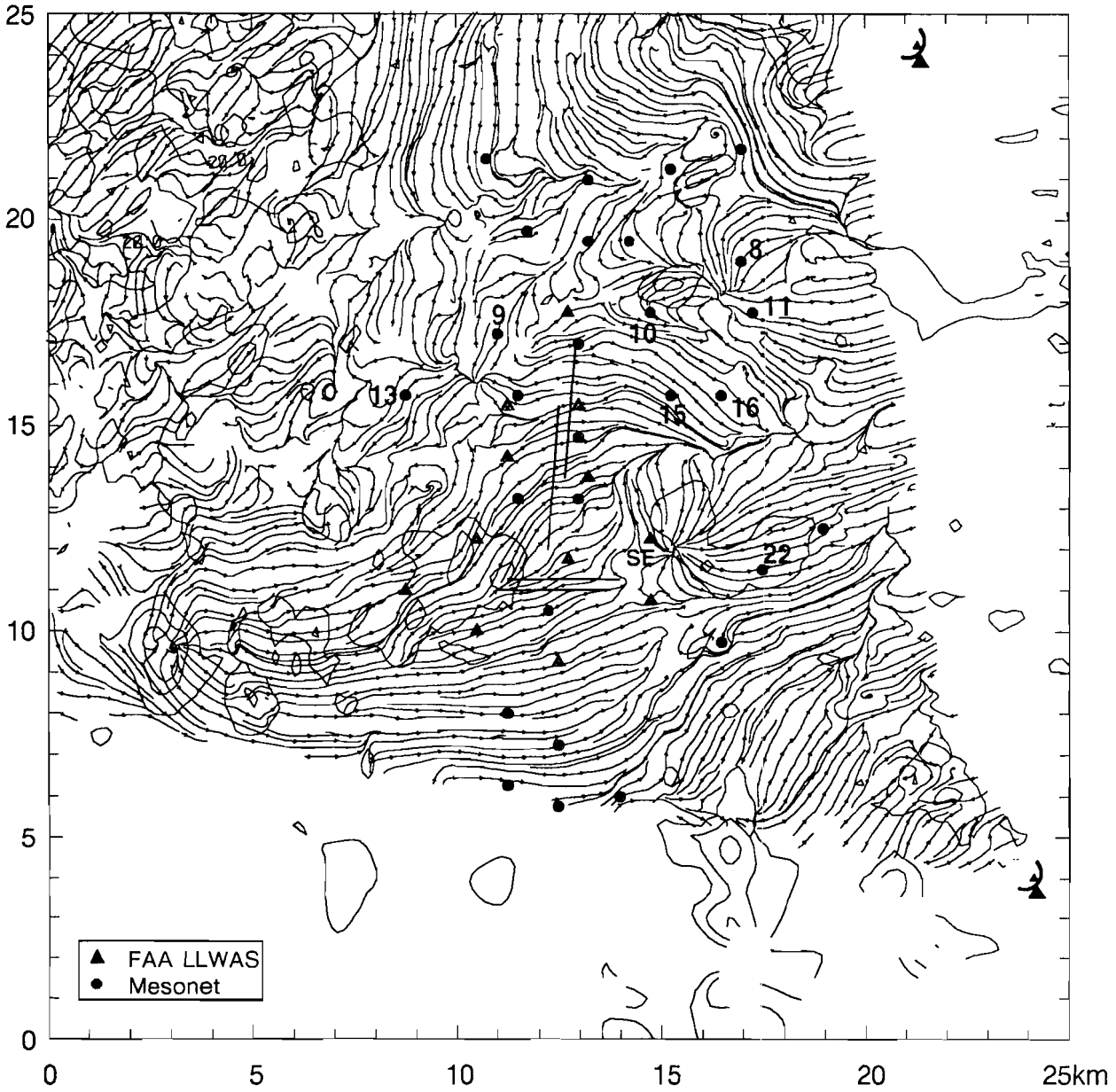

Figure VIII-8b. Dual Doppler plot of the streamline and reflectivity field at 2253:22 UTC on 2 September 1987. This image shows the microbursts more clearly than the wind vector image in Fig. VIII-8a.

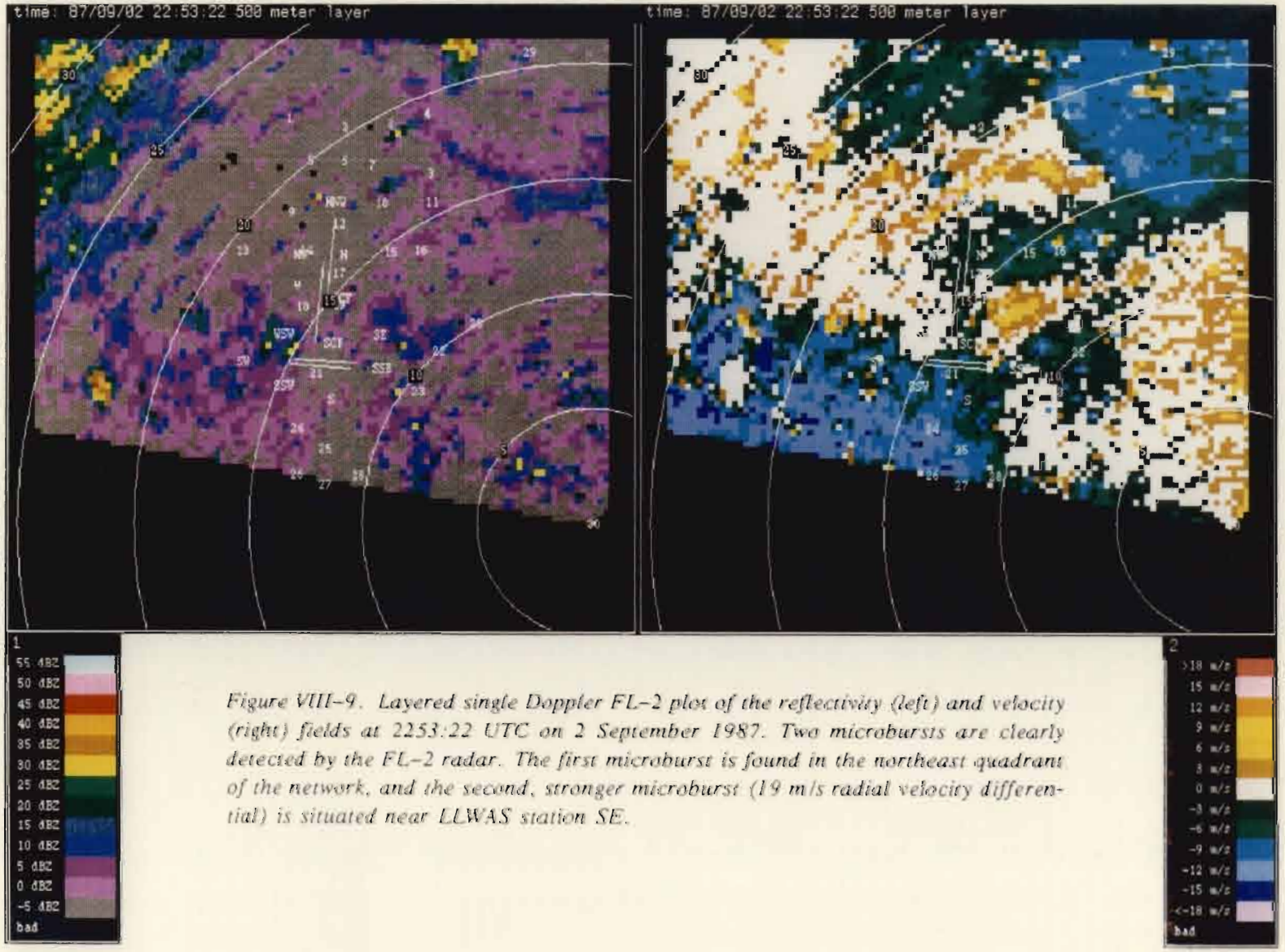

Figure VIII–9. Layered single Doppler FL–2 plot of the reflectivity (left) and velocity (right) fields at 2253:22 UTC on 2 September 1987. Two microbursts are clearly detected by the FL–2 radar. The first microburst is found in the northeast quadrant of the network, and the second, stronger microburst (19 m/s radial velocity differential) is situated near LLWAS station SE.

bining it with the unsmoothed FL-2 velocity field in the dual Doppler analysis procedure (see Appendix A). DiStefano (1988) thresholded the FL-2 velocities at 6 dB signal-to-noise ratio, and found that microburst E could no longer be identified.* This type of microburst, with a shallow outflow and very weak reflectivity return will always be difficult to detect with Doppler radar.

Figure VIII-9 also shows nicely the two gust fronts present at this time. A thin reflectivity line and strong convergence in the Doppler velocity field give evidence of the southward-moving gust front 7 km northeast of Stapleton, while only the Doppler signature reveals the (even stronger) northward-moving gust front southwest of the airport. The progression of these two gust fronts can be seen in Fig. VIII-4.

By 2307 UTC, the intersection of these two gust fronts over the northern runway produced a small cyclonic circulation (counter-clockwise rotation) between stations 12 and N. This circulation persisted for 10 minutes as it moved rapidly toward the east. After the two gust fronts had collided over the northern runway (2311 UTC), winds shifted into the west and northwest throughout the network, and a maximum wind speed of 15.6 m/s was detected over the airport by the FL-2 single Doppler radar (not shown).

* This microburst case is discussed in depth by DiStefano (1988), who classified it as "undetected" by the FL-2 Doppler radar, but "detected" by the LLWAS and mesonet.

IX. SUMMARY

The FAA evaluation of the enhancements to the LLWAS at Denver Stapleton International Airport took place from 3 August through 4 September, 1987. Lincoln Laboratory's responsibilities included providing a color workstation display showing Doppler radar data fields over Stapleton for use in real-time by FAATC and SEIC meteorologists, providing terminals for alphanumeric LLWAS message display, collecting data with 1-minute resolution from a 30-station mesonet sited around Stapleton, and collecting radar data in a dual Doppler mode (with the FL-2 and UND Doppler radars) when wind shear events impacted the airport.

This report has documented the seven wind shear cases that occurred during the LLWAS evaluation period that were requested by FAATC for in-depth analysis. A chapter of this report was devoted to each wind shear case. Each chapter contained a description of the available data sent to FAATC and examples of wind shear as indicated by the mesonet and LLWAS wind fields. For the four cases for which dual Doppler analyses were calculated, a description of the synoptic situation (surface weather conditions, upper level wind conditions, and satellite cloud maps) for the state of Colorado for the time period of interest was also included. A figure summarizing the wind shear events occurring during the requested time periods, and examples of the wind shear signatures as documented by mesonet/LLWAS synoptic wind plots, dual Doppler wind fields, and color FL-2 single Doppler plots were also included for these cases.

In discussing the examples of wind shear, several discrepancies between the different forms of data were noted. These differences should be taken into consideration when using the provided Doppler radar and mesonet data to evaluate the performance of the enhanced LLWAS.

REFERENCES

Barnes, S.L., 1980: Report on a meeting to establish a common Doppler radar data exchange format. *Bull. Amer. Meteor. Soc.*, **61**, 1401–1404.

DiStefano, J.T.,1988: Observability of microbursts using Doppler weather radar and surface anemometers during 1987 in Denver, CO. *MIT, Lincoln Laboratory Project Report ATC–161, FAA Report No. FAA–RD–PS/88/12*, 77 pp.

Doviak, R.J., R.G. Strauch and L.J. Miller, 1976: Error estimation in wind fields derived from dual–Doppler radar measurement. *J. Appl. Meteor.*, **15**, 868–878.

Evans, J.E., and D. Johnson, 1984: The FAA transportable Doppler weather radar. *Preprints, 22nd Conference on Radar Meteorology*, Zurich, Amer. Meteor. Soc., 246–250.

Evans, J.E., and D.H. Turnbull, 1985: The FAA–MIT Lincoln Laboratory Doppler weather radar program. Preprints, *2nd International Conference on the Aviation Weather System*, Montreal, Amer. Meteor. Soc., 76–79.

Goff, R.C., 1976: Vertical structure of thunderstorm induced low level wind variations. *J. Aircraft*, **14**, pp. 423–427.

Kessinger, C.J., P.S. Ray and C.E. Hane, 1987: The Oklahoma squall line of 19 May 1977. Part I: A multiple Doppler analysis of convective and stratiform structure. *J. Atmos. Sci.*, **44**, 2840–2864.

LLWAS Program Staff, 1987: Evaluation of enhancements to the Low Level Wind Shear Alert System (LLWAS) at Stapleton International Airport. Interim Report *CT–110–88–01*. FAA Technical Center, 44 pp.

Merritt, M.W., 1987: Automated detection of microburst windshear for Terminal Doppler Weather Radar. *Proc. SPIE, Vol. 846, Digital Image Processing and Visual Communications Technologies in Meteorology*, The International Society for Optical Engineering, 61.

O'Brien, P.J., 1987: Test plan for the evaluation of enhancements to the Low Level Wind Shear Alert System (LLWAS) at Stapleton Airport. Denver LLWAS Test Plan, FAA Technical Center, FAA Form 1360–38 (7–76).

Sanford, P., A. Witt, and S. Smith, 1988 (in press): Gust front/wind shift detection algorithm. *MIT, Lincoln Laboratory Project Report ATC–146, FAA Report No. DOT/FAA/PM–87–24*.

Wilson, F.W., Jr., and J.A. Flueck, 1986: A study of the methodology of low–altitude wind shear detection with special emphasis on the Low Level Wind Shear Alert concept. FAA Report No. *DOT/FAA/PM–86/4*, 109 pp.

Wolfson, M.M., 1987: The FLOWS automatic weather station network. *Preprints, Sixth Symposium on Meteorological Observations and Instrumentation*, New Orleans, Amer. Meteor. Soc., 294–299.

Appendix A
The Dual Doppler Process

There were a number of steps involved in creating the two dimensional dual Doppler analyses of wind shear events impacting the enhanced LLWAS at Stapleton International Airport. To begin with, the FL-2 and UND single Doppler radar data needed to be resampled into similar Cartesian coordinate systems. Only data from the surface up to 500 meters (input tilts equal to or lower than 0.5°) were used.

The proper Cartesian grid parameters had to be chosen to obtain the best resolution possible while still covering the entire airport area. Our grid was centered over the LLWAS network, with 100 grid points on the east-west axis and 100 points on the north-south axis, with 250 meter spacing between grid points. The center of the grid was at a range and azimuth relative to the FL-2 radar of 14.5 km at 306°, and at a range and azimuth relative to UND of 14.8 km at 217.5°.

Before combining the two single Doppler radar fields, we reviewed both the FL-2 and UND resampled Cartesian files. It was found that the UND reflectivity and velocity fields were noisy and contained several "holes", where the signal-to-noise ratio was too low for the data to be valid. A smoothing method was needed that would take out much of the noise, fill some of the "holes", and at the same time, preserve the features. A nine point median filter was chosen to smooth the resampled UND data; no filter was used on the FL-2 data.

In reviewing the resampled Cartesian files, it was also found that velocity aliasing had occurred, especially in the UND data, for a number of the high speed wind shear events. The range and azimuth limits of the aliased regions were manually determined, and the affected volume scans were re-layered with the manual dealiasing option enabled. Any necessary smoothing steps were performed after the fields were dealiased.

Another parameter that had to be chosen was the limiting between-beam angle for the calculation of the horizontal wind field. The wind field will be most accurate when the radar beams intersect at exactly 90 degrees. However, in order to increase the region covered by dual Doppler processing, a smaller intersection angle must be accepted. A minimum beam angle of 30° between the radars was used. Also, since only the two dimensional surface wind field was required, none of the issues associated with deriving the vertical velocity had to be considered.

The final criteria to consider was the time difference between the FL-2 and UND scans. Throughout nearly all of the cases, the radars were scanning at less than a 15 second time differential, although time differences of up to 2 minutes were allowed. After all of these steps were completed, we combined, at each grid point, the single Doppler radar measurements from the FL-2 Doppler radar with those from the UND Doppler radar, to produce the two dimensional surface wind fields.

Appendix B
The Lincoln Laboratory Cartesian Exchange Format (CEF)*

Introduction

This document describes the format for the exchange of Cartesian product data.

Recording medium and format

The data are recorded on 9-track magnetic tape at a density of 1600 bits per inch (BPI) or 6250 BPI.

Each file on the tape contains header information and product data for one product only, and for a single altitude "slice". Each file is terminated by an end of file mark (EOF), and the last file on the tape is followed by a second "EOF".

Header information and product data are organized as a series of 128 byte ASCII physical records.

Data organization

Each file on tape has a series of header information records, followed by a blank record (to signify the end of comments), and a number of data records.

The header information is organized so that there is only one "type" of data stored per header record.

The product data to be conveyed is a rectangular Cartesian grid. The grid consists of rows (horizontal orientation) and columns (vertical orientation). The rows and columns may have different numbers of data elements. "Row elements" correspond to x axis positions whose actual locations are dependent on the resolution of the row. "Column elements" are the corresponding y axis positions, whose actual locations are dependent on the resolution of the column. Hence, "row elements" may be read as "x elements", and "column elements" may be read as "y elements".

The "origin" of the rectangular grid is defined to be the lower left hand corner of the grid (unless otherwise stated), and the location of that origin in space is measured in meters East and North of the radar location. Rows are oriented West to East, and columns are oriented South to North.

* Appendix B has been taken from information provided by B.H. Stevens.

Header records

All header information records consist of 48 ASCII characters of a descriptive nature, followed by up to 80 ASCII characters of either character or numerical data.

The order of information in the header records is constant. Any comments will appear last, and the end of these comments (and the end of the header data) will be signified by a record whose first 48 characters (the description), at least, are blank.

The following table defines the construction of the header records; because all descriptive characters are written into a 48 character alphanumeric field (FORTRAN FORMAT A48) only the format for the actual data will be specified here. It should be noted that all data formats begin in column (byte) 49 of a 128 byte record.

48 Descriptive characters	Data description	Data format
a) SOURCE ORGANIZATION	80 ASCII characters	A80
b) SOURCE RADAR	80 ASCII characters	A80
c) SOURCE SITE	80 ASCII characters	A80
d) SOURCE PROJECT	80 ASCII characters	A80
e) DATE COLLECTED	month day year hour minute second	I2,5(1X,I2)
f) DATA TYPE CODE	1=<type_code=<3	I1
g) PRODUCT NAME	80 ASCII characters	A80
h) PRODUCT CODE	1=<product_code	I2
i) DISPLACEMENT OF ORIGIN FROM RADAR (m)	east_displ, north_displ	I7,1X,I7
j) NUMBER OF ELEMENTS IN ROWS AND COLUMNS	row_elems, col_elems	I4,1X,I4
k) RESOLUTION OF ROWS AND COLUMNS (m)	row_res, col_res	I5,1X,I5
l) ALITUDE LIMITS OF LAYER (m)	bot_alt, top_alt	I5,1X,I5
m) ELEV/AZIMUTH ANGLE (°)	angle	F6.1
n) UNAMBIGUOUS VELOCITY (m/s)	unambig_vel	F5.1
o) SCALE FACTOR	scale	F9.4
p) COMMENT	80 ASCII characters	A80
. .	.	.
. .	.	.
. .	.	.
?) (blank line signifying end of header records)		

The "DATA TYPE CODE" (record f) refers to the way the Cartesian field was generated. This code can be any of the following values, with the associated meanings:

type_code = 1 for true layered product
= 2 for resampled PPI
= 3 for resampled RHI

The "PRODUCT CODE" (record h) can currently have the following values and associated meanings for product data:

Product	Product code	Data units
Reflectivity	1	dBz
Radial velocity	2	m/s
Turbulence	3	$(cm^{2/3})/s$
Radial shear	4	$1/s \times 10^{-3}$
Tangential shear	5	$1/s \times 10^{-3}$
Total shear	6	$1/s \times 10^{-3}$
Echo tops	7	kft
Predicted reflectivity	8	dBz

For PPI and RHI data, the "ALTITUDE LIMITS" (record l) has no meaning. For true layered data, the "ELEV/AZIMUTH ANGLE" (record m) has no meaning. For a PPI, the angle is to be interpreted as an elevation angle; for an RHI, the angle is an azimuth angle.

Product data

Product data are stored with 32 values per record, with each data value recorded in an I4 format (using the FORTRAN statement FORMAT(32I4)). All data values are rounded to the nearest integer value; bad or missing data have the value "9999".

The actual product data are stored an entire row at a time. The first row stored is the bottom-most, i.e., the row which starts at the origin of the Cartesian field.

If one were to consider the Cartesian field to be a two dimensional array, with the first dimension being the index to an element in a row, and the second the index to an element in a column, then one might say that the data are stored by looping over all column elements, and by looping over all row elements for a given column element.

Since there are 32 values stored per record, the number of records required per row is given by:

$$\text{records per row} = \frac{\text{number of row elements}}{32}$$

The total number of records required to hold the entire Cartesian field is given by:

total records required = records per row X number of column elements

It should be noted that a new record is begun at the start of a new row, regardless of whether or not the previous record was completely filled.

FORTRAN-77 code for reading header descriptives and data

The following FORTRAN-77 code (only pertinent statements are shown) is intended as a demonstration of a method of reading the header information from a CEF file. The header descriptives are discarded once read; they could actually be skipped when reading by use of the appropriate FORMAT specification, except in the case of reading comments. A blank record signifies the end of header records.

```
C
C      Variable declarations
C
       CHARACTER*48 DESCRIPTION
       CHARACTER*80 ORGANIZATION
       CHARACTER*80 RADAR
       CHARACTER*80 SITE
       CHARACTER*80 PROJECT
       INTEGER*4    MONTH, DAY, YEAR, HOUR, MINUTE
       INTEGER*4    SECOND
       CHARACTER*80 PROD_NAME
       INTEGER*4    PROD_CODE, DATA_TYPE
       INTEGER*4    ORIG_EAST_DISPL, ORIG_NORTH_DISPL
       INTEGER*4    N_ROW_ELEMENTS, N_COL_ELEMENTS
       INTEGER*4    ROW_RESOLUTION, COL_RESOLUTION
       INTEGER*4    BOT_ALTITUDE, TOP_ALTITUDE
       REAL*4       EVELATION_ANGLE
       REAL*4       AZIMUTH_ANGLE
       REAL*4       UNAMBIG_VELOCITY, SCALE
C
C      Declarations for reading comments
C      (The maximum number of comments to be read is
C      set to 20 as an example)
C
       INTEGER*4    N_COMMENTS, MAX_COMMENTS
       PARAMETER   (MAX_COMMENTS = 20)
       CHARACTER*80 TEMP_STRING, COMMENT(MAX_COMMENTS)
C
```

```
C     Declaration for reading elevation/azimuth angle
C
      REAL*4        ANGLE
C
C     Variable for input logical unit (tape drive)
C        (logical unit 1 is used as an example)
C
      INTEGER*4     INPUT_LU
      PARAMETER    (INPUT_LU = 1)
            .
            .
            .
C
C     Read source organization
C
      READ(INPUT_LU,100) DESCRIPTION, ORGANIZATION
  100 FORMAT(A48,A80)
C
C     Read source radar
C
      READ(INPUT_LU,200) DESCRIPTION, RADAR
  200 FORMAT(A48,A80)
C
C     Read source site
C
      READ(INPUT_LU,300) DESCRIPTION, SITE
  300 FORMAT(A48,A80)
C
C     Read source project
C
      READ(INPUT_LU,400) DESCRIPTION, PROJECT
  400 FORMAT(A48,A80)
C
C     Read date data was collected
C
      READ(INPUT_LU,500) DESCRIPTION, MONTH, DAY, YEAR,
     &                                HOUR, MINUTE, SECOND
  500 FORMAT(A48,I2,5(1X,I2))
C
C     Read data type code
C
      READ(INPUT_LU,600) DESCRIPTION, DATA_TYPE
  600 FORMAT(A48,I)
```

```
C
C     Read product name
C
      READ(INPUT_LU,700) DESCRIPTION, PROD_NAME
  700 FORMAT(A48,A80)
C
C     Read product code
C
      READ(INPUT_LU,800) DESCRIPTION, PROD_CODE
  800 FORMAT(A48,I2)
C
C     Read displacement of origin from radar (meters)
C
      READ(INPUT_LU,900) DESCRIPTION, ORIG_EAST_DISPL,
     &                                ORIG_NORTH_DISPL
  900 FORMAT(A48,I7,1X,I7)
C
C     Read number of row and column elements
C
      READ(INPUT_LU,1000) DESCRIPTION, N_ROW_ELEMENTS,
     &                                 N_COL_ELEMENTS
 1000 FORMAT(A48,I4,1X,I4)
C
C     Read row and column resolution (meters/element)
C
      READ(INPUT_LU,1100) DESCRIPTION, ROW_RESOLUTION,
     &                                 COL_RESOLUTION
 1100 FORMAT(A48,I5,1X,I5)
C
C     Read altitude limits of layer (meters)
C        (no meaning if PPI or RHI)
C
      READ(INPUT_LU,1200) DESCRIPTION, BOT_ALTITUDE,
     &                                 TOP_ALTITUDE
 1200 FORMAT(A48,I5,1X,I5)
C
C     Read elevation/azimuth angle (degrees)
C        (no meaning if layered data)
C
      READ(INPUT_LU,1300) DESCRIPTION, ANGLE
 1300 FORMAT(A48,F6.1)
C
C     If a PPI...
```

```
C
      IF(DATA_TYPE .EQ. 2) THEN
C
C        Store angle as elevation
C
         ELEVATION_ANGLE = ANGLE
C
C     If an RHI...
C
      ELSE IF(DATA_TYPE .EQ. 3) THEN
C
C        Store angle as azimuth
C
         AZIMUTH_ANGLE = ANGLE
         ENDIF
C
C     Read unambiguous velocity (meters/sec)
C
      READ(INPUT_LU,1400) DESCRIPTION, UNAMBIG_VELOCITY,
     &                    SCALE
 1400 FORMAT(A48,F5.1,F9.4)
C
C     Loop to read comments
C
C     Initialize comment count
C
      N_COMMENTS = 0
C
C     Loop...
C
 1500 CONTINUE
C
C        Read a comment line
C
         READ(INPUT_LU,1600) DESCRIPTION, TEMP_STRING
 1600    FORMAT(A48,A80)
C
C        See if description is non-blank and if we
C        haven't reached our maximum number of comments
C        yet - if ok, then save comment
C
         IF(DESCRIPTION .NE. ' ' .AND.
        &   N_COMMENTS .LT. MAX_COMMENTS) THEN
```

```
            N_COMMENTS = N_COMMENTS + 1
            COMMENT(N_COMMENTS) = TEMP_STRING
            ENDIF
C
C        Continue to loop if description is not blank
C
         IF(DESCRIPTION .NE. ' ') GO TO 1500
C
C     Done with header records
C
```

FORTRAN-77 code for reading product data

The following FORTRAN-77 code (only pertinent statements are shown) is intended as a demonstration of a method of reading the product data from a CEF file.

```
C
C     Variable declarations
C          (The number of row elements and column ele-
C          ments are set to 256 as an example; this
C          allows proper dimensioning of PROD_DATA.
C          Since N_ROW_ELEMENTS AND N_COL_ELEMENTS would
C          most likely be read from the header records
C          at some point, it would be likely that some
C          other scheme for dimensioning PROD_DATA would
C          be generally more appropriate. For the
C          purpose of this example code, however, this
C          limited approach allows correct and complete
C          code to be written).
C
      INTEGER*4 N_ROW_ELEMENTS, N_COL_ELEMENTS
      PARAMETER (N_ROW_ELEMENTS = 256)
      PARAMETER (N_COL_ELEMENTS = 256)
      INTEGER*4 PROD_DATA(N_ROW_ELEMENTS,N_COL_ELEMENTS)
      INTEGER*4 ROW_ELEMENT, COL_ELEMENT
C
C     Variable for input logical unit (tape drive)
C        (logical unit 1 is used as an example)
C
      INTEGER*4 INPUT_LU
      PARAMETER (INPUT_LU = 1)
```

```
C
C     Loop over all column elements
C
      DO 200 COL_ELEMENT = 1, N_COL_ELEMENTS
C
C        Read a row of data (loop over all row elements)
C
         READ(INPUT_LU,100)(PROD_DATA(ROW_ELEMENT,
        &    COL_ELEMENT), ROW_ELEMENT=1,
        &    N_ROW_ELEMENTS)
  100    FORMAT(32I4)
C
C        Next column element...
C
  200    CONTINUE
C
C     Done with this product data. (Remember to divide
C     the integer PROD_DATA by the real SCALE (store as
C     a real) to get the correct values.)
C
```

Appendix C
Procedures For Requesting FAA-Lincoln Laboratory Dual Doppler Weather Radar Data

1. Contact: Dr. James E. Evans
MIT Lincoln Laboratory, HW-10
P.O. Box 73
Lexington, MA 02173

in writing to request the radar, mesonet, LLWAS or dual Doppler data. Include your name, mailing address and telephone number.

2. The single Doppler radar data will be provided on magnetic tape (6250 bpi) in the Universal Common Doppler Radar Data Exchange Format (see Barnes, 1980). We can also provide data in a B-scan printout format if necessary.

3. The mesonet and LLWAS data will be provided on magnetic tape (1600 or 6250 bpi) in the Common Mesonet Format (CMF) being used at the National Center for Atmospheric Research. A complete description of the format will be provided.

4. Dual Doppler (2-dimensional) surface wind fields (when available) will be provided on magnetic tape (1600 or 6250 bpi) in the Lincoln Laboratory Cartesian Exchange Format (see Appendix B). Wind vector plots and streamline plots can also be provided.

5. We ask that you send us one new tape for each tape that you receive. No additional data requests will be filled until the blank tapes for the previous request are received. Feel free to contact us with any questions that arise in using the data.

6. If you publish any results that are based on or that make use of our data we ask that you do the following:

a) Include the following acknowledgement:

"The data used in this report were provided by MIT Lincoln Laboratory under sponsorship from the Federal Aviation Administration".

b) Cite this Project Report when discussing the data.

c) Provide us with one copy of your publication (send to J.E. Evans).

7. The tapes are provided for the exclusive use of the requesting organization in scientific studies. Further distribution of the data is not authorized.